

# STUDY OF NATURAL CONVECTIVE FLOW IN A SATURATED POROUS MEDIUM

A Thesis Submitted  
in Partial Fulfilment of the Requirements  
for the Degree of  
DOCTOR OF PHILOSOPHY

*by*  
AJAY KUMAR SINGH

*to the*  
DEPARTMENT OF MATHEMATICS  
INDIAN INSTITUTE OF TECHNOLOGY, KANPUR  
AUGUST, 1990

TO  
MY PARENTS

115237

23 DEC 1991

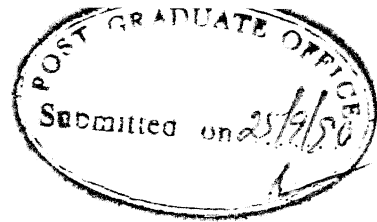
CENTRAL LIBRARY

1000 40000

Acc No. **112537**

TH  
519.4  
Si 64 S

MATH-1990-D-SIN-STU



## CERTIFICATE

It is certified that the work contained in the thesis entitled, "Study of Natural Convective Flow in a Saturated Porous Medium" by Ajay Kumar Singh, has been carried out under our supervision and that the work has not been submitted elsewhere for a degree.

A handwritten signature in cursive script, appearing to read "K. A. Narayan".

( K. A. Narayan )  
Assistant Professor  
Chemical Engineering Dept.  
Indian Institute of Technology  
Kanpur 208 016  
INDIA

A handwritten signature in cursive script, appearing to read "Purnyatma Singh".

( Purnyatma Singh )  
Professor  
Mathematics Department  
Indian Institute of Tech.  
Kanpur 208 016  
INDIA



## ACKNOWLEDGEMENT

I am deeply indebted to my thesis supervisors, Professor Punyatma Singh and Dr. Kumar Abhay Narayan for their invaluable advice and criticism to the completion of this work.

My deepest gratitude to Dr. T. Sundararajan, Dept. of Mechanical Engineering, Indian Institute of Technology, Kanpur, without whose timely advice and perennial support this investigation would not have been possible.

Special words of thanks go to Professor B. Singh, Director and Dr. B.D. Banerjee, Scientist, Central Mining Research Station, Dhanbad, for their due help in completing my research work at IIT Kanpur.

My special thanks are also due to Professor B.L.Dhoopar and Dr. Peeyush Chandra, for the concern they showed for the progress of my work. I appreciate the company of Daya Shankar, Ramakant, Shailesh, Umesh, Ashutosh, Neeraj, Puneet, Ibha, Kalika and Pratibha who gave me healthy cooperation and boosted my morale for my work.

I can never say in words how grateful I am to my dear parents, brothers and sisters, who have been a constant source of inspiration and encouragement throughout the course of this work. I record my sincere thanks to my wife Abha, for her unfailing affection and care and to my daughter Garima, who always encouraged me with persistent smiles during the course of the present work.

Finally, I wish to thank Swami Anand Chaitanya, for his painstaking typing and to Mr. J.C. Verma for his meticulous drawing of figures. Thanks to all others who helped me in one way or other to carry out the present investigation.

August, 1990.

*Ajay Kumar Singh*  
Ajay Kumar Singh

## CONTENTS

	Page
CERTIFICATE	iii
ACKNOWLEDGEMENTS	iv
SYNOPSIS	viii
CHAPTER I : INTRODUCTION	
1.1 Overview	1
1.2 Description and properties of porous media	3
1.3 Governing equations for convection through porous media	6
1.4 The boundary layer equations in porous media	14
1.5 Background of the present work	16
References	28
CHAPTER II : NATURAL CONVECTION ABOUT A SEMI INFINITE VERTICAL FLAT PLATE IN A POROUS MEDIUM	
2.1 Introduction	35
2.2 Basic equations and boundary conditions for constant wall temperature	36
2.3 Solutions by finite difference method	38
2.4 Free convection with wall temperature a function of position	44
2.5 Results and discussion	46
References	49
Figures	50

CHAPTER III : NATURAL CONVECTION IN A RECTANGULAR POROUS  
ENCLOSURE WITH HEATED WALLS

3.1	Introduction	54
3.2	Problem statement	56
3.3	Numerical procedure	59
3.4	Results and discussion	68
	References	74
	Figures	76

CHAPTER IV : NATURAL CONVECTION IN A VERTICAL CYLINDRICAL  
ANNULUS FILLED WITH A POROUS MATERIAL

4.1	Introduction	84
4.2	The Basic equations	86
4.3	Development of finite elemental equations	88
4.4	Matrix formulation and solution procedure	93
4.5	Results and discussion	95
	References	101
	Figures	102

CHAPTER V : A NUMERICAL STUDY OF OSCILLATORY CONVECTIVE  
FLOW THROUGH A POROUS MEDIUM

5.1	Introduction	110
5.2	Governing equations	112
5.3	Solution of the temperature field	113
5.4	Numerical solution for the velocity field	114
5.5	Results and discussion	115
	References	119
	Figures	120

CHAPTER VI : APPLICATION OF A THERMODYNAMIC METHOD  
TO BENARD CONVECTION IN HORIZONTAL  
POROUS LAYER

6.1	Introduction	123
6.2	The dual field method	126
6.3	Formulation of GPDP for Benard-Darcy Problem	129
6.4	Application of dual field method	133
6.5	Solution for rigid surfaces	137
6.6	Results and discussion	142
	References	144

## SYNOPSIS

The present thesis outlines a combined numerical and theoretical study of convective heat transfer in a fluid saturated porous medium.

The subject of convective transport processes in porous materials has received a great deal of attention in recent years owing to its importance in many practical applications such as the development of geothermal energy technology, petroleum reservoirs and building thermal insulation systems.

The analysis of fluid flow and heat transfer is based on the transport equations and one has to consider the appropriate form of governing equations in the context of flow through porous media. The use of Darcy's law as the momentum conservation equation has now become common place and it is well known that this law does not take into account the effects of a solid boundary and the inertial forces. Instead of considering only the potential nature of the Darcy's equation, some researchers use the Brinkman model which also includes the viscous shear term while some others use Forchheimer-extended Darcy model to deal with the inertial forces. There is yet another group of researchers who prefer to use Navier-Stokes type equation with Darcy resistance term included.

One of the primary objectives of the present work is to study buoyancy induced flows in a saturated porous medium based on a generalized momentum equation which contains the non-linear

convective terms as well as the viscous shear terms in addition to the Darcy resistance term. Numerical techniques as well as the analytical method is employed to obtain the solution of governing non-linear coupled partial differential equations.

The first chapter is introductory and is concerned with the general background of the work presented in this thesis. Description and various properties of a porous medium along with the conservation equations of mass, momentum and energy are discussed in brief. Literature survey of the published work related to the different problems analyzed here, is presented.

The second chapter deals with the prediction of steady natural convection adjacent to a semi-infinite vertical surface embedded in a saturated porous medium, subject to a prescribed constant wall temperature or the wall temperature as a power function of distance from the leading edge. Finite difference method, based on highly implicit scheme with variable mesh size, is employed. It is found that the vertical velocity component reaches a maximum a little way out from the wall and then decreases. The horizontal velocity component is always directed towards the wall. The temperature decreases monotonically away from the wall.

Third chapter is concerned with the study of steady, two-dimensional buoyancy induced flow in a rectangular vertical porous enclosure with specified temperature on all the four boundaries. The governing equations in stream function vorticity form are numerically solved by upwind finite difference method. A line-by-line numerical procedure is

adopted to reduce the difference equations in the tridiagonal form. The stream function, vorticity and temperature fields are obtained for various values of the dimensionless parameters. Flow patterns and isotherms are plotted and results on local and average Nusselt numbers are reported. The flow is unicellular filling the entire half of the enclosure. The velocities are higher near the wall and lower near the line of symmetry. The isotherm patterns are more distorted when the convection is dominant.

In the fourth chapter, free convective heat transfer in a vertical porous annulus whose inner wall is heated at a constant temperature, outer wall is isothermally cooled and the top and bottom are insulated, is investigated. The governing equations are axisymmetric form of two-dimensional continuity equation, generalized momentum equation and the energy equation. The velocity and pressure formulation is used and finite element method based on Galerkin approach is applied to solve the governing equations. Velocity and temperature fields and the local Nusselt number are shown as a function of the dimensionless parameters of the problem. Results on average Nusselt number along the heated wall are also presented.

In the fifth chapter, the problem of convective flow along an infinite vertical wall of constant temperature is analyzed. The far stream temperature is also constant but differs from that of the wall. The free stream oscillates about a constant mean and the effect of natural convection on oscillatory flow

is studied. Finite difference method with Crank Nicolson scheme is used to predict the velocity field. Skin friction at the wall is also calculated.

A variational principle based on Onsager's linear theory of irreversible processes is applied to study the thermohydrodynamical stability of natural convection in a horizontal porous layer bounded by two rigid walls in the last chapter. The critical wave numbers and the corresponding Rayleigh-Darcy numbers are obtained for various values of Darcy number.



# CHAPTER I

## INTRODUCTION

### 1.1 OVERVIEW

The transport of heat by convection in porous media is a process that finds frequent application in a broad spectrum of disciplines ranging from chemical engineering to geophysics. Examples of convection through porous media may be found in insulation systems, petroleum and reservoir engineering and ceramic industry. The same processes play a vital role in the design procedures for putting down the fire in goaf areas of coal mines and also in the design of pebble bed nuclear reactors and nuclear waste storage devices. Since convective heat transfer through porous media has such an overwhelming impact on our life, a good knowledge of these processes is necessary for the concerned scientists and engineers. An attempt is made here to study the flow of energy carrying fluids through porous media. The subject matter covered is the mathematical description of fluid flow and heat transfer through saturated porous media, with emphasis on the numerical solution of the governing partial differential equations. The improved numerical methods have permitted the use of general mathematical models capable of handling complex problems without approximating the actual flow problems by a simpler one.

Numerous studies of convection in porous media have been conducted using the Darcy's law which expresses that the

velocity is proportional to the pressure gradient. The Darcy's model neglects the effects of a solid boundary and inertial forces. When the porous medium is bounded by impermeable surface, the no-slip condition must be applied and the usual Darcy equation is then improper to describe the flow, at least, near the surface. Brinkman (1947) was the first to include the viscous shear term in addition to the Darcy resistance term in the flow equation. The viscous shear stress term takes into consideration the boundary effect and removes the inconsistency of Darcy's law with the no-slip condition. The inertia forces become significant in the case of porous media with high permeabilities and also if the fluid velocity is high. To incorporate the inertia effects, Forchheimer (1901) considered additional velocity square term in the Darcy equation which approximately accounts for the losses in the pressure due to flow separation in the pores. In many applications, the inertia forces are treated by adding non-linear convective terms in the flow equations. The boundary and inertia effects not included in Darcy's model, may alter the velocity fields and heat transfer characteristics. It is seen that these effects reduce the heat transfer rate for a given flow driving force.

Current research is focussed on generalizing some interesting flows of viscous fluid through porous medium using such kinds of equations that take into account the effects of the viscous stress as well as the inertia forces. Some typical cases of convection in porous media are studied while the ensuing system of partial differential equations are solved by

finite difference or finite element methods and in one case irreversible thermodynamics is employed. The velocity and temperature distributions along with the heat transfer rates have been obtained.

## 1.2 DESCRIPTION AND PROPERTIES OF POROUS MEDIA

It is first of all necessary to describe some of the basic concepts associated with the physics of flow through porous media. We begin with the term "porous media". A great variety of natural and artificial materials are porous. Soil, sand filters, fibrous aggregates and sandstones are examples of porous media. To give a precise definition of the term porous media is not very easy. Bear, Zaslavsky and Irmay (1968) define porous medium as a portion of space occupied by heterogeneous or multiphase matter. It should include a solid phase distributed throughout the medium. The solid phase is referred to as solid matrix and the space which is not a part of the solid matrix is called void space or pore space. At least some of the pores are interconnected and the pores which are not interconnected are considered as the part of the solid matrix. While the microscopic behaviour of a single particle or fluid in a single pore obeys well-known physical laws, the macroscopic behaviour of the porous material is described by average properties. A porous medium is characterized by a variety of geometrical properties. Following are some of the main characteristics of porous media.

**Porosity:**

One of the most important properties of porous media is porosity which is a measure of pore space and hence of the fluid capacity of the medium. Porosity is defined as the ratio of the void space to the total volume and is expressed either as a fraction of one or in percent.

One may distinguish two types of porosities, namely, absolute and effective. Absolute porosity is the percentage of total void space with respect to the bulk volume regardless of the interconnection of the pores. A porous structure may have considerable absolute porosity and yet have no conductivity to fluid for lack of pore interconnection. Effective porosity is the percentage of interconnected void space with respect to the bulk volume. It is an indication of conductivity to fluid but not necessarily a measure of it.

**Permeability:**

The permeability of a porous material may be defined as its fluid conductivity, or ability to let fluid flow within its interconnected pore network. Hence it is natural to expect a relation between permeability of a medium and effective porosity but not necessarily with absolute porosity. All factors, namely, grain size, grain packing, grain angularity, grain size distribution, cementation and consolidation, which influence effective porosity also influence permeability.

**Specific Surface:**

The specific surface of a porous material is defined as the interstitial surface area of the pores per unit bulk volume of porous material.

**Fluid Saturation:**

There is yet another important factor to influence the dynamics of fluid flow through porous media — the fluid content of the porous structure. Saturated flow is a term used to describe the flow of a fluid through a porous medium where the entire void space is filled with the fluid. The void space of a porous medium may be partially filled, the remaining void space being occupied by air. On the other hand, two or more immiscible liquids may jointly fill the void space, for example, petroleum reservoir rocks normally contain both petroleum hydrocarbons and water. The saturation of a porous medium with respect to a particular fluid is defined as the fraction of the void volume of the medium filled by the fluid in question.

All these macroscopic properties of porous media have significance only for samples of porous materials containing relatively large number of pores. A complete description of these bulk properties, their experimental determination procedures and some theories showing their interrelation are discussed by Muskat (1946), Scheidegger (1957), Collins (1961) and Bear (1972).

### 1.3 GOVERNING EQUATIONS FOR CONVECTION THROUGH POROUS MEDIA

The problem of complete investigation of fluid flow and heat transfer characteristics is to study the velocity distribution, the temperature distribution, the pressure and density of the fluid. These are functions of spatial coordinates and time. The path of heat and fluid flow through a porous medium is complex and the flow geometry changes continuously from one region of the material to another; for example, the velocity is large in small pores and small in the larger ones. Although the flow of fluid and energy through porous media is complicated, it usually is sufficient to determine average velocities, average temperature distribution, average flow paths, or the pressure distribution in the material. Here, the conservation equations for porous media flow and heat transfer are discussed in brief.

#### I. Mass Conservation:

The mass balance equation results from the consideration that no fluid can be produced or destroyed in any infinitesimal volume of the material filled with fluid. Mathematically, for a three-dimensional average flow the mass conservation statement reads ,

$$\frac{D\rho}{Dt} + \rho \operatorname{div} \mathbf{q} = 0 , \quad (1.1)$$

where,  $\mathbf{q}$  is the volume averaged velocity vector,  $\rho$  is the density of the fluid and  $t$  is the time. The symbol  $\frac{D\rho}{Dt}$  denotes here the substantive derivative which consists of the local

contribution (in non-steady flow)  $\frac{\partial \rho}{\partial t}$ , and the convective variation (due to translation),  $\mathbf{q} \cdot \text{grad } \rho$ . For an incompressible fluid with  $\rho = \text{constant}$ , the mass conservation equation (1.1) assumes the simplified form,

$$\text{div } \mathbf{q} = 0 . \quad (1.2)$$

## II. Momentum Conservation

The momentum equation in the fluid mechanics of porous media originated in the nineteenth century in connection with the engineering of public fountains in the city of Dijon, France. Most of the information regarding the experiment performed by the French engineer Henry P.G. Darcy (1856) and his law in its simplest form with discussion on its limitations and some of its modifications may be found in the books by Muskat (1946), Scheidegger (1957), Collins (1961) and Bear (1972). Based on his experiments Darcy (1856) discovered that the rate of fluid flow  $Q$  through a filter bed is directly proportional to the area  $A$  of the bed and to the difference  $(h_1 - h_2)$  between the fluid heads at the inlet and outlet faces of the bed and inversely proportional to the thickness  $L$  of the bed, to establish the Darcy's formula,

$$Q = \frac{\text{constant} \times A(h_1 - h_2)}{L} . \quad (1.3)$$

This form of Darcy's law has only a very restricted use which can be summarized in a more useful form to state that the area-averaged velocity through a column of porous material is directly proportional to the pressure gradient established along the column. Denoting the area-averaged velocity by  $u$  and the

pressure gradient in the channel by  $\frac{dp}{dx}$ , the Darcy's law may be expressed in the differential form as ,

$$u = \text{constant} \times \frac{dp}{dx} . \quad (1.4)$$

Subsequent research workers established that the area-averaged velocity of the fluid seeping through a porous material is inversely proportional to the viscosity of the fluid. Therefore, the Darcy's law for one-dimensional flow can be written as,

$$u = \frac{K}{\mu} \left( - \frac{dp}{dx} \right) , \quad (1.5)$$

where,  $\mu$  is the coefficient of viscosity. The constant of proportionality  $K$  is called the permeability and as stated earlier, is a property of the porous medium.

It is now possible to define the permeability of a porous medium as the volume of a fluid of unit viscosity passing through a unit cross-section of the medium in unit time under the action of a unit pressure gradient. It is determined only by the structure of the medium and is entirely independent of the nature of the fluid. Its dimensions are those of an area.

In practical problems, the flow is rarely rectilinear and neither the direction of the flow nor the magnitude of the pressure gradient is known. In vectorial notation, the three dimensional generalization of equation (1.5) including the body force term is,

$$\mathbf{q} = - \frac{K}{\mu} (\nabla p - \rho \mathbf{g}) , \quad (1.6)$$

where,  $\mathbf{q}$  is the volume rate of flow through a unit



cross-sectional area of the porous medium under the action of a pressure gradient  $\nabla p$ , and  $g$  is the acceleration due to gravity. The quantities  $\rho$  and  $p$  are averaged over a region available to flow that is large with respect to the pore size. The permeability  $K$  may vary from point to point and may not be the same in all directions. However, it will generally suffice to consider the medium to be isotropic in which  $K$  is independent of direction. Thus the above three-dimensional generalization of Darcy's law is applicable to the flow of an incompressible fluid through a homogeneous and isotropic porous medium. Carman (1956) gives an excellent exposition of the principles of flow of gases through porous media. The case of compressible fluid flow is beyond the scope of the present investigation.

Equation (1.6) is essentially a balance of bulk viscous force, gravitational force and the pressure gradient and it was soon noticed that Darcy's law possibly can be valid only in a certain seepage velocity domain, outside which more general flow equations must be used to describe the flow correctly. In many practical systems, the porous medium has a high permeability and consequently the speed in the porous bed is not small, making Darcy's law inapplicable because it neglects the inertial forces. Forchheimer (1901) modified the Darcy's law by including a second order term in the velocity and proposed the relations of the form,

$$\frac{dp}{dx} + au + bu^2 = 0, \quad (1.7)$$

and later added a third order term to give,

$$\frac{dp}{dx} + au + bu^2 + cu^3 = 0 . \quad (1.8)$$

Here,  $u$  is as usual the seepage velocity,  $p$  is the pressure (gravity is neglected), and  $a, b, c$  are empirical constants. The quadratic and cubic terms were added to make the equation fit experimental data better. When the flow is two or three - dimensional the obvious formal generalization of Forchheimer extended model (Choudhary et al. 1976) may be,

$$\nabla p - \rho g + \frac{\mu}{K} \mathbf{q} + \frac{\rho b}{K} |\mathbf{q}| \mathbf{q} = 0 , \quad (1.9)$$

where,  $|\mathbf{q}|$  is the absolute velocity and  $\frac{\mu}{K}$  and  $\frac{\rho b}{K}$  take the place of  $a$  and  $b$  respectively, in equation (1.7). The Forchheimer equations were postulated to account for the flow separation as it occurs in flow through the pores over the rigid matrix. Nevertheless, the Forchheimer relations are valid only if the fluid velocity is very high.

Deviations from Darcy's law have been observed not only at high flow rates but also near a solid boundary. Mathematically, since the order of Darcy's law is lower than that of the Navier-Stokes equation, the no-slip boundary condition is not required to be imposed on the impermeable boundary. This motivated Brinkman(1947) to modify Darcy's law by adding the classical frictional terms resulting in the famous Brinkman model which in vectorial notation is,

$$\nabla p - \rho g + \frac{\mu}{K} \mathbf{q} - \mu \nabla^2 \mathbf{q} = 0 , \quad (1.10)$$

where ,  $\nabla^2$  is the Laplacian.

Attempts have also been made to study the significance of nonlinear convective terms in the equation of motion (Hamel 1934, Yih 1965, Raats 1972, Yamamoto and Yoshida 1974). Analytical work of Yamamoto and Iwamura (1976) has considered the convective acceleration terms and frictional terms in a generalized equation of motion to include inertia and boundary effects in the Darcy's law. Following Yamamoto and Iwamura (1976), the momentum conservation equation for unsteady flow of an incompressible fluid through a homogeneous, isotropic and saturated porous medium may be taken to be,

$$\rho \frac{Dq}{Dt} = \rho g - \nabla p + \mu \nabla^2 q - \frac{\mu}{K} q . \quad (1.11)$$

Equation (1.11) is often referred to as the generalized momentum equation for a porous medium. It reduces to the Brinkman model when the inertial term on the left-hand side is omitted and can be further reduced to ordinary Darcy's law when the term of viscous stress on the right-hand side is also negligible. Moreover, for  $K \rightarrow \infty$ , i.e. no solid matrix present, this generalized momentum equation for flow through porous media is converted to the Navier-Stokes equation which is the momentum conservation equation for a pure fluid region. In addition to giving the appropriate limiting solutions as discussed above it is also expected that the generalized momentum equation will give good results in the case of highly porous media.

### III. ENERGY CONSERVATION

The theory of heat transfer in porous media is based on the existence of local thermal equilibrium between the fluid phase and the solid matrix. This equilibrium is required in order to apply local volume averaging but is not always guaranteed (Chan and Banerjee 1981). However, most of the analytical work on fluid flow and heat transfer through porous media has been carried out by assuming such equilibrium. Neglecting the viscous dissipation, the energy equation obtained by Wooding (1957) to study cellular convection in a geothermal reservoir is,

$$\rho C q \cdot \nabla T = \nabla \cdot (k \nabla T) , \quad (1.12)$$

where,  $T$  is the temperature of both the fluid and solid phases,  $C$  is the specific heat of the fluid and  $k$  is the effective thermal conductivity of the porous medium. For an isotropic homogeneous porous medium, the energy conservation equation under unsteady conditions is of the form (Cheng 1978, Bejan 1984),

$$S \frac{\partial T}{\partial t} + q \cdot \nabla T = \alpha \nabla^2 T . \quad (1.13)$$

Here,  $\alpha = \frac{k}{\rho C}$  is the thermal diffusivity of the porous medium and  $S$  is the heat capacity ratio of the fluid-filled porous medium to that of the fluid .

The mass, momentum and energy conservation equations discussed above constitute the fundamental equations for the study of fluid flow and heat transfer through porous media.

Many analytical investigations have been made to establish these conservation equations and are summarized by Cheng (1978) and Bejan (1984) among others. Vafai and Tien (1981) have developed the governing equations, alongwith an indication of physical limitations and assumptions made in the derivation.

For theoretical studies of convective heat transfer through a porous medium, the governing equations are obtained with the help of Boussinesq approximation in which the density  $\rho$  is treated as a constant in all terms in the equations of motion except the one in the body force term. The dependence of  $\rho$  on temperature is given by,

$$\rho_a - \rho = \rho\beta (T - T_a) , \quad (1.14)$$

where, suffix 'a' stands for the value of the quantities in the ambient medium and  $\beta$  is the coefficient of thermal expansion.

In natural convection flows, the body force term can be expressed as buoyancy term. The hydrostatic pressure with the body force acting on the fluid constitutes the driving mechanism for the natural convective flows. The local pressure  $p$  may be broken down to two terms, one due to the motion of the fluid,  $P$ , known as the viscous pressure and the other due to the hydrostatic pressure  $p_a$ , that is,

$$p = P + p_a . \quad (1.15)$$

The vector  $(\rho \mathbf{g} - \nabla p)$  in the momentum equation (1.11) can be expressed as,

$$\rho \mathbf{g} - \nabla p = \rho \mathbf{g} - (\nabla p_a + \nabla P) = \rho \mathbf{g} - (\rho_a \mathbf{g} + \nabla P) ,$$

where, we have used  $\nabla p_a = \rho_a g$  in the gravitational field. Using (1.14), finally we get,

$$\rho g - \nabla p = (\rho - \rho_a) g - \nabla p = -\rho\beta (T - T_a) g - \nabla p .$$

Hence the equation of motion (1.11) for natural convection in a saturated porous medium takes the form,

$$\frac{Dq}{Dt} = -g\beta (T - T_a) - \frac{1}{\rho} \nabla p + \nu \nabla^2 q - \frac{\nu}{K} q , \quad (1.16)$$

where,  $\nu$  represents the kinematic viscosity of the fluid and the term  $-g\beta (T - T_a)$  is known as the buoyancy term. It is to be noted that in natural convection, the velocity and temperature fields are coupled.

#### 1.4 THE BOUNDARY LAYER EQUATIONS IN POROUS MEDIA

The basic concepts in employing the boundary layer approximation to fluid flow and heat transfer through porous media are very similar to those in the classical viscous theory originated by Ludwig Prandtl in 1904 for forced flow. If a solid body of temperature  $T_0$  is placed in a uniform fluid stream  $U_\infty$  and temperature  $T_\infty$ , then the velocity changes from zero to  $U_\infty$  and the temperature varies from  $T_0$  to  $T_\infty$  in a region situated relatively close to the solid body. The thin layer in which the velocity increases from zero to its full value is called viscous boundary layer and in a similar way, the temperature varies from  $T_0$  to  $T_\infty$  in a thermal boundary layer. Boundary layer analysis is applicable to natural convection flows also in which the pressure in the region beyond the boundary layer is hydrostatic unlike in the case of forced flow where it is being imposed by

an external flow. According to the boundary layer concept, therefore, the flow field is divided into two regions, first the slender boundary layer in which convection of momentum and energy occur and the other, outside the boundary layer where inviscid flow prevails. Such a division of the flow field brings about a considerable simplification to the mathematical theory of the motion of fluid of low viscosity. The boundary layer equations are derived by comparing the magnitude of the various terms in the momentum and energy equations. Certain expressions in the differential equations governing the flow are neglected due to their relative smallness as compared to those retained.

The first paper dealing with the boundary layers in porous media appears to be that of Wooding (1963) to treat the problem of free convection about a line source and a point source, as well as for free convection about two finite heated vertical plates embedded in a porous medium. Wooding pointed out that when the dimensions of a convective system in a saturated porous medium are sufficiently great, diffusion effects can be neglected except in regions where the gradients of fluid properties are very large. A boundary layer theory was developed for vertical plane flows in such regions. The boundary layer approximations were also invoked by McNabb (1965) who studied free convection flows in a saturated porous medium above a horizontal heated plate. The book by Bejan (1984) contains an excellent coverage on boundary layers in porous media.

Making the usual boundary layer assumptions, the generalized momentum equation for a steady two-dimensional incompressible fluid flow takes the form,

$$\rho \left( u \frac{\partial u}{\partial x} + v \frac{\partial u}{\partial y} \right) = - \frac{dp}{dx} + \mu \frac{\partial^2 u}{\partial y^2} - \frac{\mu}{K} u, \quad (1.17)$$

and the energy equation becomes,

$$\rho C \left( u \frac{\partial T}{\partial x} + v \frac{\partial T}{\partial y} \right) = k \frac{\partial^2 T}{\partial y^2}, \quad (1.18)$$

where,  $u$  and  $v$  are the velocity components in  $x$  and  $y$  directions and  $T$  is the temperature. For natural convection the two-dimensional momentum equation in steady state assumes the following form,

$$\rho \left( u \frac{\partial u}{\partial x} + v \frac{\partial u}{\partial y} \right) = \rho g \beta (T - T_{\infty}) + \mu \frac{\partial^2 u}{\partial y^2} - \frac{\mu u}{K}. \quad (1.19)$$

## 1.5 BACKGROUND OF THE PRESENT WORK

A considerable amount of work has been published in the past five decades on thermal convection in porous medium. Early research credit goes to Horton and Rogers (1945), Morrison et al. (1948), Rogers and Morrison (1950) and Rogers et al. (1951). These authors considered this kind of flow in attempting to find the distribution of salt in subterranean sand layers. The problem of setting up of convection currents to discuss the possibility of convective flow in a porous medium was investigated theoretically by Lapwood (1948) and confirmed experimentally by Katto and Masuoka (1967). Eversince, this field has never lost its momentum because of its wide applications in science and technology. Wooding (1957-1963) and Elder (1967) made significant contributions to this area in



connection with the studies of transport processes occurring in geothermal reservoirs. The basic development of the use of boundary layer approximation to examine the convective flow through porous media was done by Wooding (1963) and McNabb (1965). Much of the previous work on heat transfer in porous media and geothermal systems is to be found in extensive review article by Cheng (1978).

Numerous investigations have been devoted to the natural convection in a porous medium adjacent to flat plates. The first investigation on free convection flow about a vertical flat plate embedded in a porous medium using boundary layer approximation was reported by Cheng and Minkowycz (1977), who obtained similarity solutions with the assumption that wall temperature is a power function of distance from the origin. Cheng (1977) revealed that solution to problems of prescribed heat flux can be obtained by a simple transformation of variables. Using an order of magnitude estimate Cheng (1978) obtained the boundary layer equations for a porous layer adjacent to a heated vertical surface and analyzed the problem using integral method with different assumed profiles. The local Nusselt number obtained from the integral method appeared to be in good agreement with that of the similarity solution. Cheng and Chang (1979) applied perturbation method to the problem of natural convection adjacent to vertical or horizontal heated surfaces. They assumed the power law variation in the wall temperature and solved perturbation equations of first order to give boundary layer solutions. The numerical solution

of the boundary layer equations was given by Na and Pop (1983) to predict the steady natural convection heat transfer from an impermeable vertical surface in a saturated porous medium subject to a prescribed non-uniform wall temperature or to a prescribed non-uniform wall heat flux. Higher-order effects of Darcian free convection boundary layer flow adjacent to a semi-infinite vertical flat plate with a power law variation of wall temperature were examined theoretically by Cheng and Hsu (1984) using the method of matched asymptotic expansions. Natural convection from vertical plates in porous media was analyzed by Ingham and Pop (1987) for cases where the leading edge of heating plate is at an arbitrary distance above an impermeable horizontal boundary and the plate is maintained at a constant temperature or uniform heat flux. Govindarajulu and Malarvizhi (1987) considered the problem for various wall temperatures and injection velocity conditions to obtain approximate series solution.

Boundary layer analysis for natural convection in a fluid saturated porous medium, adjacent to horizontal surfaces with wall temperature being a power function of distance from the leading edge, was performed by Cheng and Chang (1976). Similarity solutions for the convective flow above a heated horizontal impermeable surface or below a cooled horizontal impermeable surface are obtained and applications to convective flow above the heated bedrock or below the cooled caprock in a liquid-dominated geothermal reservoir were discussed. Free convection about an impermeable horizontal surface in a porous

medium with prescribed wall temperature was considered by Chang and Cheng (1983) and solutions were obtained by asymptotic matching procedures. Chandrasekhara et al. (1984) also found similarity solutions for free convection about an impermeable horizontal surface in a saturated porous medium of variable permeability. The results of the analysis had a bearing on convective flows in geothermal reservoirs. Natural convection for horizontal surface in porous media bounded by an impermeable vertical wall was examined by Ingham and Pop (1987) who applied the method of matched asymptotic expansions for mathematical treatment.

Little attention has been given to transient convection in a porous medium. Johnson and Cheng (1978) carried out a systematic research of similarity solutions for free convection about flat plates in porous media for steady and transient situations. Similarity solutions were shown to exist for steady free convection about vertical surfaces when the temperature difference between the wall and the environment varies either in power-law or exponential forms and for horizontal surfaces according to power law form. Several very specific solutions for unsteady free convection about flat plates in a porous medium were shown to exist. The problems of transient free convection in a porous medium adjacent to a vertical semi-infinite flat plate with a step increase in wall temperature and surface heat flux were considered by Cheng and Pop (1984). Ingham et al. (1982) presented solutions of the boundary layer equations which describe the transient free

convection flow in a saturated porous medium near a vertical flat impermeable surface which is suddenly cooled to the ambient fluid temperature.

Much work has been done on the study of convection in enclosed porous medium bounded by solid plane surfaces. Theoretical and experimental studies of natural convection in confined porous media were carried out by Holst and Aziz (1972). Critical Rayleigh number for convection in a rectangular box filled with fluid saturated porous material heated from below was determined by Beck (1972). Natural convection in a vertical porous layer of large temperature difference between the vertical walls was studied theoretically by Weber (1975) with the assumption that boundary layers develop along the vertical walls. Bejan (1979) modified the Weber's theory for convection in a vertical porous layer by combining Weber's boundary layer solution with zero energy flux boundary conditions at the top and bottom walls. Convection in a cavity enclosing a Darcy medium driven by heating in the horizontal was analyzed by Walker and Homsy (1978) where the solutions are governed by dimensionless parameters of Darcy-Rayleigh number and the cavity aspect ratio. Bejan and Tien (1978) have reported an analytical method to study the corner effects in shallow cavities. Steady convective motion inside a rectangular cavity filled with a porous material were examined by Simpkins and Blythe (1980) in the large Rayleigh number limit for flows driven by horizontal temperature gradient. An integral relations approach was used to determine the boundary layer structure on the side walls.

Numerical solutions for horizontal porous layer through the Galerkin form of the finite element method are due to Hickox and Gartling (1981). Heat transfer rates were presented for aspect ratio ranging from 0.1 to 0.5 and Rayleigh numbers in the range 25 to 200. Heat transfer results for low Rayleigh number are also due to Bankvall (1974) and Burns et al. (1976), both via numerical solutions.

The results of a numerical simulation of natural convection in a vertical rectangular porous enclosure subjected to a horizontal temperature differential were presented by Shiralkar et al. (1983) for substantially larger values of the Darcy-Rayleigh number. The effects of aspect ratio on flow behaviour and heat transfer rates in a rectangular porous cavity have been reported by Prasad and Kulacki (1984a). In another paper Prasad and Kulacki (1984b) presented numerical results for two-dimensional, steady, free convection for a rectangular cavity with constant heat flux on one vertical wall, the other vertical wall being isothermally cooled. The numerical solution of Prasad (1987) deals with convection in a rectangular cavity filled with a heat generating Darcy porous medium.

Recently natural convection in vertical annuli has also been studied in the presence of rigid matrix in Darcy's regime. By using a finite element numerical method, Hickox and Gartling (1982) have obtained heat transfer results for tall annulus with the inner wall heated at a constant temperature and the outer wall isothermally cooled, the top and bottom being insulated. Similar problem was considered by Havstad and

Burns (1982) who used finite difference method, perturbation technique and an approximate analysis for investigation. The results obtained by the above authors are applicable for only low Rayleigh number heat transfer. The work of Philip (1982) also describes free convection at small Rayleigh number. Prasad and Kulacki (1984c) considered the same thermal boundary conditions but for larger ranges of Rayleigh number and radius ratio. A numerical and experimental investigation of natural convection in saturated porous media in the annulus between vertical concentric cylinders with small aspect ratio was reported by Prasad and Kulacki (1985). As the radius ratio (outside/inside) was increased, smaller aspect ratios were required to introduce multicellular flow structures. Prasad (1986) numerically examined the convective heat transfer in a vertical annulus when its inner wall is heated by applying a constant heat flux.

In describing heat transfer in porous media, many studies have dealt with non-Darcy flow model. The buoyancy induced boundary layer adjacent to vertical wall was analyzed by Plumb and Huenefeld (1981) using a velocity square term in the momentum equation. Deviations from Darcy's law were shown to occur for larger values of modified Grashof number. Forchheimer model was also used by Bejan and Poulikakos (1984) to study the intermediate and non-Darcy flow regimes for natural convection along vertical plate embedded in a porous medium. Lai and Kulacki (1987) studied steady non-Darcy convection from a heated horizontal surface. Inertial (non-Darcy) effects at high

Rayleigh number in a vertical porous layer subjected to uniform heat fluxes at the sides were numerically evaluated using the Forchheimer model (Poulikakos 1985). Numerical experiments in a porous layer heated from the side were carried out by Poulikakos and Bejan (1985) to confirm the non-Darcy flow prediction of an analytical solution and to illustrate the regime between Darcy flow and flow affected by inertia. Nield and Joseph (1985) demonstrated that the effects of inertia are significant in natural convection at realistically large values of the Rayleigh number in thin layers of saturated porous media with small Prandtl number. Inertia effects on buoyancy-driven flow and heat transfer in a vertical porous cavity were examined by Prasad and Tuntomo (1987). A Forchheimer-extended Darcy model was shown to give superior predictions in the inertial flow regime.

Several works have been published by using the Brinkman extended Darcy model where the viscous dissipation term is included in the momentum equation. The Benard problem from viscous flow limit to Darcy's limit has been considered by Katto and Masuoka (1967), as well as by Walker and Homsy (1977). These investigators used Brinkman model as the momentum equation. Rudraiah et al. (1980) and Rudraiah and Balachandra Rao (1983) also used the same model to understand the onset of convection in porous medium made up of sparse distribution of particles. Using matched asymptotic solutions for a three-layer model for natural convection at a semi-infinite vertical plate in saturated porous media, the Brinkman model was incorporated

(Hsu and Cheng 1985). The boundary effect was shown to be important at larger Rayleigh numbers and higher Darcy numbers. The Brinkman model was employed by Chan et al. (1970) for analyzing heat transfer in a rectangular porous enclosure filled with gas. Tong and Subramanian (1985) have presented a boundary layer analysis for the Brinkman model to investigate the effect of the no-slip boundary condition in rectangular enclosures containing a porous medium. They reported significant contributions of the diffusion term at high Rayleigh and Darcy numbers. Tong and Orangi (1986) and Sen (1987) studied natural convection in porous cavities incorporating the viscous terms in the equation of motion.

Although as early as 1976, Yamamoto and Iwamura considered the transport and viscous terms in a generalized equation of motion, only a limited effort has been made to study the significance of these terms for convection in porous media. Two-dimensional free convection flow through a porous medium bounded by a vertical infinite surface was analyzed by using the generalized momentum equation for steady state case (Raptis et al. 1981) and also for unsteady state situation (Raptis and Perdikis 1983). Raptis (1983) and Singh et al. (1986) used this model to study unsteady free convective flow through a porous medium bounded by an infinite vertical plate, when the plate temperature is oscillating with time about a constant value. Raptis and Perdikis (1985) examined the effects of free stream oscillations on this geometry and Raptis and Singh (1985) considered the case of moving vertical wall. Very recently,



Lauriat and Prasad (1987) made a dimensional analysis of the Brinkman-extended Darcy formulation, with the transport term in the equation of motion to study the effects of transport and viscous terms on natural convection in vertical porous cavity.

It should be noted that attempts to consider the transport and viscous terms for analyzing convection in porous medium are limited. Recent investigations suggest the incorporation of these terms in the momentum equation. The work in this thesis is devoted to the study of some convection problems in porous media using the generalized momentum equation, which contains nonlinear transport term and a term of viscous stress also. We consider the equation with and without boundary layer approximation depending on the nature of the problem. The results are generated by solving the complete two-dimensional coupled governing equations by finite difference or finite element numerical methods. Irreversible thermodynamics is employed to the classical Benard-Darcy problem.

The problem of natural convection heat transfer from an impermeable semi-infinite vertical surface embedded in a saturated porous medium subject to a prescribed constant wall temperature or the wall temperature as a function of position from the leading edge is considered first. The analysis is based on boundary layer approximation. A numerical marching technique based on highly implicit finite difference method with variable mesh size is applied for the solution. The velocity and temperature fields are obtained together with the rate of heat transfer.

The next problem chosen deals with natural convection in an enclosed porous medium bounded by solid plane surfaces. The geometry is limited to a rectangular one with no-slip and isothermal boundary conditions on all four surfaces. The stream-function and vorticity formulation is used and an upwind finite difference scheme is employed for discretization of the vorticity and energy equations. The results are presented in terms of theoretical streamlines and isotherms for the dimensionless parameters, the Rayleigh-Darcy number, the Darcy number, aspect ratio and the top wall temperature. Results are compared with those obtained by finite element method based on Galerkin approach.

In the fourth chapter, free convective heat transfer in a vertical porous annulus whose inner wall is heated and the outer wall is isothermally cooled, the top and bottom being insulated, is investigated. The governing equations are axisymmetric form of two-dimensional continuity equation, generalized momentum equations and the energy equation. The velocity pressure formulation in which the generalized momentum equations are considered as they are, is chosen. The velocity components, pressure and temperature are all obtained simultaneously, at each node by finite element method. The algorithm developed here is very general and is suitable for a wide range of problems.

In the fifth chapter, transient convective flow through a porous medium is considered. The buoyancy effect on fluctuating flow through a porous medium bounded by an infinite vertical

wall is studied. The free stream velocity oscillates about a non-zero mean and the surface absorbs the fluid with a constant velocity. The temperature of the wall is constant and it differs from free stream temperature. The governing equations are solved by Crank-Nicolson finite difference method and the results are obtained for various values of Grashof number, the permeability parameter and the amplitude parameter.

In the last chapter of the thesis, a variational principle based on Onsager's linear theory of irreversible processes is used to study the thermohydrodynamical stability of natural convection in a porous medium bounded by two horizontal walls. The balance equations of mass, momentum and energy are considered to study the natural convection in a thin horizontal layer of saturated porous medium heated from below. The problem is treated by linear perturbation analysis when both the bounding surfaces are rigid. The critical wave numbers and the corresponding Rayleigh-Darcy numbers are obtained for various values of Darcy number.

## REFERENCES

- Bankvall, C.G., 1974, "Natural convection in a vertical permeable space", *Wärme-und Stoffübertragung*, Vol. 7, pp. 22-30.
- Bear, J., 1972, *Dynamics of Fluids in Porous Media*, American Elsevier, New York.
- Bear, J., Zaslavsky, D., and Irmay, S., 1968, *Physical Principles of Water Percolation and Seepage*, UNESCO, Paris.
- Beck, J.L., 1972, "Convection in a box of porous material saturated with fluid", *Phys. Fluids*, Vol. 15, pp. 1377 - 1383.
- Bejan, A., 1979, "On the boundary layer regime in a vertical enclosure filled with a porous medium", *Letters in Heat and Mass Transfer*, Vol. 6, pp. 93-102.
- Bejan, A., 1984, *Convection Heat Transfer*, John Wiley and Sons, New York.
- Bejan, A., and Poulikakos, D., 1984, "The non-Darcy regime for vertical boundary layer natural convection in a porous medium", *Int. J. Heat Mass Transfer*, Vol. 27, pp. 717 - 722.
- Bejan, A., and Tien, C.L., 1978, "Natural convection in a horizontal porous medium subjected to an end - to - end temperature difference", *Trans. ASME J. Heat Transfer*, Vol. 100, pp. 191-198.
- Brinkman, H.C., 1947, "A calculation of the viscous force exerted by a flowing fluid on a dense swarm of particles", *Appl. Sci. Res., Sect. A1*, pp. 27-34.
- Burns, P.J., Chow, L.C., and Tien, C.L., 1977, "Convection in a vertical slot filled with porous insulation", *Int. J. Heat Mass Transfer*, Vol. 20, pp. 919-926.
- Carman, P.C., 1956, *Flow of Gases through Porous Media*, Butterworths Scientific Pub., London.
- Chan, B.K.C., Ivey, C.M., and Barry, J.M., 1970, "Natural convection in enclosed porous media with rectangular boundaries", *Trans. ASME J. Heat Transfer*, Vol. 2, pp. 21-27.
- Chan, Y.T., and Banerjee, S., 1981, "Analysis of transient three dimensional natural convection in porous media", *Trans. ASME J. Heat Transfer*, vol. 103, pp. 242-248.

Chandrasekhara, B.C., Namboodiri, P.M.S., and Hanumanthappa, A.R., 1984, "Similarity solutions for buoyancy induced flows in a saturated porous medium adjacent to horizontal surfaces", *Wärme-und Stoffübertragung*, Vol. 18, 17-23.

Chang, I.D., and Cheng, P., 1983, "Matched asymptotic expansions for free convection about an impermeable horizontal surface in a porous medium", *Int. J. Heat Mass Transfer*, Vol. 26, pp. 163-174.

Cheng, P., 1977, "Constant surface flux heat solutions for porous layer flows", *Letters in Heat and Mass Transfer*, Vol. 4, pp. 119-128.

Cheng, P., 1978a, "Convective heat transfer in porous layers by integral methods", *Letters in Heat and Mass Transfer*, Vol. 5, pp. 243-252.

Cheng, P., 1978b, "Heat transfer in geothermal systems", *Adv. Heat Transfer*, Vol. 14, pp. 1-105.

Cheng, P., and Chang, I.D., 1976, "Buoyancy induced flow in a saturated porous medium adjacent to impermeable horizontal surfaces", *Int. J. Heat Mass Transfer*, Vol. 19, pp. 1267-1272.

Cheng, P., and Chang, I.D., 1979, "Convection in a porous medium as a singular perturbation problem", *Letters in Heat and Mass Transfer*, Vol. 6, pp. 253 - 258.

Cheng, P., and Hsu, C.T., 1984, "Higher-order approximations for Darcian free convective flow about a semi-infinite vertical flat plate", *Trans. ASME J. Heat Transfer*, Vol. 106, pp. 143-151.

Cheng, P., and Minkowycz, W.J., 1977, "Free convection about a vertical flat plate embedded in a porous medium with application to heat transfer from a dike", *J. Geophys. Res.*, Vol. 82, pp. 2040-2044.

Cheng, P., and Pop, I., 1984, "Transient free convection about a vertical flat plate embedded in a porous medium", *Int. J. Engng. Sci.*, Vol. 22, pp. 253-264.

Choudhary, M., Propster, M., and Szekely, J., 1976, "On the importance of the inertial terms in the modeling of flow maldistribution in packed beds", *AIChE J.*, Vol. 22, pp. 600-603.

Collins, R.E., 1961, *Flow of Fluids through Porous Materials*, Reinhold Publishing Corporation, New York.

Darcy, H.P.G., 1856, *Les Fontaines Publiques de la Ville de Dijon*, Victor Dalmont, Paris.

Elder, J.W., 1967a, "Steady free convection in a porous medium heated from below", *J. Fluid Mech.*, Vol. 27, pp. 29-48.

- Elder, J.W., 1967b, "Transient convection in a porous medium", J. Fluid Mech., Vol. 27, pp. 609-623.
- Forchheimer, P.H., 1901, "Wasserbewegung durch Boden", Z. Ver. Dtsch. Ing., Vol. 45, pp. 1782-1788.
- Govindrajulu, T., and Malarvizhi, G., 1987, "A note on the solution of free convection boundary layer flow in a saturated porous media", Int. J. Heat Mass Transfer, Vol. 30, pp. 1769 - 1771.
- Hamel, G., 1934, "Über Grundwasserströmung", Z. angew. Math. Mech., Vol. 14, pp. 129-157.
- Havstad, M.A., and Burns, P.J., 1982, "Convective heat transfer in vertical cylindrical annuli filled with a porous medium", Int. J. Heat Mass Transfer, Vol. 25, pp. 1755-1766.
- Hickox, C.E., and Gartling, D.K., 1981, "A numerical study of natural convection in a horizontal porous layer subjected to an end-to-end temperature difference", Trans. ASME J. Heat Transfer, Vol. 103, pp. 797-802.
- Hickox, C.E., and Gartling, D.K., 1982, "A numerical study of natural convection in a vertical, annular, porous layer", ASME Paper No. 82-HT-68.
- Holst, P.H., and Aziz, K., 1972a, "A theoretical and experimental study of natural convection in a confined porous medium", Canadian J. Chem. Engng., Vol. 50, pp. 232-241.
- Holst, P.H., and Aziz, K., 1972b, "Transient three-dimensional convection in a confined porous medium", Int. J. Heat Mass Transfer, Vol. 15, pp. 73 - 90.
- Horton, C.W., and Rogers, F.T., Jr., 1945, "Convection currents in a porous medium", J. App. Physics, Vol. 16, pp. 367 - 370.
- Hsu, C.T., and Cheng, P., 1985, "The Brinkman model for natural convection about a semi-infinite vertical flat plate in a porous medium", Int. J. Heat Mass Transfer, Vol. 28, pp. 683-697.
- Ingham, D.B., Merkin, J.H., and Pop. I., 1982, "Flow past a suddenly cooled vertical flat surface in a saturated porous medium", Int. J. Heat Mass Transfer", Vol. 25, pp. 1916-1919.
- Ingham, D.B., and Pop. I., 1987a, "Darcian free convective flow about an impermeable horizontal surface bounded by a vertical wall", Int. J. Engng. Sci., Vol. 25, pp. 373 - 383.
- Ingham, D.B., and Pop., I., 1987b, "Free convection from a semi-infinite vertical surface bounded by a horizontal wall in a porous medium", Int. J. Heat Mass Transfer, Vol. 30, pp. 1615 - 1622.

Johnson, C.H., and Cheng, P., 1978, "Possible similarity solutions for free convection boundary layers adjacent to flat plates in porous media", Int. J. Heat Mass Transfer, Vol. 21, pp. 709-718.

Katto, Y., and Masuoka, T., 1967, "Criterion for the onset of convective flow in a fluid in a porous medium", Int. J. Heat Mass Transfer, Vol. 10, pp. 297-309.

Lai, F.C., and Kulacki, F.A., 1987, "Non-Darcy convection from horizontal impermeable surfaces in saturated porous media", Int. J. Heat Mass Transfer, Vol. 30, pp. 2189-2192.

Lapwood, E.R., 1948, "Convection of a fluid in a porous medium", Proc. Camb. Phil. Soc., Vol. 44, pp. 508-521.

Lauriat, G., and Prasad, V., 1987, "Natural convection in a vertical porous cavity : a numerical study for Brinkman-extended Darcy formulation", Trans. ASME J. Heat Transfer, Vol. 109, pp. 688-696.

Morrison, H.L., Rogers, F.T. Jr., and Horton, C.W., 1949, "Convection currents in porous media, II observation of conditions at onset of convection", J. App. Physics, Vol. 20, pp. 1027 - 1029.

McNabb, A., 1965, "On convection in a saturated porous medium", Proceedings of the 2nd Australian Conference on Hydraulics and Fluid Mechanics, pp. C161-C171, The University of Auckland Press, New Zealand.

Muskat, M., 1946, The Flow of Homogeneous Fluids through Porous Media, McGraw-Hill, New York, (1937); 2nd printing by Edwards, Ann Arbor, Michigan.

Na, T.Y., and Pop, I., 1983, "Free convection flow past a vertical flat plate embedded in a saturated porous medium", Int. J. Engng. Sci., Vol. 21, pp. 517-526.

Nield, D.A., and Joseph, D.D., 1985, "Effects of quadratic drag on convection in a saturated porous medium", Phys. Fluids, Vol. 28, pp. 995 - 997.

Philip, J.R., 1982, "Axisymmetric free convection at small Rayleigh number in porous cavities", Int. J. Heat Mass Transfer, Vol. 25, pp. 1689-1699.

Plumb, O.A., and Huenefeld, J.C., 1981, "Non-Darcy natural convection from heated surfaces in saturated porous media", Int. J. Heat Mass Transfer, Vol. 24, pp. 765-768.

Poulikakos, D., 1985, "A departure from the Darcy model in boundary layer natural convection in a vertical porous layer with uniform heat flux from the side", Trans ASME J. Heat Transfer, Vol. 107, pp. 716-720.

Poulikakos, D., and Bejan, A., 1985, "The departure from Darcy flow in natural convection in a vertical porous layer", Phys. Fluids, Vol. 28, pp. 3477-3484.

Prasad, V., 1986, "Numerical study of natural convection in a vertical, porous annulus with constant heat flux on the inner wall", Int. J. Heat Mass Transfer, Vol. 29, pp. 841 - 853.

Prasad, V., 1987, "Thermal convection in a rectangular cavity filled with a heat generating Darcy porous medium", Trans. ASME J. Heat Transfer, Vol. 109, pp. 697 - 703.

Prasad, V., and Kulacki, F.A., 1984a, "Convective heat transfer in a rectangular porous cavity-effect of aspect ratio on flow structure and heat transfer", Trans. ASME J. Heat Transfer, Vol. 106, pp. 158-165.

Prasad, V., and Kulacki, F.A., 1984b, "Natural convection in a rectangular porous cavity with constant heat flux on one vertical wall", Trans. ASME J. Heat Transfer, Vol. 106, pp. 152-157.

Prasad, V., and Kulacki, F.A., 1984c, "Natural convection in a vertical porous annulus", Int. J. Heat Mass Transfer, Vol. 27, pp. 207-219.

Prasad, V., and Kulacki, F.A., 1985, "Natural convection in porous media bounded by short concentric cylinders", Trans. ASME J. Heat Transfer, Vol. 107, pp. 147-154.

Prasad, V., and Tuntomo, A., 1987, "Inertia effects on natural convection in a vertical porous cavity", Numerical Heat Transfer, Vol. 11, pp. 295-320.

Raats, P.A.C., 1972, "The role of inertia in the hydrodynamics of porous media", Arch. Rational Mech. Anal., Vol. 44, pp. 267-280.

Raptis, A., 1983, "Unsteady free convective flow through a porous medium", Int. J. Engng. Sci., Vol. 21, pp. 345-348.

Raptis, A., and Perdikis, C. 1983, "Flow of a viscous fluid through a porous medium bounded by a vertical surface", Int. J. Engng. Sci., Vol. 21, pp. 1327-1330.

Raptis, A., and Perdikis, C., 1985, "Oscillatory flow through a porous medium by the presence of free convective flow", Int. J. Engng. Sci., Vol. 23, pp. 51-55.



Raptis, A., Perdikis, C., and Tzivanidis, G., 1981, "Free convection flow through a porous medium bounded by a vertical surface", J. Phys. D: Appl. Phys., Vol. 14, pp. L 99-L 102.

Raptis, A., and Singh, A.K., 1985, "Free-convection flow past an impulsively started vertical plate in a porous medium by finite difference method", Astrophysics and Space Science, Vol. 112, pp. 259-265.

Rogers, F.T., Jr., and Morrison, H.L., 1950, "Convection currents in porous media, III Extended theory of the critical gradient", J. App. Physics, Vol. 21, pp. 1177 - 1180.

Rogers, F.T., Jr., Schilberg, L.E., and Morrison, H.L., 1951, "Convection currents in porous media, IV Remarks on the theory", J. App. Physics, Vol. 22, pp. 1476 - 1479.

Rudraiah, N., and Balachandra Rao, S., 1983, "Study of nonlinear convection in a sparsely packed porous medium using spectral analysis", App. Sci. Res., Vol. 40, pp. 223-245.

Rudraiah, N., Veerappa, B., and Balachandra Rao, S., 1980, "Effects of nonuniform thermal gradient and adiabatic boundaries on convection in porous media", Trans ASME, J. Heat Transfer, Vol. 102, pp. 254-260.

Scheidegger, A.E., 1957, The Physics of Flow through Porous Media, University of Toronto Press, Toronto.

Sen, A.K., 1987, "Natural convection in a shallow porous cavity - the Brinkman model", Int. J. Heat Mass Transfer, Vol. 30, pp. 855 - 868.

Shiralkar, G.S., Haajizadeh, M. and Tien, C.L., 1983, "Numerical study of high Rayleigh number convection in a vertical porous enclosure", Numerical Heat Transfer, Vol. 6, pp. 223-234.

Simpkins, P.G., and Blythe, P.A., 1980, "Convection in a porous layer, Vol. 23, pp. 881-887.

Singh, P., Misra, J.K. and Narayan, K.A., 1986, "A mathematical analysis of unsteady flow and heat transfer in porous medium", Int. J. Engng. Sci., Vol. 24, pp. 277-287.

Tong, T.W. and Orangi, S., 1986, "A numerical analysis for high modified Rayleigh number natural convection in enclosures containing a porous medium", Proceedings, 8th International Heat Transfer Conference, San Francisco, USA, pp. 2647-2652.

Tong, T.W. and Subramanian, E., 1985, "A boundary-layer analysis for natural convection in vertical porous enclosures - use of the Brinkman-extended Darcy model", Int. J. Heat Mass Transfer, Vol. 28, pp. 563-571.

Vafai, K., and Tien, C.L., 1981, "Boundary and inertia effects on flow and heat transfer in porous media", Int. J. Heat Mass Transfer, Vol. 24, pp. 195-203.

Walker, K., and Homsy, G.M., 1977, "A note on convective instabilities in Boussinesq fluids and porous media", Trans. ASME J. Heat Transfer, Vol. 99, pp. 338-339.

Walker, K.L., and Homsy, G.M., 1978, "Convection in a porous cavity", J. Fluid Mech., Vol. 87, pp. 449-474.

Weber, J.E., 1975, "The boundary-layer regime for convection in a vertical porous layer", Int. J. Heat Mass Transfer, Vol. 18, pp. 569-573.

Wooding, R.A., 1957, "Steady state free thermal convection of liquid in saturated permeable medium", J. Fluid Mech., Vol. 2, pp. 273 - 285.

Wooding, R.A., 1958, "An experiment on free thermal convection of water in saturated permeable material", J. Fluid Mech., Vol. 3, pp. 582 - 600.

Wooding, R.A., 1960a, "Instability of viscous liquid of variable density in a vertical Hele - Shaw cell", J. Fluid Mech., Vol. 7, pp. 501 - 515.

Wooding, R.A., 1960b, "Rayleigh instability of thermal boundary layer in flow through a porous medium", J. Fluid Mech., Vol. 9, pp. 183-192.

Wooding, R.A., 1962, "Free convection of fluid in a vertical tube filled with porous material", J. Fluid Mech., Vol. 13, pp. 129 - 144.

Wooding, R.A., 1963, "Convection in a saturated porous medium at large Rayleigh number or Peclet number", J. Fluid Mech., Vol. 15, pp. 527-544.

Yamamoto, K., and Iwamura, N., 1976, "Flow with convective acceleration through a porous medium", J. Engng. Maths., Vol. 10, pp. 41-54.

Yamamoto, K., and Yoshida, Z., 1974, "Flow through a porous wall with convective acceleration", J. Phys. Soc. Japan, Vol. 37, pp. 774-779.

Yih, C.S., 1965, Dynamics of Nonhomogeneous Fluids, Macmillan Co., New York.

## CHAPTER II

# NATURAL CONVECTION ABOUT A SEMI INFINITE VERTICAL FLAT PLATE IN A POROUS MEDIUM

### 2.1 INTRODUCTION

The study of natural convection adjacent to heated vertical surfaces embedded in a fluid saturated porous medium has been the subject of several recent investigations. The introduction of boundary layer approximation in porous medium literature intensified the research efforts on analytical studies of convective heat transfer about heated surfaces. Within the framework of boundary layer approximation similar to those invoked by Wooding (1963) and McNabb (1965). Cheng and Minkowycz (1977) obtained the analytical expression for boundary layer thickness and heat transfer coefficients to study convective heat transfer about an isothermal dike intruded in an aquifer. Johnson and Cheng (1978) analyzed free convection boundary layers in porous medium adjacent to flat plates including unsteady cases and thermal stratification. A comprehensive review of the early literature has been presented by Cheng (1978). The earlier works rely heavily on Darcy's law. Plumb and Huenefeld (1981) used the Forchheimer extended Darcy model and Hsu and Cheng (1985) used Brinkman model to study the problem. With few exceptions, most of the earlier theoretical studies are devoted to the problem of finding similarity solutions for steady free convection about the vertical

surfaces. In all these analysis power form variations of wall temperature distribution are assumed. A numerical solution of the problem has been obtained by Na and Pop (1983).

The objective of the present analysis is to predict the steady natural convection heat transfer from an impermeable vertical surface in a saturated porous medium subject to a prescribed constant wall temperature or the wall temperature as a function of position from the leading edge. The generalized momentum equation in which the convection and viscous terms are taken into account has been considered. Several studies have been made on the basis of this generalized momentum equation (Singh et al. 1986, Raptis et al. 1987 and Raptis and Takhar 1987 ). The method of solution, applied here, is close to that used by Hornbeck (1961), who has developed a numerical marching technique based on highly implicit finite difference method with variable mesh size. Thus, the numerical solution of the boundary layer equations are obtained to the required accuracy.

## 2.2 BASIC EQUATIONS AND BOUNDARY CONDITIONS FOR CONSTANT WALL TEMPERATURE

A two-dimensional steady flow through a fluid saturated porous medium occupying a semi-infinite region of the space bounded by a vertical impermeable surface is considered. The X-axis is taken along the surface and the Y-axis is normal to the surface. The boundary layer and Boussinesq approximations are assumed and the properties of the fluid and the isotropic

porous matrix are constant. The governing equations with inertia and viscous terms are,

$$\frac{\partial U}{\partial X} + \frac{\partial V}{\partial Y} = 0, \quad (2.1)$$

$$U \frac{\partial U}{\partial X} + V \frac{\partial V}{\partial Y} = \nu \frac{\partial^2 U}{\partial Y^2} + g\beta (T - T_\infty) - \frac{\nu U}{K}, \quad (2.2)$$

$$U \frac{\partial T}{\partial X} + V \frac{\partial T}{\partial Y} = \alpha \frac{\partial^2 T}{\partial Y^2}, \quad (2.3)$$

where,  $U$  and  $V$  are the velocity components in the  $X$  and  $Y$ -directions respectively,  $T$  is the temperature,  $\nu$  is the kinematic viscosity,  $g$  is the acceleration due to gravity,  $\beta$  is the coefficient of volume expansion of the fluid,  $\alpha$  is the thermal diffusivity and  $K$  is the permeability of the porous medium. The subscript  $\infty$  denotes the condition near the edge of the boundary layer. The boundary conditions are,

$$\begin{aligned} X = 0 : U = 0, \quad T = T_\infty, \\ Y = 0 : U = 0, \quad V = 0, \quad T = T_w, \\ Y \rightarrow \infty : U \rightarrow 0, \quad T \rightarrow T_\infty. \end{aligned} \quad (2.4)$$

The equations (2.1) - (2.3) and the boundary conditions (2.4) are put in dimensionless form by using the following transformations,

$$\begin{aligned} x &= \frac{\nu^2 X}{g\beta (T_w - T_\infty) L^4} = \frac{X}{L Gr}, \quad y = \frac{Y}{L}, \\ u &= \frac{\nu U}{g\beta (T_w - T_\infty) L^2} = \frac{UL}{\nu Gr}, \quad v = \frac{VL}{\nu}, \\ \theta &= \frac{T - T_\infty}{T_w - T_\infty}, \quad Da = \frac{K}{L^2}, \quad Gr = \frac{g\beta (T_w - T_\infty) L^3}{\nu^2}, \quad Pr = \frac{\nu}{\alpha}. \end{aligned} \quad (2.5)$$

where,  $L$  is the characteristic length in the  $X$ -direction,  $Da$  is the Darcy number,  $Gr$  is the Grashof number and  $Pr$  is the Prandtl number. In terms of the new variables, basic equations become,

$$\frac{\partial u}{\partial x} + \frac{\partial v}{\partial y} = 0, \quad (2.6)$$

$$u \frac{\partial u}{\partial x} + v \frac{\partial u}{\partial y} = \frac{\partial^2 u}{\partial y^2} + \theta - \frac{u}{Da}, \quad (2.7)$$

$$u \frac{\partial \theta}{\partial x} + v \frac{\partial \theta}{\partial y} = \frac{1}{Pr} \frac{\partial^2 \theta}{\partial y^2}. \quad (2.8)$$

The boundary conditions are rewritten in the form,

$$\begin{aligned} x = 0 : u = 0, \theta = 0, \\ y = 0 : u = 0, v = 0, \theta = 1, \\ y \rightarrow \infty : u = 0, \theta = 0. \end{aligned} \quad (2.9)$$

### 2.3 SOLUTIONS BY FINITE DIFFERENCE METHOD

Equations (2.6) - (2.8) are now written in finite difference form by superposing a two-dimensional rectangular mesh on the flow field. Step sizes  $\Delta x$  and  $\Delta y$  are taken respectively in the  $x$  and  $y$  directions. Subscripts  $(i, j)$  indicate positions in the  $(x, y)$  directions respectively so that  $i = 0$  corresponds to  $x = 0$  and  $j = 0$  to  $y = 0$ ; a positive change  $\Delta x$  in the  $x$  coordinate increases  $i$  by 1 and a positive change  $\Delta y$  increases  $j$  by 1. Let the plate be represented by  $j = 0$  and the edge of the boundary layer by  $j = n+1$ . The finite difference equations are written as (Hornbeck 1961),

$$\frac{u_{i+1,j+1} - u_{i,j+1}}{\Delta x} + \frac{v_{i+1,j+1} - v_{i+1,j}}{\Delta y} = 0, \quad (2.10)$$

$$\begin{aligned}
u_{i+1,j} &= \frac{u_{i+1,j} - u_{i,j}}{\Delta x} + v_{i+1,j} \frac{u_{i+1,j+1} - u_{i+1,j-1}}{2(\Delta y)} \\
&= \frac{u_{i+1,j-1} - 2u_{i+1,j} + u_{i+1,j+1}}{(\Delta y)^2} + \theta_{i+1,j} - \frac{u_{i+1,j}}{Da},
\end{aligned} \quad (2.11)$$

$$\begin{aligned}
u_{i+1,j} &= \frac{\theta_{i+1,j} - \theta_{i,j}}{\Delta x} + v_{i+1,j} \frac{\theta_{i+1,j+1} - \theta_{i+1,j-1}}{2(\Delta y)} \\
&= \frac{1}{Pr} \frac{\theta_{i+1,j-1} - 2\theta_{i+1,j} + \theta_{i+1,j+1}}{(\Delta y)^2} + \theta_{i+1,j} - \frac{u_{i+1,j}}{Da}.
\end{aligned} \quad (2.12)$$

The difference form stated here is highly implicit, that is, not only all  $y$ -derivatives are evaluated at  $(i+1)$  but the coefficients of non-linear convective terms are also evaluated at  $(i+1)$ . The discretization is of second order accuracy in  $\Delta y$  for  $u$  and  $\theta$  and is suitable for the marching procedure along the  $x$ -direction in conformity with the parabolic nature of equations (2.7) and (2.8). An iterative scheme is required to solve the non-linear difference equations. The difference equations (2.10) - (2.12) are rewritten in the linearized form as,

$$\frac{u_{i+1,j+1}^{k+1} - u_{i,j+1}^{k+1}}{\Delta x} + \frac{v_{i+1,j+1}^{k+1} - v_{i+1,j}^{k+1}}{\Delta y} = 0, \quad (2.13)$$

$$\begin{aligned}
u_{i+1,j}^k &= \frac{u_{i+1,j}^{k+1} - u_{i,j}^{k+1}}{\Delta x} + v_{i+1,j}^k \frac{u_{i+1,j+1}^{k+1} - u_{i+1,j-1}^{k+1}}{2(\Delta y)} \\
&= \frac{u_{i+1,j-1}^{k+1} - 2u_{i+1,j}^{k+1} + u_{i+1,j+1}^{k+1}}{(\Delta y)^2} + \theta_{i+1,j}^k - \frac{u_{i+1,j}^{k+1}}{Da},
\end{aligned} \quad (2.14)$$

$$\begin{aligned}
u_{i+1,j}^{k+1} \frac{\theta_{i+1,j}^{k+1} - \theta_{i,j}^{k+1}}{\Delta x} + v_{i+1,j}^{k+1} \frac{\theta_{i+1,j+1}^{k+1} - \theta_{i+1,j-1}^{k+1}}{2(\Delta y)} \\
= \frac{1}{Pr} \frac{\theta_{i+1,j-1}^{k+1} - 2\theta_{i+1,j}^{k+1} + \theta_{i+1,j+1}^{k+1}}{(\Delta y)^2} \quad (2.15)
\end{aligned}$$

The superscripts  $k$  and  $(k+1)$  indicate values obtained on  $k$ th and  $(k+1)$ th iteration respectively.

Equation (2.14) is, finally, written in the simplified form,

$$\begin{aligned}
\left[ -\frac{1}{(\Delta y)^2} - \frac{v_{i+1,j}^k}{2(\Delta y)} \right] u_{i+1,j-1}^{k+1} \\
+ \left[ \frac{2}{(\Delta y)^2} + \frac{u_{i+1,j}^k}{\Delta x} + \frac{1}{Da} \right] u_{i+1,j}^{k+1} \\
+ \left[ -\frac{1}{(\Delta y)^2} + \frac{v_{i+1,j}^k}{2(\Delta y)} \right] u_{i+1,j+1}^{k+1} \\
= \frac{u_{i+1,j}^k}{\Delta x} u_{i,j} + \theta_{i+1,j}^k \quad (2.16)
\end{aligned}$$

Similarly equations (2.13) and (2.15) are rewritten in more useful forms as,

$$v_{i+1,j+1}^{k+1} = v_{i+1,j}^{k+1} - \frac{\Delta y}{\Delta x} (u_{i+1,j+1}^{k+1} - u_{i,j+1}), \quad (2.17)$$



$$\begin{aligned}
& \left[ -\frac{1}{Pr(\Delta y)^2} - \frac{v_{i+1,j}^{k+1}}{2(\Delta y)} \right] \theta_{i+1,j-1}^{k+1} \\
& + \left[ -\frac{2}{Pr(\Delta y)^2} + \frac{u_{i+1,j}^{k+1}}{\Delta x} \right] \theta_{i+1,j}^{k+1} \\
& + \left[ -\frac{1}{Pr(\Delta y)^2} + \frac{v_{i+1,j}^{k+1}}{2(\Delta y)} \right] \theta_{i+1,j+1}^{k+1} \\
& = \frac{u_{i+1,j}^{k+1}}{\Delta x} \theta_{i,j}^{k+1}. \quad (2.18)
\end{aligned}$$

The linearized difference form (2.16) of the momentum equation written for  $j = 1(1)n$  leads to a set of  $n$  linear equations for  $n$  unknown values of  $u$  at the  $x$ -location  $i+1$ . This linearized tridiagonal set is solved by Gaussian elimination method and then the solution of (2.17) for  $v$  at the  $x$ -location  $i+1$  is obtained in a stepwise manner working outward from the plate. Once values of  $u$  and  $v$  have been determined at  $i+1$ , the discretized energy equation (2.18) written for  $j = 1(1)n$  leads to a tridiagonal set of  $n$  linear equations that can be easily solved for the  $n$  unknown values of  $\theta$  at the location  $i+1$ . Equations (2.16) - (2.18) are solved iteratively until the values obtained on a given iteration agree with those obtained on the previous iteration within some predetermined accuracy. For the convergence of the iterative process underrelaxation is employed. The quantities  $u_{i+1,j}^k$ ,  $v_{i+1,j}^k$  and  $\theta_{i+1,j}^k$  appearing in the difference equations (2.16) - (2.18) are modified after each iteration as follows.

$$\begin{aligned}
 u_{i+1,j}^k &\leftarrow u_{i+1,j}^k + \lambda (u_{i+1,j}^{k+1} - u_{i+1,j}^k) , \\
 v_{i+1,j}^k &\leftarrow v_{i+1,j}^k + \lambda (v_{i+1,j}^{k+1} - v_{i+1,j}^k) , \\
 \theta_{i+1,j}^k &\leftarrow \theta_{i+1,j}^k + \lambda (\theta_{i+1,j}^{k+1} - \theta_{i+1,j}^k) ,
 \end{aligned} \tag{2.19}$$

where,  $\lambda$  is a relaxation parameter and values of  $\lambda$  in the range  $0 \leq \lambda < 1$  correspond to underrelaxation. In the present calculation underrelaxation factor is found to be 0.6. This completes the solution at the x-location  $i+1$ . A repetition of the above steps allows to march in upward direction along the wall.

The computer program takes care of the fact that the velocity and temperature profiles vary rapidly near the wall and hence a fine mesh is required near the wall. A relatively coarse mesh has been used in the regions away from the wall. If  $\Delta y$  is uniform across the boundary layer thickness, the number of simultaneous equations increases excessively. Solution of such large number of equations not only requires excessive computer time but also involves large round-off error. Non-uniform  $\Delta y$  therefore has been used. This requires the technique of combining large and small mesh sizes.

If the mesh size is to be changed from  $\Delta y_1$  to a larger value  $\Delta y_2$  at the y location  $j = p$  as shown in Figure 1, the central difference form for the first or second order derivative at  $j = p$  requires the values of the dependent variable at a fictitious point  $j = q$  which is  $\Delta y_1$  above the point  $j = p$ . A dependent variable  $Q_{i+1,q}$  at the point  $j = q$  is determined by

passing a parabola through the values  $Q_{i+1,p-1}$ ,  $Q_{i+1,p}$  and  $Q_{i+1,p+1}$  and then interpolating for  $Q_{i+1,q}$  yielding,

$$Q_{i+1,q} = \frac{\phi-1}{\phi+1} Q_{i+1,p-1} + 2(1-\phi) Q_{i+1,p} + \frac{2\phi^2}{1+\phi} Q_{i+1,p+1} \quad (2.20)$$

$$\text{where, } \phi = \frac{\Delta y_1}{\Delta y_2}.$$

The derivatives at  $j = p$  are approximated as,

$$\left. \frac{\partial Q}{\partial y} \right|_{j=p} = \frac{Q_{i+1,q} - Q_{i+1,p-1}}{2(\Delta y_1)} \quad (2.21)$$

$$\left. \frac{\partial^2 Q}{\partial y^2} \right|_{j=p} = \frac{Q_{i+1,q} - 2Q_{i+1,p} + Q_{i+1,p-1}}{(\Delta y_1)^2} \quad (2.22)$$

where,  $Q_{i+1,q}$  is given by equation (2.20).

At the points of step size change, equations (2.21) and (2.22) are used in the momentum and energy equations and at these points equations are rewritten, as they involve central differences in transverse direction. This modification is not required in the continuity equation because only first order forward differences in the transverse direction are involved. It is ensured that the proper mesh size is used in the appropriate region.

The local Nusselt number in the non-dimensional form is given by,

$$Nu_x = - \left. \frac{\partial \theta}{\partial y} \right|_{y=0} \quad (2.23)$$

This has been calculated numerically by the following difference formula,

$$Nu_x = \left[ \frac{3\theta_{i+1,0} - 4\theta_{i+1,1} + \theta_{i+1,2}}{2(\Delta y)} \right] . \quad (2.24)$$

## 2.4 FREE CONVECTION WITH WALL TEMPERATURE A FUNCTION OF POSITION

In section 2.2, the problem has been formulated for the case of constant wall temperature. The problem must be reformulated if the wall temperature is a function of position. The governing differential equations remain the same as (2.1) - (2.3). The boundary conditions in this case are,

$$\begin{aligned} X = 0 : U = 0, \quad T = T_\infty, \\ Y = 0 : U = 0, \quad V = 0, \quad T = T_w(X), \\ Y \rightarrow \infty : U \rightarrow 0, \quad T \rightarrow T_\infty. \end{aligned} \quad (2.25)$$

If  $T_{w0}$  is the wall temperature at  $X = 0$ , a new set of dimensionless variables are defined as follows,

$$\begin{aligned} x = \frac{\nu^2 X}{g\beta (T_{w0} - T_\infty) L^4} = \frac{X}{LGr}, \quad y = \frac{Y}{L}, \\ u = \frac{\nu U}{g\beta (T_{w0} - T_\infty) L^2} = \frac{UL}{\nu Gr}, \quad v = \frac{VL}{\nu}, \quad \theta = \frac{T - T_\infty}{T_{w0} - T_\infty}, \quad (2.26) \\ Pr = \frac{\nu}{\alpha}, \quad Gr = \frac{g\beta (T_{w0} - T_\infty) L^3}{\nu^2}, \quad Da = \frac{K}{L^2}. \end{aligned}$$

Introducing the dimensionless variables (2.26), the governing partial differential equations and the corresponding boundary conditions take the following form,

$$\frac{\partial u}{\partial x} + \frac{\partial v}{\partial y} = 0 ,$$

$$u \frac{\partial u}{\partial x} + v \frac{\partial u}{\partial y} = \frac{\partial^2 u}{\partial y^2} + \theta - \frac{u}{Da} ,$$

$$u \frac{\partial \theta}{\partial x} + v \frac{\partial \theta}{\partial y} = \frac{1}{Pr} \frac{\partial^2 \theta}{\partial y^2} ,$$

$$x = 0 : u = 0, \quad \theta = 0 ,$$

$$y = 0 : u = 0, \quad v = 0, \quad \theta = \theta_w(x) = \frac{T_w(x) - T_\infty}{T_{w0} - T_\infty} , \quad (2.27)$$

$$y \rightarrow \infty : u = 0, \quad \theta = 0 .$$

It is to be noted that the governing partial differential equations in the dimensionless form remain the same as (2.6) - (2.8) in the case of constant wall temperature.  $\theta_w(x)$  may be any function of  $x$  relevant to practical and engineering applications. For the sake of convenience, in the present investigation,  $\theta_w(x)$  is defined as,

$$\theta_w(x) = x^n ,$$

where,  $n$  is a real number. The fundamental steps for solving the differential equations are similar to those specified in Section 2.3.

## 2.5 RESULTS AND DISCUSSION

No quantitative statement can be made about the choice of step sizes. In the regions of more rapidly changing velocity and temperature profiles a fine mesh size is required. Since implicit formulation is used there is no restriction on the selection of step sizes  $\Delta x$  from the point of view of stability. The computations are carried out on DEC-1090 computer for  $\Delta x = 0.02$  and variable mesh size employed in  $y$ -direction are as follows,

$\Delta y = 0.02$  for first 50 steps,

$\Delta y = 0.05$  for next 130 steps,

$\Delta y = 0.1$  for next 5 steps.

These step sizes have been finally selected by approximating the thickness of the boundary layer formed which corresponds to 8.0 in the present calculations. The underrelaxation factor is chosen to be 0.6. Different step sizes and underrelaxation factors were used and the above mentioned values were found to generate the best results with minimum CPU time.

All the values of  $v$  are found to be negative which indicate that the horizontal velocity component is always directed towards the wall. The vertical velocity component  $u$  reaches a maximum a little way out from the wall and then decreases. The temperature  $\theta$  decreases monotonically away from the wall.

In Figure 2 the vertical velocity field is plotted against  $y$  when the wall temperature is constant. The value of Prandtl number  $Pr$  is taken as 0.73 and that of  $x$  as 0.2, the curves are

plotted for different values of  $Da$ . It is observed that  $u$ -velocity increases significantly as the value of  $Da$  increases.

The value of temperature at a point increases as the Darcy number  $Da$  decreases. However, this effect has not been shown in a pictorial diagram.

The range of  $n$  for which the problem is physically consistent is considered. To this end the method given by Cheng and Minkowycz (1977) is followed. Since the wall temperature begins to deviate from  $T_{\infty}$  at  $x = 0$  and convective flow must start at this point, horizontal velocity and boundary layer thickness must therefore increase or at least remain constant with  $x$ . This implies that the exponent of  $x$  must be greater than or equal to zero, which results in the limit  $0 \leq n \leq 1$ .

Figure 3 shows the variation of  $u$  - velocity with  $y$  for different values of  $n$ , which is the exponent of wall temperature. The values of  $n$  are chosen to be 0.0, 0.25, 0.5 and 0.75. The velocity at any point is found to be decreasing with the increase in  $n$ .

Figure 4 shows the temperature profiles for different values of  $n$ . These curves are plotted for  $n = 0.0, 0.25, 0.5$  and 0.75 and for fixed values of  $x$ ,  $Pr$  and  $Da$ . The value of temperature at a point decreases with  $n$ . The value  $n = 0.0$  corresponds to the case of constant wall temperature.

It is customary that when a numerical method is applied to a problem, the results so obtained are compared with the available numerical solution or exact solutions to determine the error involved in the results. Since non-similar results are

not available in the existing literature for the problem considered in this investigation, the numerical solutions are obtained by setting  $Da \rightarrow \infty$  and  $n = 0.0$ . In this case the governing equations correspond to free convection flow along vertical wall of constant temperature in the absence of porous matrix. The results of local heat transfer calculated for  $Pr = 0.733$  are compared with those given by Schlichting (1968) and the agreement is seen to be very good. It is found that the local Nusselt number for  $x = 0.5$  and  $1.0$  are  $0.4359$  and  $0.3634$  by the present method while it is  $0.4272$  and  $0.3592$  respectively as reported by Schlichting (1968).



## REFERENCES

- Cheng, P., 1978, "Heat transfer in geothermal systems", Adv. Heat Transfer, Vol. 14, pp. 1-105.
- Cheng, P., and Minkowycz, W.J., 1977, "Free convection about a vertical flat plate embedded in a porous medium with application of heat transfer from a dike", J. geophys. Res., Vol. 82, pp. 2040-2044.
- Hornbeck, R.W., 1961, "The Entry Problem in Pipes with Porous Walls", Ph.D. Thesis, Carnegie Inst. Tech.
- Hsu, C.T., and Cheng, P., 1985, "The Brinkman model for natural convection about a semi-infinite vertical flat plate in a porous medium", Int. J. Heat Mass Transfer, Vol. 28, pp. 683-697.
- Johnson, C.H., and Cheng, P., 1978, "Possible similarity solutions for free convection boundary layers adjacent to flat plates in porous media", Int. J. Heat Mass transfer, Vol. 21, pp. 709-718.
- McNabb, A., 1965, "On convection in a porous medium", Proceedings of 2nd Australian Conference on Hydraulics and Fluid Mechanics", University of Auckland, Auckland, New Zealand, pp. C 161-C 171.
- Na, T.Y., and Pop, I., 1983, "Free convection flow past a vertical flat plate embedded in a saturated porous medium", Int. J. Engng. Sci., Vol. 21, pp. 517-526.
- Plumb, O.A., and Huenefeld, J.C., 1981, "Non-Darcy natural convection from heated surfaces in saturated porous media", Int. J. Heat Mass Transfer, Vol. 24, pp. 765-768.
- Raptis, A., Singh, A.K., and Rai, K.D., 1987, "Finite difference analysis of unsteady free convective flow through a porous medium adjacent to a semi-infinite vertical plate", Mech. Res. Comm., Vol. 14, pp. 9-16.
- Raptis, A., and Takhar, H.S., 1987, "Flow through a porous medium", Mech. Res. Comm., Vol. 14, pp. 327-329.
- Schlichting, H., 1968, "Boundary Layer Theory", McGraw Hill, New York.
- Singh, P., Misra, J.K., and Narayan, K.A., 1986, "A mathematical analysis of unsteady flow and heat transfer in porous medium", Int. J. Engng. Sci., Vol. 24, pp. 277-287.
- Wooding, R.A., 1963, "Convection in a saturated porous medium at large Rayleigh number or Peclet number", J. fluid Mech., Vol. 15, pp. 527-544.

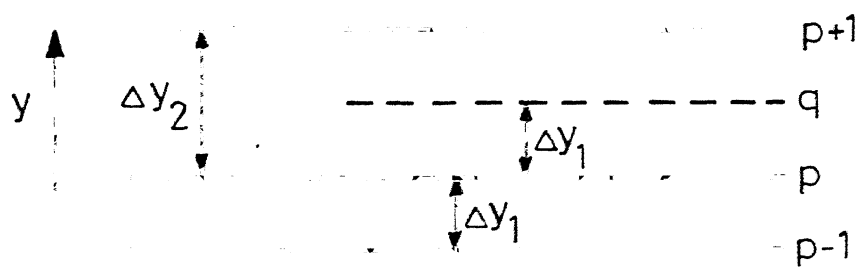


Figure 1 Mesh size change

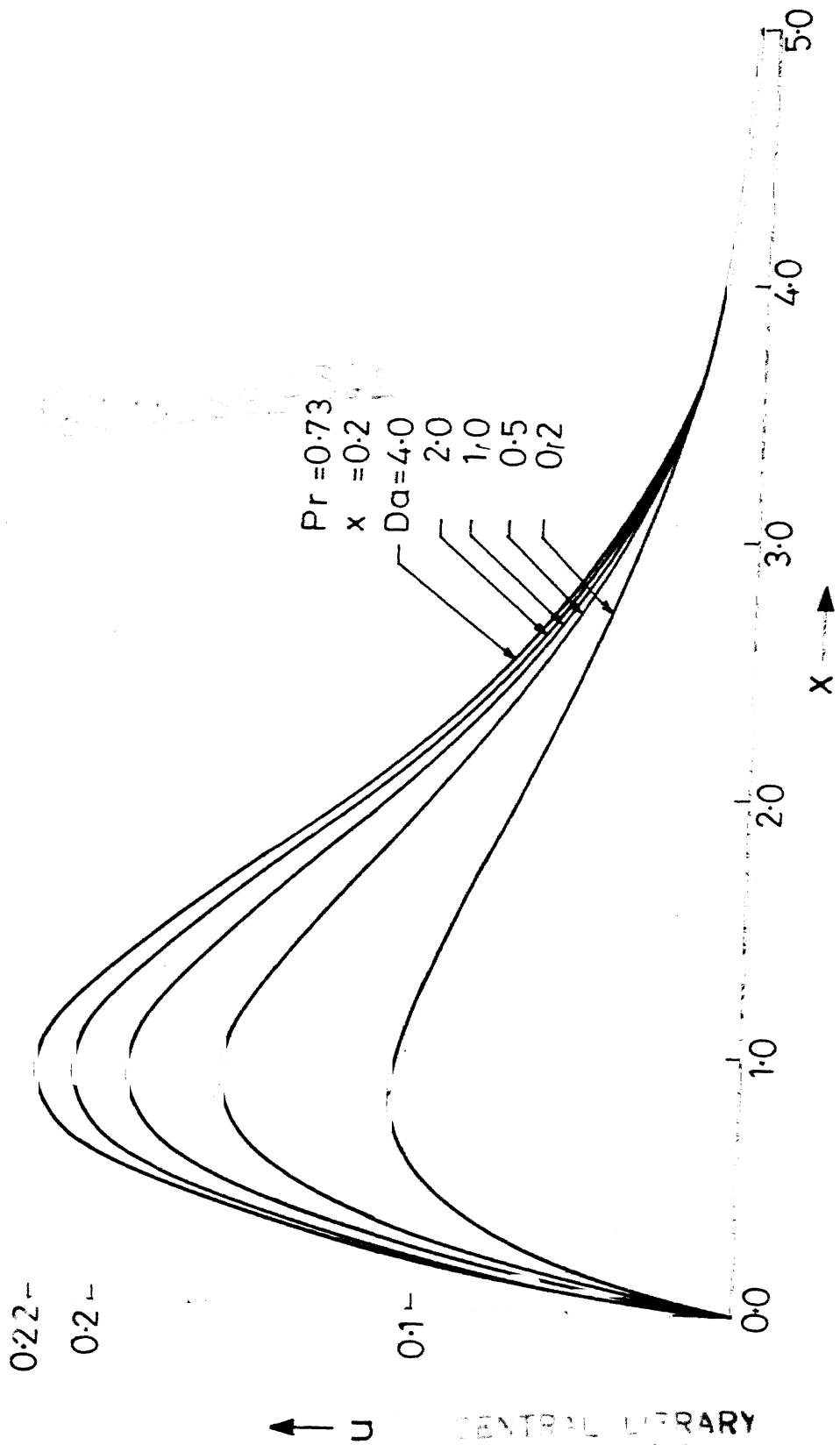
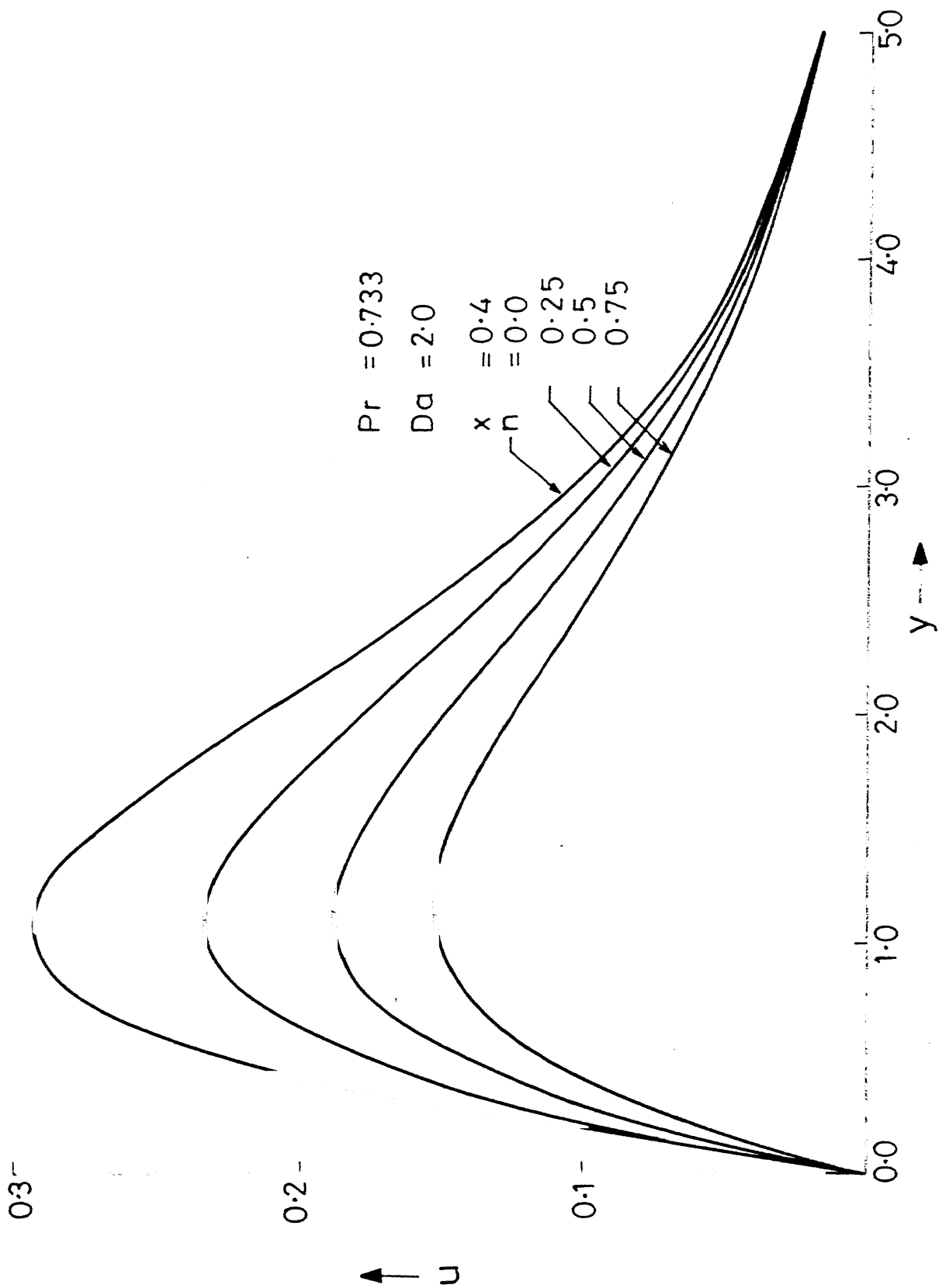


Figure 2 Horizontal velocity profile



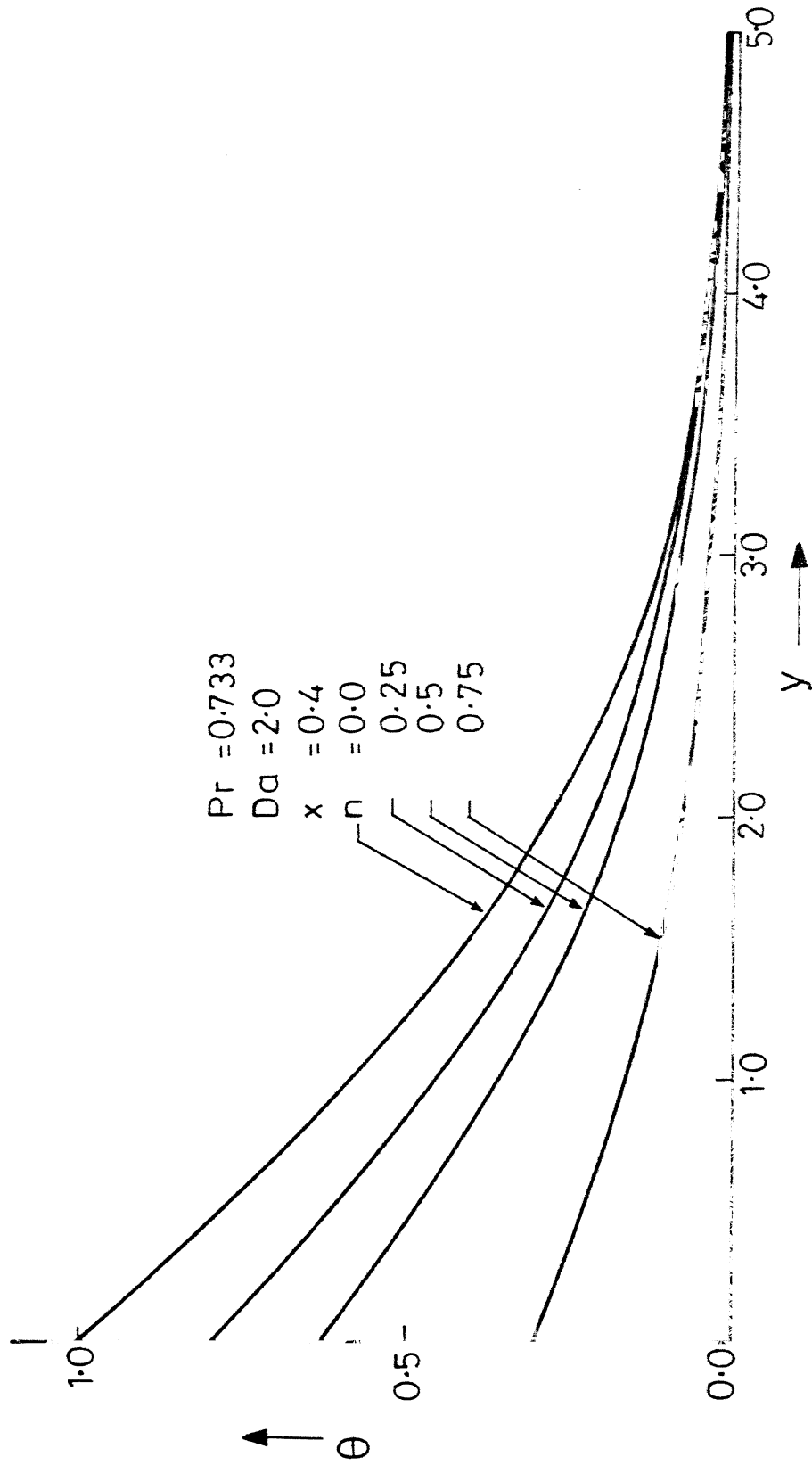


Figure 4 Temperature profile

## CHAPTER III

### NATURAL CONVECTION IN A RECTANGULAR POROUS ENCLOSURE WITH HEATED WALLS

#### 3.1 INTRODUCTION

Natural convection in fluid saturated porous enclosures has received considerable attention for its application in a variety of engineering problems. A number of analytical, numerical and experimental studies have been performed for natural convection in vertical rectangular porous enclosures with isothermal vertical walls and adiabatic horizontal walls. The assumption of insulated horizontal walls may be of fundamental interest but there are some physical situations in which vertical heat transfer through horizontal boundaries, is not negligible. Investigations that focus on natural convection in rectangular enclosures in which the side walls, top wall and the bottom wall are at constant but different temperatures, are few in number. This condition permits heat transfer across all the boundaries, which results in considerable variation of the flow field. Examples of such situations include geothermal applications and coal mine fires in the goaf areas. Christopher (1986) has analyzed transient natural convection for the case when all the four walls are isothermal.

Furthermore, in most of these studies it is assumed that Darcy's law is applicable. Analytical studies by Weber (1975),

Walker and Homsy (1978), Bejan (1979) and Simpkins and Blythe (1980) and numerical studies by Holst and Aziz (1972), Hickox and Gartling (1981), Shiralkar et al. (1983), Prasad and Kulacki (1984) and Christopher (1986) are based on Darcy's law. Chan et al. (1970), Tong and Subramanian (1985) and Tong and Orangi (1986) used the Brinkman-extended Darcy model, which included the viscous force terms in their analysis and the no-slip boundary conditions were satisfied. Poulikakos and Bejan (1985) and Prasad and Tuntomo (1987) have analyzed the inertia effects by using Forchheimer-extended Darcy equation of motion and the significance of Forchheimer's velocity square term are examined. Recently, Lauriat and Prasad (1987) have performed a numerical study for a generalized momentum equation and have included viscous force terms and inertial force terms simultaneously. All the above investigations except the one by Christopher (1986) describe convective heat transfer in rectangular porous enclosures with two adiabatic walls.

The present investigation is concerned with the steady, two dimensional buoyancy-induced convection in a vertical porous rectangular enclosure with specified temperature on all the four surfaces. The boundaries are impermeable and the results are based on inclusion of boundary and inertia effects. The pressure field appearing in the momentum equation is eliminated and the stream function vorticity equation together with the energy equation is solved by the upwind finite difference method. This method leads to a simple and straight forward analysis and possesses a highly desirable property of numerical

stability. The stream function, vorticity and temperature fields and the local and average Nusselt numbers are obtained for four dimensionless parameters, namely, the Rayleigh-Darcy number, Darcy number, aspect ratio and the top wall temperature.

### 3.2 PROBLEM STATEMENT

The physical system shown in Figure 1 is a two dimensional fluid saturated porous medium enclosed by four isothermal and impermeable walls. The two vertical side walls are maintained at the same temperature  $T_s$  and the top and bottom horizontal walls are kept at two different temperatures  $T_t$  and  $T_b$  respectively. Subject to the Boussinesq approximation, the continuity, momentum and energy equations for the flow of a Newtonian fluid are,

$$\frac{\partial U}{\partial X} + \frac{\partial V}{\partial Y} = 0, \quad (3.1)$$

$$\rho(U \frac{\partial U}{\partial X} + V \frac{\partial U}{\partial Y}) = - \frac{\partial P}{\partial X} + \mu(\frac{\partial^2 U}{\partial X^2} + \frac{\partial^2 U}{\partial Y^2}) - \frac{\mu U}{K}, \quad (3.2)$$

$$\rho(U \frac{\partial V}{\partial X} + V \frac{\partial V}{\partial Y}) = - \frac{\partial P}{\partial Y} + \mu(\frac{\partial^2 V}{\partial X^2} + \frac{\partial^2 V}{\partial Y^2}) - \frac{\mu V}{K} + \rho g \beta (T - T_s), \quad (3.3)$$

$$U \frac{\partial T}{\partial X} + V \frac{\partial T}{\partial Y} = \alpha (\frac{\partial^2 T}{\partial X^2} + \frac{\partial^2 T}{\partial Y^2}). \quad (3.4)$$

The boundary conditions for the problem are,

$$\begin{aligned} X = 0: & U = 0, V = 0, T = T_s, \\ X = A: & U = 0, V = 0, T = T_s, \\ Y = 0: & U = 0, V = 0, T = T_b, \\ Y = B: & U = 0, V = 0, T = T_t. \end{aligned} \quad (3.5)$$



where,  $U$  and  $V$  are the horizontal and vertical velocity components in the  $X$  and  $Y$  directions respectively,  $P$  is the pressure,  $T$  the temperature,  $\rho$  is the density of the fluid,  $\mu$  the viscosity,  $\alpha$  is the thermal diffusivity,  $\beta$  the coefficient of thermal expansion,  $g$  is the acceleration due to gravity,  $K$  is the permeability of the porous medium and  $A$  and  $B$  are respectively the width and height of the enclosure.

The problem may now be restated in the dimensionless form. The dimensionless variables chosen are ,

$$\begin{aligned}
 x &= \frac{X}{A}, \quad y = \frac{Y}{A}, \quad u = \frac{UA}{\alpha}, \quad v = \frac{VA}{\alpha}, \quad p = \frac{PA^2}{\rho\alpha^2}, \quad \theta = \frac{T - T_s}{T_b - T_s}, \\
 \theta_t &= \frac{T_t - T_s}{T_b - T_s}, \quad Pr = \frac{\mu}{\rho\alpha}, \quad Da = \frac{K}{A^2}, \quad As = \frac{B}{A}, \\
 Ra^* &= \frac{\rho g \beta (T_b - T_s) KA}{\mu \alpha}, \quad (3.6)
 \end{aligned}$$

where,  $Da$  and  $Ra^*$  are Darcy number and Rayleigh-Darcy number respectively,  $Pr$  is the Prandtl number and  $As$  is the aspect ratio. In terms of these dimensionless variables, the equations (3.1) - (3.4) may be rewritten as,

$$\frac{\partial u}{\partial x} + \frac{\partial v}{\partial y} = 0, \quad (3.7)$$

$$u \frac{\partial u}{\partial x} + v \frac{\partial u}{\partial y} = - \frac{\partial p}{\partial x} + Pr \left( \frac{\partial^2 u}{\partial x^2} + \frac{\partial^2 u}{\partial y^2} \right) - \frac{Pr}{Da} u, \quad (3.8)$$

$$u \frac{\partial v}{\partial x} + v \frac{\partial v}{\partial y} = - \frac{\partial p}{\partial y} + Pr \left( \frac{\partial^2 v}{\partial x^2} + \frac{\partial^2 v}{\partial y^2} \right) + \frac{Pr}{Da} (Ra^* \theta - v), \quad (3.9)$$

$$u \frac{\partial \theta}{\partial x} + v \frac{\partial \theta}{\partial y} = \frac{\partial^2 \theta}{\partial x^2} + \frac{\partial^2 \theta}{\partial y^2} . \quad (3.10)$$

subject to the boundary conditions,

$$\begin{aligned} x = 0 : u = 0, v = 0, \theta = 0 , \\ x = 1 : u = 0, v = 0, \theta = 0 , \\ y = 0 : u = 0, v = 0, \theta = 1 , \\ y = As : u = 0, v = 0, \theta = \theta_t . \end{aligned} \quad (3.11)$$

Since the pressure field is unknown, it is eliminated from the equations (3.8) and (3.9). Stream function  $\psi$  and vorticity  $\omega$  are defined as,

$$u = \frac{\partial \psi}{\partial y} , \quad v = - \frac{\partial \psi}{\partial x} \quad (3.12)$$

$$\text{and} \quad \omega = \frac{\partial u}{\partial y} - \frac{\partial v}{\partial x} . \quad (3.13)$$

The equation of continuity (3.7) is automatically satisfied by (3.12) and the vorticity can be written in terms of  $\psi$  as,

$$\omega = \frac{\partial^2 \psi}{\partial x^2} + \frac{\partial^2 \psi}{\partial y^2} . \quad (3.14)$$

The momentum equations (3.8) and (3.9) are transformed into the vorticity equation,

$$\frac{\partial \psi}{\partial y} \frac{\partial \omega}{\partial x} - \frac{\partial \psi}{\partial x} \frac{\partial \omega}{\partial y} = \text{Pr} \left( \frac{\partial^2 \omega}{\partial x^2} + \frac{\partial^2 \omega}{\partial y^2} \right) - \frac{\text{Pr}}{\text{Da}} \left( \omega + \text{Ra}^* \frac{\partial \theta}{\partial x} \right) . \quad (3.15)$$

The energy equation (3.10) now takes the form,

$$\frac{\partial \psi}{\partial y} \frac{\partial \theta}{\partial x} - \frac{\partial \psi}{\partial x} \frac{\partial \theta}{\partial y} = \frac{\partial^2 \theta}{\partial x^2} + \frac{\partial^2 \theta}{\partial y^2} . \quad (3.16)$$

The boundary conditions to be satisfied by  $\psi$  and  $\theta$  are,

$$\begin{aligned}
 x = 0 : \psi &= 0, \frac{\partial \psi}{\partial x} = 0, \theta = 0, \\
 x = 1 : \psi &= 0, \frac{\partial \psi}{\partial x} = 0, \theta = 0, \\
 y = 0 : \psi &= 0, \frac{\partial \psi}{\partial y} = 0, \theta = 1, \\
 y = As : \psi &= 0, \frac{\partial \psi}{\partial y} = 0, \theta = \theta_t.
 \end{aligned}
 \tag{3.17}$$

The advantage of stream function vorticity formulation is that instead of working with the continuity equation and two momentum equations only two second order equations are to be considered and the number of unknown variables is also reduced by one with the elimination of the pressure term. The principal difficulty in this formulation is that, in general, vorticity is unknown apriori along solid boundaries and hence is not useful in situations with moving boundaries, for example in solidification or melting problems for which velocity boundary conditions must be imposed on the moving boundary. However, the problem under consideration may easily be treated with this formulation and it appears to require less computational time than the velocity pressure formulation described in Chapter IV.

### 3.3 NUMERICAL PROCEDURE

The governing equations are coupled non-linear partial differential equations for which an iterative procedure of solution is natural. Finite difference equations are derived using upwind differences for convective terms and central differences for other terms. The upwind difference

approximation of the convective terms depends on the flow directions in which a derivative is replaced by a backward difference if the velocity in the concerned direction is positive and by a forward difference if that is negative. The resulting finite difference equation is only first order accurate but leads to a diagonally dominant matrix and to a numerically stable scheme independent of the step sizes. The governing equations (3.14) - (3.16) are approximated in the following difference forms,

$$\frac{\psi_{i-1,j} - 2\psi_{i,j} + \psi_{i+1,j}}{(\Delta x)^2} + \frac{\psi_{i,j-1} - 2\psi_{i,j} + \psi_{i,j+1}}{(\Delta y)^2} = \omega_{i,j}, \quad (3.18)$$

$$\begin{aligned} & \frac{|\Delta\psi_j|}{2\Delta y} \left( \frac{\omega_{i,j} - \omega_{i\pm 1,j}}{\Delta x} \right) + \frac{|\Delta\psi_i|}{2\Delta x} \left( \frac{\omega_{i,j} - \omega_{i,j\pm 1}}{\Delta y} \right) \\ &= \text{Pr} \left( \frac{\omega_{i-1,j} - 2\omega_{i,j} + \omega_{i+1,j}}{(\Delta x)^2} + \frac{\omega_{i,j-1} - 2\omega_{i,j} + \omega_{i,j+1}}{(\Delta y)^2} \right) \\ & \quad - \frac{\text{Pr}}{\text{Da}} \left( \omega_{i,j} + \text{Ra}^* \frac{\theta_{i+1,j} - \theta_{i-1,j}}{2\Delta x} \right), \end{aligned} \quad (3.19)$$

$$\begin{aligned} & \frac{|\Delta\psi_j|}{2\Delta y} \left( \frac{\theta_{i,j} - \theta_{i\pm 1,j}}{\Delta x} \right) + \frac{|\Delta\psi_i|}{2\Delta x} \left( \frac{\theta_{i,j} - \theta_{i,j\pm 1}}{\Delta y} \right) \\ &= \frac{\theta_{i-1,j} - 2\theta_{i,j} + \theta_{i+1,j}}{(\Delta x)^2} + \frac{\theta_{i,j-1} - 2\theta_{i,j} + \theta_{i,j+1}}{(\Delta y)^2}, \end{aligned} \quad (3.20)$$

where,  $\Delta\psi_i = \psi_{i+1,j} - \psi_{i-1,j}$ ,  $\Delta\psi_j = \psi_{i,j+1} - \psi_{i,j-1}$  and  $\Delta x$  and  $\Delta y$  are the mesh sizes in the  $x$  and  $y$  directions respectively. The subscripts  $i$  and  $j$  correspond to  $x$  and  $y$  directions.

The difference equations (3.18) - (3.20) are solved by line-by-line method presented by Patankar (1980). This method has the advantage of being simple and easy to apply, involving the solution of tridiagonal sets of equations along the lines parallel to  $x$  and  $y$ -axis alternately called horizontal and vertical sweeps. Starting from below, all the horizontal lines except those with prescribed boundary conditions are swept one by one during the horizontal sweep. For a fixed  $j$ , the unknown variables corresponding to the node points  $(i, j+1)$  and  $(i, j-1)$  are assumed to be known from an initial guess or previous iteration or the most recently available values. A tridiagonal system is set up for the unknowns corresponding to the nodes  $(i-1, j)$ ,  $(i, j)$  and  $(i+1, j)$  which is easily solved by tridiagonal algorithm. After the horizontal sweeps, vertical sweeps are performed starting from left to right in which the nodal variables at  $(i+1, j)$  and  $(i-1, j)$  are considered as known and a tridiagonal system is solved for the nodal values at  $(i, j-1)$ ,  $(i, j)$  and  $(i, j+1)$  for a fixed  $i$ . The process is repeated for several iterations till convergence at all grid points is obtained.

Assuming  $r_1 = \frac{2\Delta x}{\Delta y}$  and  $r_2 = \frac{2\Delta y}{\Delta x}$  equation (3.19) may be expressed in a tridiagonal form for horizontal and vertical sweeps as follows ,

## Horizontal Sweep

$$\begin{aligned}
& (-|\Delta\psi_j| - 2r_2Pr) \omega_{i-1,j} + (|\Delta\psi_i| + |\Delta\psi_j| + 4r_1Pr + 4r_2Pr \\
& \quad + 2 \Delta x \Delta y \frac{Pr}{Da}) \omega_{i,j} - 2r_2Pr \omega_{i+1,j} \\
& = 2r_1Pr \omega_{i,j-1} + (|\Delta\psi_i| + 2r_1Pr) \omega_{i,j+1} \\
& \quad - \Delta y \frac{Ra^*Pr}{Da} (\theta_{i+1,j} - \theta_{i-1,j}), \text{ for } \Delta\psi_j > 0 \text{ and } \Delta\psi_i > 0, \\
& (-|\Delta\psi_j| - 2r_2Pr) \omega_{i-1,j} + (|\Delta\psi_i| + |\Delta\psi_j| + 4r_1Pr + 4r_2Pr \\
& \quad + 2 \Delta x \Delta y \frac{Pr}{Da}) \omega_{i,j} - 2r_2Pr \omega_{i+1,j} \\
& = (|\Delta\psi_i| + 2r_1Pr) \omega_{i,j-1} + 2r_1Pr \omega_{i,j+1} \\
& \quad - \Delta y \frac{Ra^*Pr}{Da} (\theta_{i+1,j} - \theta_{i-1,j}), \text{ for } \Delta\psi_j > 0 \text{ and } \Delta\psi_i < 0, \\
& -2r_2Pr \omega_{i-1,j} + (|\Delta\psi_i| + |\Delta\psi_j| + 4r_1Pr + 4r_2Pr \\
& \quad + 2 \Delta x \Delta y \frac{Pr}{Da}) \omega_{i,j} + (-|\Delta\psi_j| - 2r_2Pr) \omega_{i+1,j} \\
& = 2r_1Pr \omega_{i,j-1} + (|\Delta\psi_i| + 2r_1Pr) \omega_{i,j+1} \\
& \quad - \Delta y \frac{Ra^*Pr}{Da} (\theta_{i+1,j} - \theta_{i-1,j}), \text{ for } \Delta\psi_j < 0 \text{ and } \Delta\psi_i > 0, \\
& \text{and} \\
& -2r_2Pr \omega_{i-1,j} + (|\Delta\psi_i| + |\Delta\psi_j| + 4r_1Pr + 4r_2Pr \\
& \quad + 2 \Delta x \Delta y \frac{Pr}{Da}) \omega_{i,j} + (-|\Delta\psi_j| - 2r_2Pr) \omega_{i+1,j} \\
& = (|\Delta\psi_i| + 2r_1Pr) \omega_{i,j-1} + 2r_1Pr \omega_{i,j+1} \\
& \quad - \Delta y \frac{Ra^*Pr}{Da} (\theta_{i+1,j} - \theta_{i-1,j}), \text{ for } \Delta\psi_j < 0 \text{ and } \Delta\psi_i < 0.
\end{aligned}$$

(3.21)

## Vertical Sweep

$$\begin{aligned}
& -2r_1 Pr \omega_{i,j-1} + (|\Delta\psi_i| + |\Delta\psi_j| + 4r_1 Pr + 4r_2 Pr \\
& \quad + 2 \Delta x \Delta y \frac{Pr}{Da}) \omega_{i,j} + (-|\Delta\psi_i| - 2r_1 Pr) \omega_{i,j+1} \\
& = (|\Delta\psi_j| + 2r_2 Pr) \omega_{i-1,j} + 2r_2 Pr \omega_{i+1,j} \\
& \quad - \Delta y \frac{Ra^*}{Da} Pr (\theta_{i+1,j} - \theta_{i-1,j}), \text{ for } \Delta\psi_j > 0 \text{ and } \Delta\psi_i > 0, \\
& (-|\Delta\psi_i| - 2r_1 Pr) \omega_{i,j-1} + (|\Delta\psi_i| + |\Delta\psi_j| + 4r_1 Pr + 4r_2 Pr \\
& \quad + 2 \Delta x \Delta y \frac{Pr}{Da}) \omega_{i,j} - 2r_1 Pr \omega_{i,j+1} \\
& = (|\Delta\psi_j| + 2r_2 Pr) \omega_{i-1,j} + 2r_2 Pr \omega_{i+1,j} \\
& \quad - \Delta y \frac{Ra^*}{Da} Pr (\theta_{i+1,j} - \theta_{i-1,j}), \text{ for } \Delta\psi_j > 0 \text{ and } \Delta\psi_i < 0, \\
& -2r_1 Pr \omega_{i,j-1} + (|\Delta\psi_i| + |\Delta\psi_j| + 4r_1 Pr + 4r_2 Pr \\
& \quad + 2 \Delta x \Delta y \frac{Pr}{Da}) \omega_{i,j} + (-|\Delta\psi_i| - 2r_1 Pr) \omega_{i,j+1} \\
& = 2r_2 Pr \omega_{i-1,j} + (|\Delta\psi_j| + 2r_2 Pr) \omega_{i+1,j} \\
& \quad - \Delta y \frac{Ra^*}{Da} Pr (\theta_{i+1,j} - \theta_{i-1,j}), \text{ for } \Delta\psi_j < 0 \text{ and } \Delta\psi_i > 0,
\end{aligned}$$

and

$$\begin{aligned}
& (-|\Delta\psi_i| - 2r_1 Pr) \omega_{i,j-1} + (|\Delta\psi_i| + |\Delta\psi_j| + 4r_1 Pr + 4r_2 Pr \\
& \quad + 2 \Delta x \Delta y \frac{Pr}{Da}) \omega_{i,j} - 2r_1 Pr \omega_{i,j+1} \\
& = (|\Delta\psi_j| + 2r_2 Pr) \omega_{i+1,j} + 2r_2 Pr \omega_{i-1,j} \\
& \quad - \Delta y \frac{Ra^*}{Da} Pr (\theta_{i+1,j} - \theta_{i-1,j}), \text{ for } \Delta\psi_j < 0 \text{ and } \Delta\psi_i < 0.
\end{aligned}$$

(3.22)

Coefficients on the left hand side and all the expressions on the right hand side in the equations (3.21) and (3.22) are evaluated from the previous iteration values of  $\Delta\psi_i$ ,  $\Delta\psi_j$ ,  $\omega_{i+1,j}$  and  $\omega_{i-1,j}$ . The boundary conditions for  $\omega$  are obtained using the no-slip condition at the right boundaries and the expression (3.14).

At  $x = 0$  :

$$\omega = \frac{\partial^2 \psi}{\partial x^2} , \quad \frac{\partial \psi}{\partial x} = 0 \quad \text{and} \quad \psi = 0 \quad (\text{no-slip}).$$

Applying central differences at a point  $(1,j)$ , one gets ,

$$\omega_{1,j} = \frac{\psi_{2,j} - 2\psi_{1,j} + \psi_{0,j}}{(\Delta x)^2} , \quad \frac{\psi_{2,j} - \psi_{0,j}}{2\Delta x} = 0 \quad \text{and} \quad \psi_{1,j} = 0 .$$

$$\text{Thus } \omega_{1,j} = \frac{2\psi_{2,j}}{(\Delta x)^2} , \quad \text{for all } j .$$

Similarly,

$$\text{at } x = 1 : \omega_{N+1,j} = \frac{2\psi_{N,j}}{(\Delta x)^2} , \quad \text{for all } j ,$$

$$\text{at } y = 0 : \omega_{i,1} = \frac{2\psi_{i,2}}{(\Delta y)^2} , \quad \text{for all } i \quad \text{and}$$

$$\text{at } y = As : \omega_{i,M+1} = \frac{2\psi_{i,M}}{(\Delta y)^2} , \quad \text{for all } i . \quad (3.23)$$

where, the number of grid points in  $x$  and  $y$  directions are  $N+1$  and  $M+1$  respectively.

In a similar fashion, the equation (3.20) is rewritten for horizontal and vertical sweeps as follows.



## Horizontal Sweep

$$\begin{aligned}
& (-|\Delta\psi_j| - 2r_2) \theta_{i-1,j} + (|\Delta\psi_i| + |\Delta\psi_j| + 4r_1 + 4r_2) \theta_{i,j} \\
& - 2r_2 \theta_{i+1,j} = 2r_1 \theta_{i,j-1} + (|\Delta\psi_i| + 2r_1) \theta_{i,j+1} , \\
& \text{for } \Delta\psi_j > 0 \text{ and } \Delta\psi_i > 0 ,
\end{aligned}$$

$$\begin{aligned}
& (-|\Delta\psi_j| - 2r_2) \theta_{i-1,j} + (|\Delta\psi_i| + |\Delta\psi_j| + 4r_1 + 4r_2) \theta_{i,j} \\
& - 2r_2 \theta_{i+1,j} = (|\Delta\psi_i| + 2r_1) \theta_{i,j-1} + 2r_1 \theta_{i,j+1} , \\
& \text{for } \Delta\psi_j > 0 \text{ and } \Delta\psi_i < 0 ,
\end{aligned}$$

$$\begin{aligned}
& - 2r_2 \theta_{i-1,j} + (|\Delta\psi_i| + |\Delta\psi_j| + 4r_1 + 4r_2) \theta_{i,j} \\
& + (-|\Delta\psi_j| - 2r_2) \theta_{i+1,j} \\
& = 2r_1 \theta_{i,j-1} + (|\Delta\psi_i| + 2r_1) \theta_{i,j+1} , \\
& \text{for } \Delta\psi_j < 0 \text{ and } \Delta\psi_i > 0 ,
\end{aligned}$$

and

$$\begin{aligned}
& - 2r_2 \theta_{i-1,j} + (|\Delta\psi_i| + |\Delta\psi_j| + 4r_1 + 4r_2) \theta_{i,j} \\
& + (-|\Delta\psi_j| - 2r_2) \theta_{i+1,j} \\
& = (|\Delta\psi_i| + 2r_1) \theta_{i,j-1} + 2r_1 \theta_{i,j+1} , \\
& \text{for } \Delta\psi_j < 0 \text{ and } \Delta\psi_i < 0 . \\
& (3.24)
\end{aligned}$$

### Vertical Sweep

$$\begin{aligned}
 & -2r_1 \theta_{i,j-1} + (|\Delta\psi_i| + |\Delta\psi_j| + 4r_1 + 4r_2) \theta_{i,j} \\
 & \quad + (-|\Delta\psi_i| - 2r_1) \theta_{i,j+1} \\
 & = (|\Delta\psi_j| + 2r_2) \theta_{i-1,j} + 2r_2 \theta_{i+1,j} \quad , \\
 & \quad \text{for } \Delta\psi_j > 0 \text{ and } \Delta\psi_i > 0.
 \end{aligned}$$

$$\begin{aligned}
 & (-|\Delta\psi_i| - 2r_1) \theta_{i,j-1} + (|\Delta\psi_i| + |\Delta\psi_j| + 4r_1 + 4r_2) \theta_{i,j} \\
 & - 2r_1 \theta_{i,j+1} = (|\Delta\psi_j| + 2r_2) \theta_{i-1,j} + 2r_2 \theta_{i+1,j} \\
 & \quad \text{for } \Delta\psi_j > 0, \text{ and } \Delta\psi_i < 0.
 \end{aligned}$$

$$\begin{aligned}
 & -2r_1 \theta_{i,j-1} + (|\Delta\psi_i| + |\Delta\psi_j| + 4r_1 + 4r_2) \theta_{i,j} \\
 & \quad + (-|\Delta\psi_i| - 2r_1) \theta_{i,j+1} \\
 & = 2r_2 \theta_{i-1,j} + (|\Delta\psi_j| + 2r_2) \theta_{i+1,j} \\
 & \quad \text{for } \Delta\psi_j < 0 \text{ and } \Delta\psi_i > 0.
 \end{aligned}$$

and

$$\begin{aligned}
 & (-|\Delta\psi_i| - 2r_1) \theta_{i,j-1} + (|\Delta\psi_i| + |\Delta\psi_j| + 4r_1 + 4r_2) \theta_{i,j} \\
 & - 2r_1 \theta_{i,j+1} = 2r_2 \theta_{i-1,j} + (|\Delta\psi_j| + 2r_2) \theta_{i+1,j} \quad , \\
 & \quad \text{for } \Delta\psi_j < 0 \text{ and } \Delta\psi_i < 0 \quad . \\
 & \quad \quad \quad (3.25)
 \end{aligned}$$

Again, assuming  $r = \frac{\Delta x}{\Delta y}$ , the equation (3.18) is subjected to the line by line procedure as follows:

### Horizontal Sweep

$$\begin{aligned} \psi_{i-1,j} - 2(1+r^2) \psi_{i,j} + \psi_{i+1,j} \\ = -r^2 \psi_{i,j-1} - r^2 \psi_{i,j+1} + (\Delta x)^2 \omega_{i,j} \end{aligned} \quad (3.26)$$

### Vertical Sweep

$$\begin{aligned} r^2 \psi_{i,j-1} - 2(1+r^2) \psi_{i,j} + r^2 \psi_{i,j+1} \\ = -\psi_{i-1,j} - \psi_{i+1,j} + (\Delta x)^2 \omega_{i,j} \end{aligned} \quad (3.27)$$

The rate of heat transfer along each wall is determined from the temperature field. The local Nusselt number along the side wall is ,

$$Nu = \left. \frac{\partial \theta}{\partial x} \right|_{x=0} \quad (3.28)$$

Along the bottom wall it is ,

$$Nu = \left. \frac{\partial \theta}{\partial y} \right|_{y=0} \quad (3.29)$$

and along the top wall, the local Nusselt number is defined as ,

$$Nu = \left. \frac{\partial \theta}{\partial y} \right|_{y=As} \quad (3.30)$$

The derivatives on the right hand side of equations (3.28)-(3.30) are computed by using a three-point finite difference formula. Once the local Nusselt number along the surfaces are determined, the average Nusselt number along each surface is evaluated by Simpson's rule of integration.

The iterative procedure adopted is summarized below,

- (a) The first iteration is started by guessing values for the fluid temperature  $\theta$ , stream function  $\psi$  and vorticity  $\omega$  at all the grid points.
- (b) Equations (3.24) and (3.25) are solved for the fluid temperature  $\theta$ .
- (c) The vorticity  $\omega$  is obtained from equations (3.21) and (3.22), using the  $\theta$  values from the previous step.
- (d) From the calculated values of  $\omega$  in step (c), the stream function  $\psi$  is obtained from equations (3.26) and (3.27).
- (e) The local Nusselt number and the average Nusselt number are estimated from the fluid temperature field.
- (f) The new guess for  $\theta$ ,  $\psi$  and  $\omega$  is evaluated from their current values using suitable relaxation parameter and steps (b-e) are repeated until convergence is reached. The convergence is presumed to have been achieved when

$$\left| \begin{array}{c} \psi_{i,j}^{k+1} - \psi_{i,j}^k \\ \psi_{i,j}^{k+1} \end{array} \right| \leq 10^{-4}$$

where, the superscripts  $k+1$  and  $k$  indicate the iteration on which that value was obtained.

### 3.4 RESULTS AND DISCUSSION

The numerical solutions have been made on a HP 9000 computer. To test the validity of the numerical procedure, the average Nusselt numbers along the side wall obtained by using the present method are compared with the results of Chen et

al.(1987) in Table 1 , for  $Pr = 7.0$  ,  $As = 1.0$  and  $10^4 \leq Ra \leq 10^6$  in the absence of porous matrix , where  $Ra$  is the Rayleigh number. The results tabulated in Table 1 are obtained for dimensionless side wall temperature = 1.0, top wall temperature = 0.7053 and bottom wall temperature = 0.0. The agreement is satisfactory and substantiates the correctness of the computational work.

At the second stage the boundary conditions for the present problem have been imposed by setting the side wall temperature = 0.0, bottom wall temperature = 1.0 and three different values of the top wall temperature = 0.0, 0.5, 1.0. Computations for different grid sizes were carried out and  $61 \times 61$ ,  $81 \times 81$  and  $101 \times 101$  grid fields showed insignificant change in the results. It was observed that a grid system of  $81 \times 81$  nodes is a good choice. The physical domain is limited by  $0 \leq x \leq 1$  and  $0 \leq y \leq As$ .

Again for the purpose of comparison, the same problem is solved by finite element method described in Chapter IV and the local Nusselt numbers along all the surfaces obtained by the two methods are presented in Tables 2, 3 and 4. The small difference between FDM and FEM is probably due to fine mesh size used in FDM calculations than that used in FEM.

Flow patterns and isotherms for various parameters are shown in Figures 2 to 9. There is a symmetry in the vortex pattern about the midplane of the enclosure, due to symmetric nature of the boundary conditions prescribed in the problem. The flow consists of a single cell filling the entire half of

the enclosure rotating in the clockwise direction but anticlockwise in the other half. The velocities are higher near the wall and lower near the line of symmetry. It is observed that the flow is almost stagnant near the corner. The circulation strength depends on  $Ra^*$ ,  $Da$ ,  $As$  and  $\theta_t$ . An increase in Rayleigh-Darcy number increases the strength of the circulation vortex. It is seen that this change in the vortex strength is nearly proportional to the Rayleigh-Darcy number. As the Darcy number decreases, the strength of the vortex decreases due to increasing resistance of the porous matrix. In order to study the effect of aspect ratio, three different sizes of the enclosures are chosen. The patterns are very similar for  $As = 0.5, 1$  and  $2$  except that the values of stream function and temperature are larger for large aspect ratio. Streamlines and isotherms are also plotted for two different values of top wall temperature =  $0.5$  and  $1.0$ . The change in the top wall temperature also alter the flow structure. The circulation pattern is smoother in the case of  $\theta_t = 1.0$  when compared to the case  $\theta_t = 0.5$ .

Furthermore, for small values of  $Ra^*$ , a pure conduction solution with parallel isotherms were obtained. As the Rayleigh-Darcy number increases, the effects of convection are noticed. For moderate values of  $Ra^*$ , the isotherms are evenly spaced curves indicating that the heat transfer is dominated by conduction and the convection effects are less. The isotherm patterns are more distorted in the case of large Rayleigh-Darcy number when the convection is dominant.

Figures 10 and 11 show the local Nusselt number along the bottom surface as a function of Rayleigh-Darcy number for different values of  $Da$  and  $\theta_t$ . The Nusselt numbers along each surface are found to increase with Rayleigh-Darcy number but decreases considerably as  $Da$  increases. Nusselt number along the bottom surface is the largest and it is the least along the top surface. Increasing  $\theta_t$  increases the Nusselt number along the top surface. Increasing the aspect ratio, decreases the Nusselt number along the top and bottom surfaces. Along the side wall, increase in the aspect ratio brings a large increase in the Nusselt number for  $\theta_t = 0$ . For larger magnitudes of  $\theta_t$ , changing the aspect ratio had little effect on the Nusselt number.

Table 1: Average Nusselt number along the side wall in absence of porous matrix for  $Pr = 7.0$ ,  $As = 1.0$ , side wall temperature = 1.0, top wall temperature = 0.7053 and bottom wall temperature = 0.0.

Ra	Comparison	Left wall	Right wall
$10^4$	Chen, Ho and Humphrey	3.5409	3.5408
	Present	3.6005	3.6005
$10^5$	Chen, Ho and Humphrey	4.3244	4.3245
	Present	4.3506	4.3507
$10^6$	Chen, Ho and Humphrey	4.8472	4.8472
	Present	5.1737	5.1737

Table 2: Local Nusselt number along the side wall for  $Pr = 1.0$ ,  $As = 1.0$ ,  $\theta_t = 0.5$ .

$Ra^* = 10, Da = 10^{-3}$				$Ra^* = 10, Da = 10^{-4}$			$Ra^* = 100, Da = 10^{-4}$		
y	0.4	0.5	0.6	0.4	0.5	0.6	0.4	0.5	0.6
FDM	1.539	1.315	1.258	1.514	1.293	1.237	1.893	2.070	2.279
FEM	1.531	1.321	1.260	1.515	1.305	1.246	1.884	2.092	2.302



Table 3: Local Nusselt number along the top wall for

$$Pr = 1.0, As = 1.0, \theta_t = 0.5.$$

$Ra^* = 10, Da = 10^{-3}$				$Ra^* = 10, Da = 10^{-4}$			$Ra^* = 100, Da = 10^{-4}$		
x	0.3	0.4	0.5	0.3	0.4	0.5	0.3	0.4	0.5
FDM	0.919	0.700	0.640	0.923	0.704	0.640	0.069	0.058	0.144
FEM	0.910	0.710	0.642	0.916	0.713	0.644	0.064	0.054	0.138

Table 4: Local Nusselt number along the bottom wall for

$$Pr = 1.0, As = 1.0, \theta = 0.5.$$

$Ra^* = 10, Da = 10^{-3}$				$Ra^* = 10, Da = 10^{-4}$			$Ra^* = 100, Da = 10^{-4}$		
x	0.3	0.4	0.5	0.3	0.4	0.5	0.3	0.4	0.5
FDM	2.278	1.841	1.663	2.316	1.850	1.714	3.500	1.994	1.313
FEM	2.290	1.834	1.680	2.316	1.861	1.720	3.610	2.110	1.351

## REFERENCES

- Bejan, A., 1979, "On the boundary layer regime in a vertical enclosure filled with a porous medium", *Letters in Heat and Mass Transfer*, Vol. 6, pp. 93-102.
- Chan, B.K.C., Ivey, C.M., and Barry, J.M., 1970, "Natural convection in enclosed porous media with rectangular boundaries", *Trans. ASME J. Heat Transfer*, vol. 92, pp. 21-27.
- Chen, K.S., Ho, J.R., and Humphrey, J.A.C., 1987, "Steady, two-dimensional, natural convection in rectangular enclosures with differently heated walls", *Trans. ASME J. Heat Transfer*, vol. 109, pp. 400-406.
- Christopher, D.M., 1986, "Transient natural convection heat transfer in a cavity filled with a fluid saturated, porous medium", *Proceedings, 8th International Heat Transfer Conference*, San Francisco, USA, pp. 2659-2664.
- Hickox, C.E. and Gartling, D.K., 1981, "A numerical study of natural convection in a horizontal porous layer subjected to an end-to-end temperature difference," *Trans. ASME J. Heat Transfer*, Vol. 103, pp. 797-802.
- Holst, P.H., and Aziz, K., 1972, "A theoretical and experimental study of natural convection in a confined porous medium", *Canadian J. Chem. Engng.*, Vol. 50, pp. 232-241.
- Lauriat, G., and Prasad, V., 1987, "Natural convection in a vertical porous cavity: a numerical study for Brinkman-extended Darcy formulation", *Trans. ASME J. Heat Transfer*, Vol. 109, pp. 688-696.
- Poulikakos, D., and Bejan, A., 1985, "The departure from Darcy flow model in natural convection in a vertical porous layer", *Phys. Fluids*, Vol. 28, pp. 3477-3484.
- Prasad, V., and Kulacki, F.A., 1984, "Convective heat transfer in a rectangular porous cavity - effect of aspect ratio on flow structure and heat transfer", *Trans. ASME J. Heat Transfer*, vol. 106, pp. 158-165.
- Prasad, V., and Tuntomo, A., 1987, "Inertia effects on natural convection in a vertical porous cavity", *Numerical Heat Transfer*, Vol. 11, pp. 295-320.
- Shiralkar, G.S., Haajizadeh, M., and Tien, C.L., 1983, "Numerical study of high Rayleigh number convection in a vertical porous enclosure", *Numerical Heat Transfer*, Vol. 6, pp. 223-234.

Simpkins, P.G., and Blythe, P.A., 1980, "Convection in a porous layer", Int. J. Heat Mass Transfer, Vol. 23, pp. 881-887.

Tong, T.W., and Orangi, S., 1986, "A numerical analysis for high modified Rayleigh number natural convection in enclosures containing a porous medium", Proceedings, 8th International Heat Transfer Conference, San Francisco, USA, pp. 2647-2652.

Tong, T.W., and Subramanian, E., "A boundary-layer analysis for natural convection in vertical porous enclosures - use of the Brinkman - extended Darcy model", Int. J. Heat Mass Transfer, Vol. 28, pp. 563-571.

Walker, K.L., and Homsy, G.M., 1978, Convection in a porous cavity", J. Fluid Mech., Vol. 97, pp. 449-474.

Weber, J.E., 1975, "The boundary - layer regime for convection in a vertical porous layer", Int. J. Heat and Mass Transfer, vol. 18, pp. 569-573.

▲ Y, V

B U=0, V=0, T=T<sub>t</sub>

▲ Y, V

As u=0, v=0, θ=θ<sub>t</sub>

U=0  
V=0  
T=T<sub>s</sub>

POROUS  
MEDIUM

U=0  
V=0  
T=T<sub>s</sub>

u=0  
v=0  
θ=0

POROUS  
MEDIUM

u=0  
v=0  
θ=0

0

U=0, V=0, T=T<sub>b</sub>

A

X, U

0

u=0, v=0, θ=1

▲ x, u

(i) Dimensional

(ii) Dimensionless

Figure 1 The Physical system

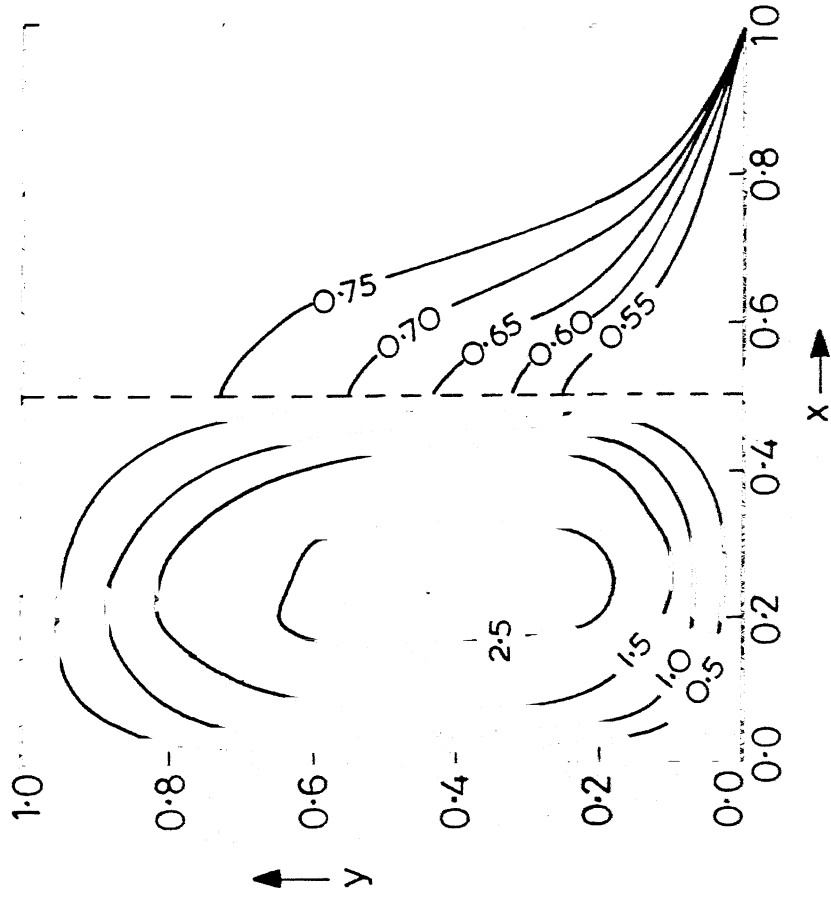


Figure 2 Streamlines and isotherms<sup>-3</sup>  
for  $\theta_t=0.5$ ,  $Pr=1$ ,  $As=1$ ,  $Ra^*=10$ ,  $Da=10$

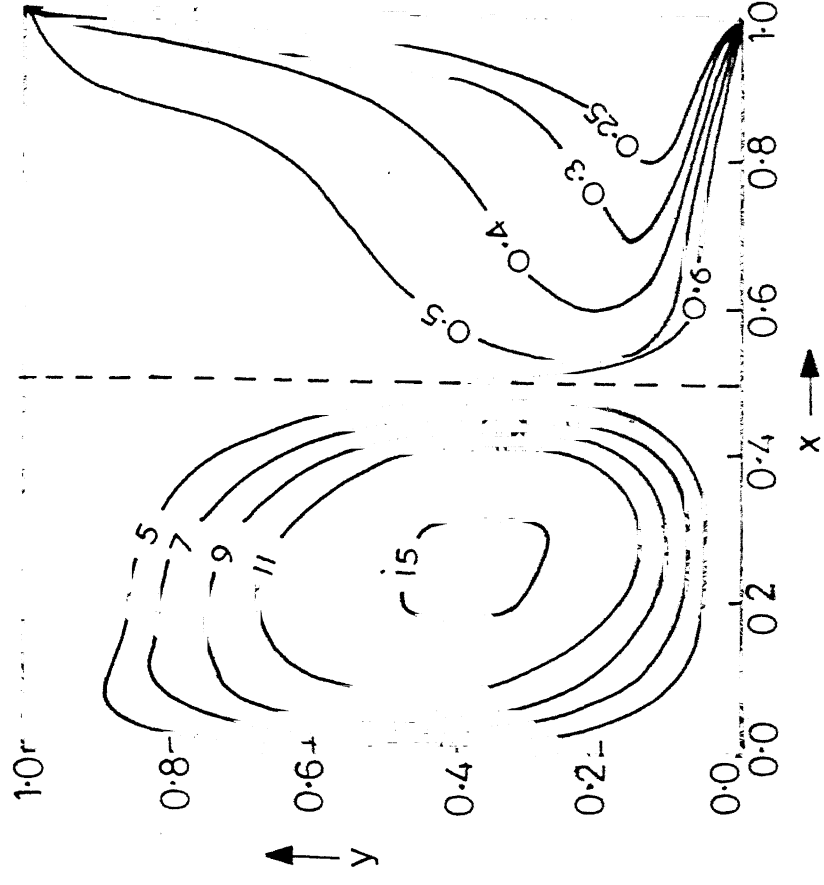


Figure 3 Streamlines and isotherms<sup>3</sup>  
for  $\theta_t=0.5$ ,  $Pr=1$ ,  $As=1$ ,  $Ra^*=10$ ,  $Da=10$

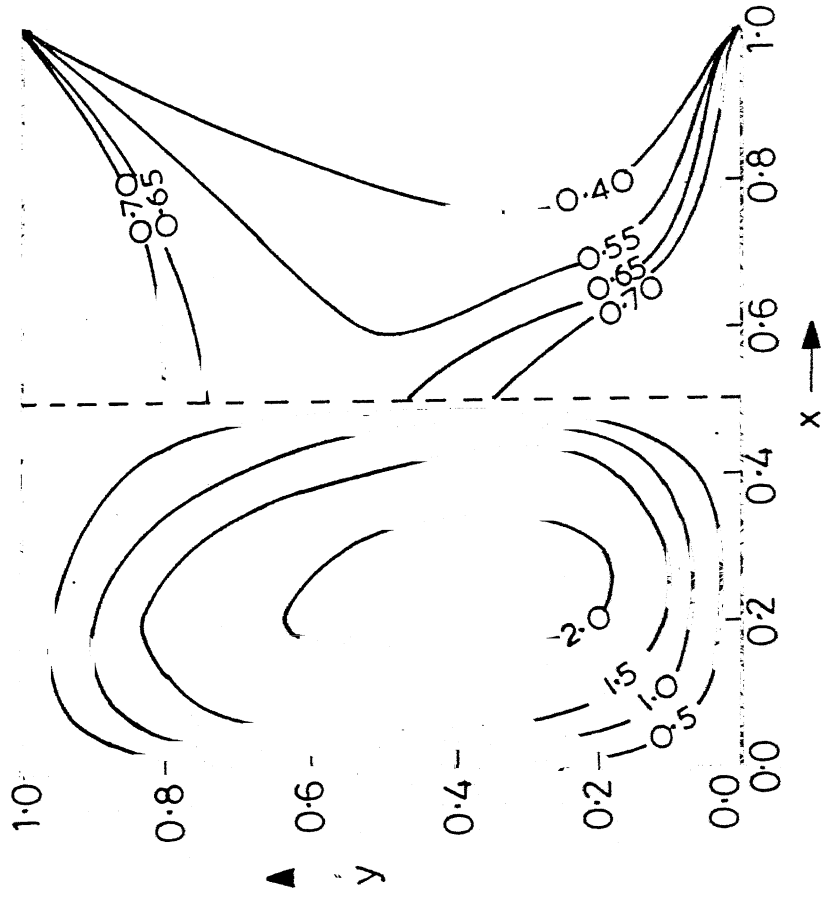


Figure 4 Streamlines and isotherms for  $\theta_f=1, Pr=1, As=1, Ra^*=10^2, Da=10^{-3}$

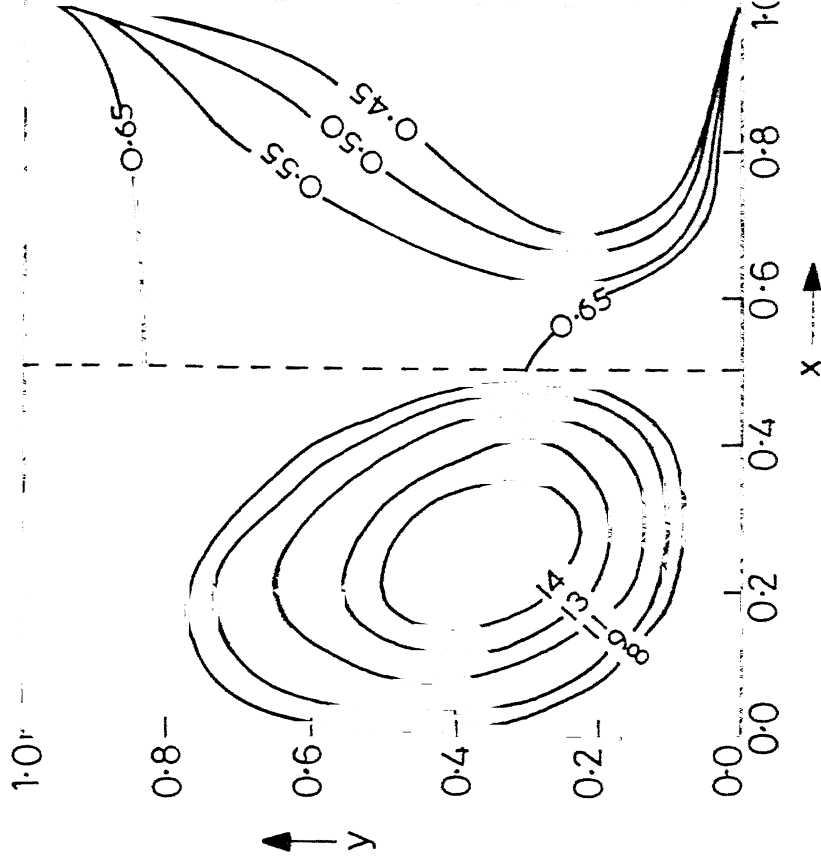


Figure 5 Streamlines and isotherms for  $\theta_f=1, Pr=1, As=1, Ra^*=10^3, Da=10^{-3}$

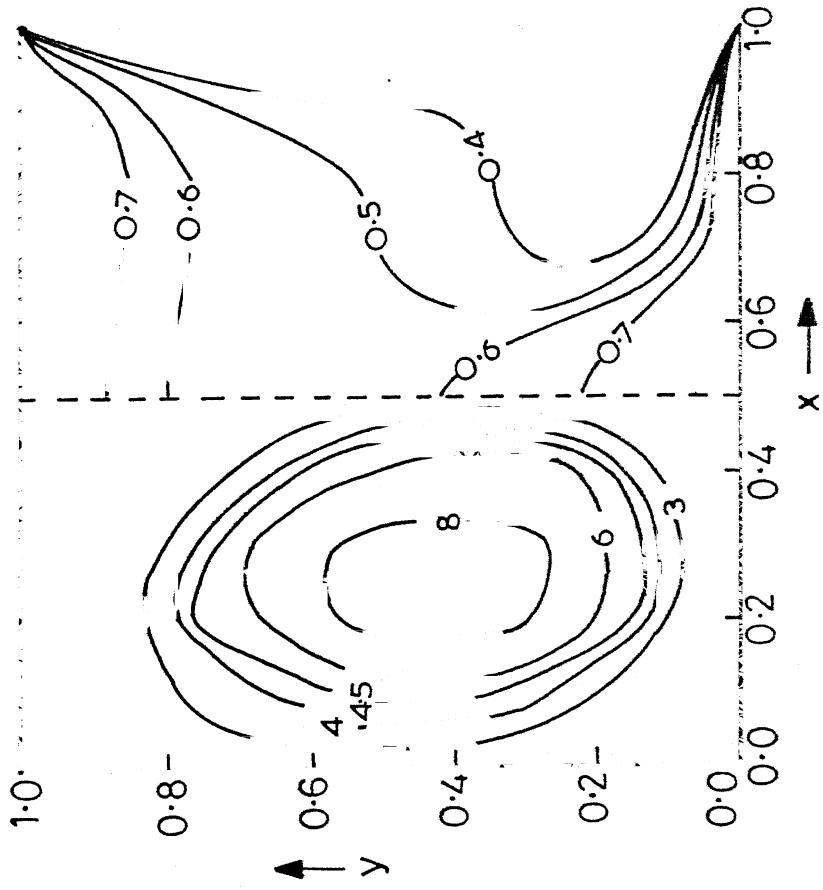


Figure 6 Streamlines and isotherms<sup>-2</sup>  
for  $\theta_t=1, Pr=1, As=1, Ra=10^3, Da=10$

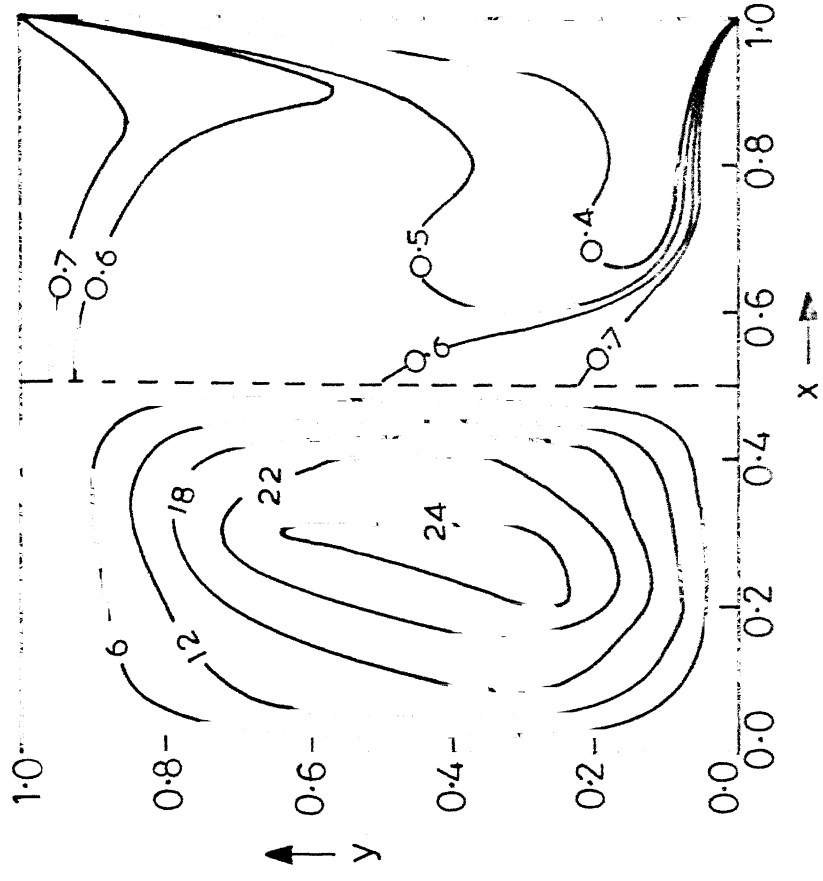


Figure 7 Streamlines and isotherms<sup>4</sup>  
for  $\theta_t=1, Pr=1, As=1, Ra=10^4, Da=10$

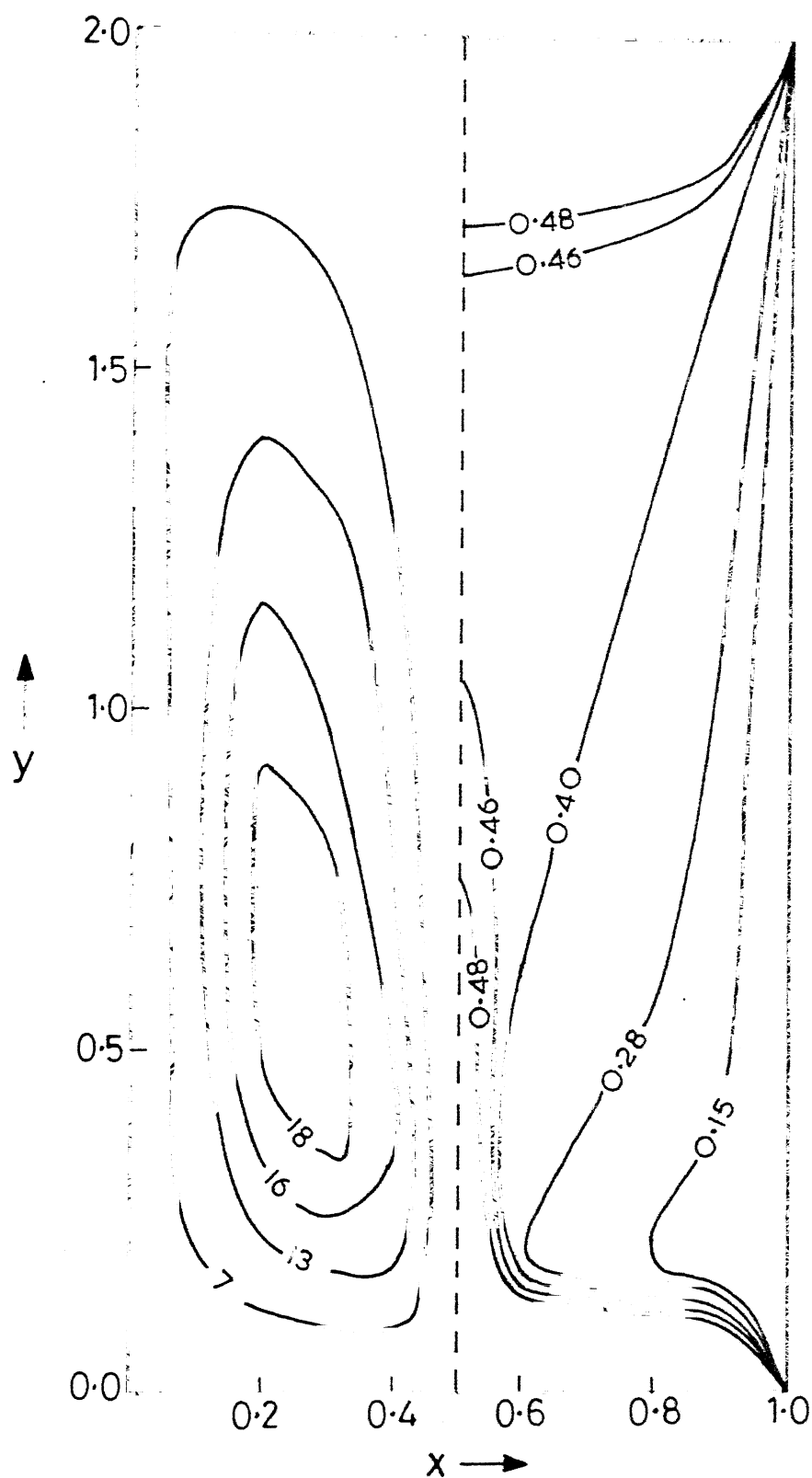


Figure 8 Streamlines and isotherms  
for  $\theta_t=1, Pr=1, As=2, Ra^*=10^3$   
 $Da=10^{-3}$



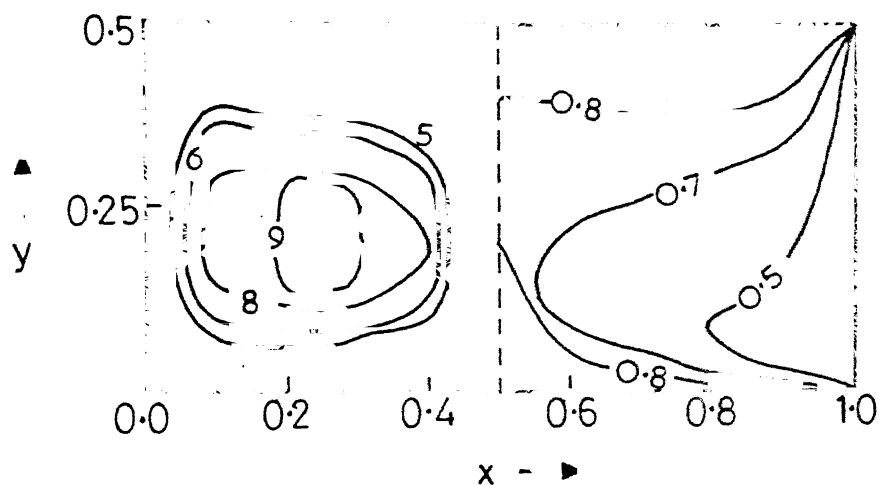


Figure 9 Streamlines and isotherms  
for  $\theta_t=1$ ,  $Pr=1$ ,  $As=1/2$ ,  $Ra=10^3$   
 $Da=10^3$

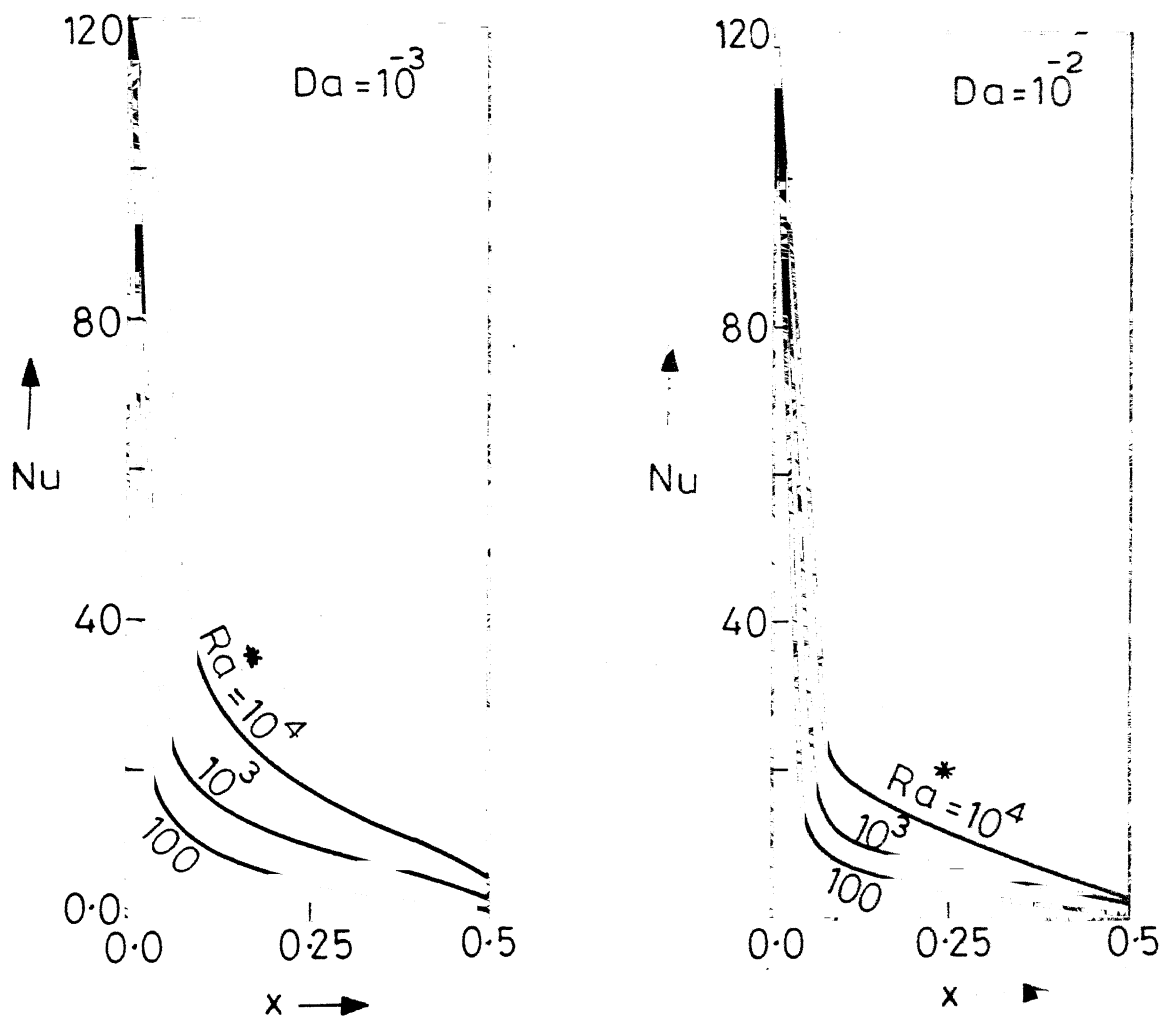


Figure 10 Local Nusselt number along the bottom wall for  $\theta_t = 1, Pr = 1, As = 1$

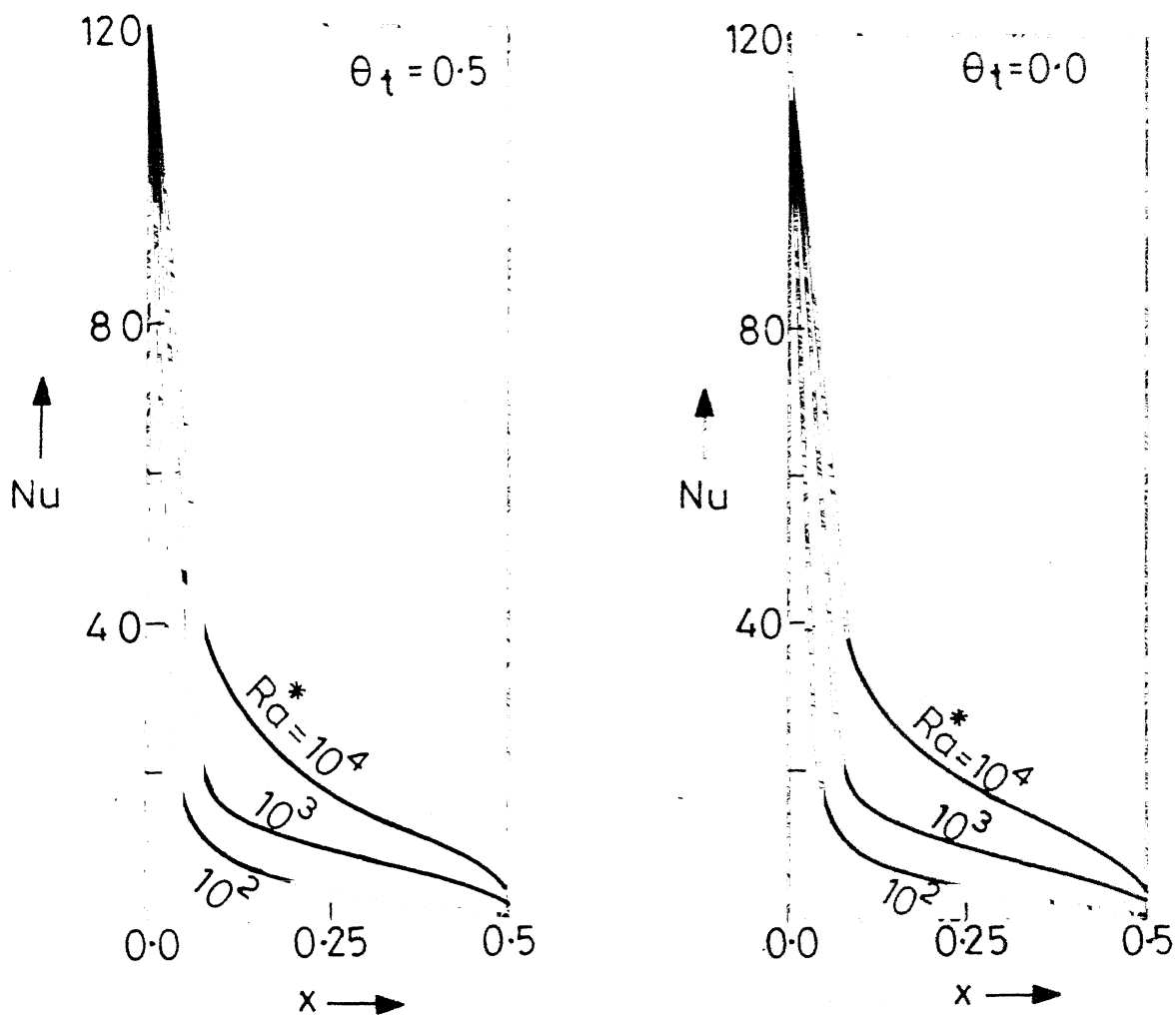


Figure 11 Local Nusselt number along the bottom wall for  $Pr = 1, As = 1, Da = 10^{-3}$

## CHAPTER IV

### NATURAL CONVECTION IN A VERTICAL CYLINDRICAL ANNULUS FILLED WITH A POROUS MATERIAL

#### 4.1 INTRODUCTION

In spite of its great practical importance in many branches of engineering, the subject of natural convection in porous media with cylindrical geometries is not nearly as well studied as the rectangular counterpart. Very recently, free convective heat transfer in cylindrical annuli filled with fluid saturated porous media has been studied experimentally and theoretically. Reda (1983), Prasad and Kulacki (1985) and Prasad et al. (1985,1986) reported some experimental results on steady state thermal field throughout an annular region bounded by a vertical inner cylinder and a concentrically placed isothermally cooled outer cylinder for different thermal conditions on the heated inner wall. In a theoretical study, Bau and Torrance (1981) examined the onset of natural convection in a fluid saturated porous medium contained between vertical coaxial cylinders of isothermal horizontal boundaries with heating from below and cooling from above. Hickox and Gartling (1982) considered natural convection in a vertical porous cylindrical annulus whose inner wall is heated at a constant temperature, the outer wall is isothermally cooled and the top and bottom are insulated. They obtained finite element numerical solutions and also used an approximate analytical method to obtain heat

transfer results for low Rayleigh numbers and high aspect ratios. Later Havstad and Burns (1982) analyzed the problem using three different methods, the finite difference numerical method, an approximate asymptotic scheme and perturbation method. Numerical results for heat transfer were presented for moderate cylinder spacings and high temperature difference. Perturbation results valid for all cylinder spacings at low temperature difference were obtained. Asymptotic solutions for very tall cylinders and all temperature difference were supplied. They also presented the effect of wall Biot number when the heat is rejected to the ambient through a conducting wall. The work of Philip (1982) is also applicable to natural convection in porous media at small Rayleigh numbers. Prasad and Kulacki (1984) reported numerical results for steady free convection in a vertical annulus filled with a saturated porous medium whose vertical walls are at constant temperatures and top and bottom are insulated. These authors considered the problem for a wide range of Rayleigh Darcy number, radius ratio parameter and aspect ratio  $\geq 1$ . Curvature effects on temperature and velocity fields were shown to be significant. In another paper Prasad and Kulacki (1985) determined heat transfer rates in short cylindrical porous annulus both numerically and experimentally for the same thermal conditions on the boundaries. Recently Prasad (1986) obtained numerical results for the case when the inner wall is heated by applying a constant heat flux which results in a higher rate of heat transfer compared to the isothermal heating. In all these

theoretical studies Darcy's law is assumed to hold and boundary and inertia effects have been totally neglected.

Consequently, the present analysis deals with free convective flow in a vertical cylindrical annulus filled with a fluid saturated porous medium without neglecting these effects. The vertical walls are at constant temperature with the inner being hot and the outer being cold. The top and bottom of the annulus are insulated. The boundaries are impermeable and the results are based on the generalized momentum equation. The problem is analyzed via finite element method based on the Galerkin form following a procedure outlined by Taylor and Hughes (1981).

#### 4.2 THE BASIC EQUATIONS

Assuming local thermal equilibrium between the solid and fluid, and also, a Boussinesq fluid, the axisymmetric two-dimensional form of the governing equations expressing conservation of mass, momentum and energy for the present problem are,

$$\frac{\partial U}{\partial R} + \frac{U}{R} + \frac{\partial V}{\partial Y} = 0, \quad (4.1)$$

$$\rho \left( U \frac{\partial U}{\partial R} + V \frac{\partial U}{\partial Y} \right) = - \frac{\partial P}{\partial R} + \mu \left\{ \frac{1}{R} \frac{\partial}{\partial R} \left( R \frac{\partial U}{\partial R} \right) - \frac{U}{R^2} + \frac{\partial^2 U}{\partial Y^2} \right\} - \frac{\mu U}{K}, \quad (4.2)$$

$$\rho \left( U \frac{\partial V}{\partial R} + V \frac{\partial V}{\partial Y} \right) = - \frac{\partial P}{\partial Y} + \mu \left\{ \frac{1}{R} \frac{\partial}{\partial R} \left( R \frac{\partial V}{\partial R} \right) + \frac{\partial^2 V}{\partial Y^2} \right\} - \frac{\mu V}{K} + \rho g \beta (T - T_0), \quad (4.3)$$

$$U \frac{\partial T}{\partial R} + V \frac{\partial T}{\partial Y} = \alpha \left\{ \frac{1}{R} \frac{\partial}{\partial R} \left( R \frac{\partial T}{\partial R} \right) + \frac{\partial^2 T}{\partial Y^2} \right\}. \quad (4.4)$$

The geometry of the cylindrical porous annulus and the coordinate system  $(R, Y)$  are shown in Figures 1 and 2.  $U$  and  $V$  represents the velocity components in  $R$  and  $Y$  directions respectively,  $\rho$  is the density of the fluid,  $\mu$  the viscosity and  $\beta$  is the thermal expansion coefficient of the fluid,  $K$  is the permeability of the isotropic porous medium and  $\alpha$  is the thermal diffusivity.  $T$ ,  $P$  and  $g$  denote the temperature, pressure and the gravitational acceleration respectively. Denoting the inner and outer cylinder radii by  $R_i$  and  $R_o$ , the cylinder height by  $H$ , gap width of the porous annulus by  $D$  and temperature at the inner and outer walls by  $T_i$  and  $T_o$ ; the appropriate boundary conditions for the problem as indicated in Figure 2 are,

$$\begin{aligned} R = R_i : U = 0, V = 0, T = T_i, \\ R = R_o : U = 0, V = 0, T = T_o, \\ Y = 0 : U = 0, V = 0, \frac{\partial T}{\partial Y} = 0, \\ Y = H : U = 0, V = 0, \frac{\partial T}{\partial Y} = 0. \end{aligned} \quad (4.5)$$

On introducing the dimensionless quantities,

$$\begin{aligned} r = \frac{R}{D}, \quad y = \frac{Y}{D}, \quad u = \frac{UD}{\alpha}, \quad v = \frac{VD}{\alpha}, \quad p = \frac{PD^2}{\rho\alpha^2}, \quad \theta = \frac{T - T_o}{T_i - T_o}, \\ r_i = \frac{R_i}{D}, \quad As = \frac{H}{D}, \quad Pr = \frac{\mu}{\rho\alpha}, \quad Ra^* = \frac{\rho g \beta K D (T_i - T_o)}{\mu\alpha}, \quad Da = \frac{K}{D^2}, \end{aligned} \quad (4.6)$$

the governing partial differential equations can be written in the following non-dimensional form,

$$u \frac{\partial u}{\partial r} + \frac{u}{r} + \frac{\partial v}{\partial y} = 0, \quad (4.7)$$

$$u \frac{\partial u}{\partial r} + v \frac{\partial u}{\partial y} = - \frac{\partial p}{\partial r} + \text{Pr} \left\{ \frac{1}{r} \frac{\partial}{\partial r} \left( r \frac{\partial u}{\partial r} \right) - \frac{u}{r^2} + \frac{\partial^2 u}{\partial y^2} \right\} - \frac{\text{Pr}}{\text{Da}} u, \quad (4.8)$$

$$u \frac{\partial v}{\partial r} + v \frac{\partial v}{\partial y} = - \frac{\partial p}{\partial y} + \text{Pr} \left\{ \frac{1}{r} \frac{\partial}{\partial r} \left( r \frac{\partial v}{\partial r} \right) + \frac{\partial^2 v}{\partial y^2} \right\} - \frac{\text{Pr}}{\text{Da}} (v - \text{Ra}^* \theta), \quad (4.9)$$

$$u \frac{\partial \theta}{\partial r} + v \frac{\partial \theta}{\partial y} = \frac{1}{r} \frac{\partial}{\partial r} \left( r \frac{\partial \theta}{\partial r} \right) + \frac{\partial^2 \theta}{\partial y^2}. \quad (4.10)$$

The boundary conditions in the non-dimensional form are,

$$\begin{aligned} r = r_i & : u = 0, \quad v = 0, \quad \theta = 1, \\ r = r_i + 1 & : u = 0, \quad v = 0, \quad \theta = 0, \\ y = 0 & : u = 0, \quad v = 0, \quad \frac{\partial \theta}{\partial y} = 0, \\ y = 0 & : u = 0, \quad v = 0, \quad \frac{\partial \theta}{\partial y} = 0. \end{aligned} \quad (4.11)$$

In the dimensionless form, the radius ratio  $\kappa = 1 + \frac{1}{r_i}$ , the aspect ratio  $As$ , the Prandtl number  $\text{Pr}$ , the Rayleigh-Darcy number  $\text{Ra}^*$  and the Darcy number  $\text{Da}$  are the important parameters.

#### 4.3 DEVELOPMENT OF FINITE ELEMENTAL EQUATIONS

First, the geometrically complex domain of the problem is represented as a collection of geometrically simple sub domains, called finite elements. Associated with each element are eight discrete node points, each of which is specified by a local co-ordinate as well as a global co-ordinate system. The eight noded isoparametric elements are chosen to accommodate parabolic



variation in the variables on the boundary and in the interior of the element. In such elements, the temperature and velocity components are specified at all the eight nodes whereas the pressure is specified only at four corner nodes. The shape function (also called as interpolation functions) for eight noded element in terms of local co-ordinates  $\xi$  and  $\eta$  are given by the following formulae.

For corner nodes :

$$N_i = \frac{1}{4} (1 + \xi_i \xi)(1 + \eta_i \eta)(\xi_i \xi + \eta_i \eta - 1) , \quad i = 1, 3, 5, 7 . \quad (4.12a)$$

For midside nodes :

$$\begin{aligned} N_i &= \frac{1}{2} (1 - \xi^2)(1 + \eta_i \eta), \text{ if } \xi_i = 0 , \quad i = 2, 6 \\ N_i &= \frac{1}{2} (1 + \xi_i \xi)(1 - \eta^2), \text{ if } \eta_i = 0 , \quad i = 4, 8 \end{aligned} \quad (4.12b)$$

For pressure, linear interpolation is used and the shape functions corresponding to four corner nodes are ,

$$\begin{aligned} M_1 &= \frac{1}{4} (1 - \xi)(1 - \eta) , \\ M_2 &= \frac{1}{4} (1 + \xi)(1 - \eta) , \\ M_3 &= \frac{1}{4} (1 + \xi)(1 + \eta) , \\ M_4 &= \frac{1}{4} (1 - \xi)(1 + \eta) . \end{aligned} \quad (4.13)$$

The advantages of using eight noded isoparametric elements and depicting the variation in pressure by shape functions of one order lower than those for defining the velocity distribution are discussed in detail by Taylor and Hughes (1981).

In terms of these shape functions, the velocity, temperature and pressure over an element are written in the following form,

$$\begin{aligned}
 u &= \sum_{i=1}^8 N_i u_i , \\
 v &= \sum_{i=1}^8 N_i v_i , \\
 \theta &= \sum_{i=1}^8 N_i \theta_i , \\
 p &= \sum_{i=1}^4 M_i p_i .
 \end{aligned}
 \tag{4.14}$$

Spatial coordinates within the element are defined in terms of all eight nodes. Using these quadratic and linear approximation functions, and employing Galerkin weighted residual approach in which the weighting functions are taken to be the shape functions themselves, equations(4.7) - (4.10) become,

$$\sum_1^{ne} \iint M_i \left( \frac{\partial N_j}{\partial r} u_j + \frac{N_j}{r} u_j + \frac{\partial N_j}{\partial y} v_j \right) r dr dy = 0 , \tag{4.15a}$$

$$\begin{aligned}
 &\sum_1^{ne} \iint N_i \left[ \left( N_k \bar{u}_k \right) \frac{\partial N_j}{\partial r} u_j + \left( N_k \bar{v}_k \right) \frac{\partial N_j}{\partial y} u_j + \frac{\partial M_l}{\partial r} p_l \right. \\
 &\quad \left. - Pr \left\{ \frac{1}{r} \frac{\partial}{\partial r} \left( r \frac{\partial N_j}{\partial r} u_j \right) - \frac{N_j}{r^2} u_j + \frac{\partial^2 N_j}{\partial y^2} u_j \right\} \right. \\
 &\quad \left. + \frac{Pr}{Da} N_j u_j \right] r dr dy = 0 , \tag{4.15b}
 \end{aligned}$$

$$\begin{aligned}
& \sum_1^{ne} \iint N_i \left[ \left( N_k \bar{u}_k \right) \frac{\partial N_j}{\partial r} v_j + \left( N_k \bar{v}_k \right) \frac{\partial N_j}{\partial y} v_j + \frac{\partial M_l}{\partial y} p_l \right. \\
& \quad \left. - Pr \left\{ \frac{1}{r} \frac{\partial}{\partial r} \left( r \frac{\partial N_j}{\partial r} v_j \right) + \frac{\partial^2 N_j}{\partial y^2} v_j \right\} \right. \\
& \quad \left. + \frac{Pr}{Da} \left( N_j v_j - Ra^* N_j \theta_j \right) \right] r dr dy = 0, \quad (4.15c)
\end{aligned}$$

$$\begin{aligned}
& \sum_1^{ne} \iint N_i \left[ \left( N_k \bar{u}_k \right) \frac{\partial N_j}{\partial r} \theta_j + \left( N_k \bar{v}_k \right) \frac{\partial N_j}{\partial y} \theta_j \right. \\
& \quad \left. - \left\{ \frac{1}{r} \frac{\partial}{\partial r} \left( r \frac{\partial N_j}{\partial r} \theta_j \right) + \frac{\partial^2 N_j}{\partial y^2} \theta_j \right\} \right] r dr dy = 0. \quad (4.15d)
\end{aligned}$$

The repeated suffixes indicate summation with the suffix running through the integral numbers 1,2,..... such that

$$l = 1, 2, 3, 4,$$

$$j = 1, 2, \dots, 8$$

and

$$k = 1, 2, \dots, 8.$$

The outer summation refers to each element in the domain. The symbols  $u_j$ ,  $v_j$ ,  $\theta_j$  and  $p_l$  etc. denote the nodal values of  $u$ ,  $v$ ,  $\theta$  and  $p$  respectively within a particular element.

Invoking Green's theorem the second order terms in the equations (4.15b) - (4.15d) are reduced and the finite elemental equations for mass, momentum and energy balance are written as

$$\sum_1^{ne} \iint M_i \left( \frac{\partial N_j}{\partial r} u_j + \frac{N_j}{r} u_j + \frac{\partial N_j}{\partial y} v_j \right) r dr dy = 0, \quad (4.16a)$$

$$\begin{aligned}
& \sum_1^{ne} \iint \left[ N_i (N_k \bar{u}_k) \frac{\partial N_j}{\partial r} u_j + N_i (N_k \bar{v}_k) \frac{\partial N_j}{\partial y} u_j + N_i \frac{\partial M_z}{\partial r} P_z \right. \\
& \quad \left. + Pr \left\{ \frac{\partial N_i}{\partial r} \frac{\partial N_j}{\partial r} u_j + \frac{\partial N_i}{\partial y} \frac{\partial N_j}{\partial y} u_j + \frac{N_i N_j}{r^2} u_j \right\} \right. \\
& \quad \left. + \frac{Pr}{Da} N_i N_j u_j \right] r dr dy = Pr \oint_{\Gamma} N_i \frac{\partial u}{\partial n} d\Gamma, \quad (4.16b)
\end{aligned}$$

$$\begin{aligned}
& \sum_1^{ne} \iint \left[ N_i (N_k \bar{u}_k) \frac{\partial N_j}{\partial r} v_j + N_i (N_k \bar{v}_k) \frac{\partial N_j}{\partial y} v_j + N_i \frac{\partial M_z}{\partial y} P_z \right. \\
& \quad \left. + Pr \left\{ \frac{\partial N_i}{\partial r} \frac{\partial N_j}{\partial r} v_j + \frac{\partial N_i}{\partial y} \frac{\partial N_j}{\partial y} v_j \right\} + \frac{Pr}{Da} (N_i N_j v_j \right. \\
& \quad \left. - Ra^* N_i N_j \theta_j) \right] r dr dy = Pr \oint_{\Gamma} N_i \frac{\partial v}{\partial n} d\Gamma, \quad (4.16c)
\end{aligned}$$

$$\begin{aligned}
& \sum_1^{ne} \iint \left[ N_i (N_k \bar{u}_k) \frac{\partial N_j}{\partial r} \theta_j + N_i (N_k \bar{v}_k) \frac{\partial N_j}{\partial y} \theta_j \right. \\
& \quad \left. + \left\{ \frac{\partial N_i}{\partial r} \frac{\partial N_j}{\partial r} \theta_j + \frac{\partial N_i}{\partial y} \frac{\partial N_j}{\partial y} \theta_j \right\} \right] r dr dy \\
& \quad = \oint_{\Gamma} N_i \frac{\partial \theta}{\partial n} d\Gamma, \quad (4.16d)
\end{aligned}$$

where  $\Gamma$  denotes the element boundary. In the nonlinear inertial terms  $\bar{u}_k$  and  $\bar{v}_k$  represent the velocity components at the  $k$ th node which are taken to be known (from the previous iteration) in order to make the equation quasilinear. The boundary integrals on the RHS of equations (4.16b) involve the derivatives of the velocity components and the temperature in the direction of the outward normal to the boundary. However,

for the present problem with boundary conditions given by (4.11), the RHS integral contributions are zero.

#### 4.4 MATRIX FORMULATION AND SOLUTION PROCEDURE

The finite element equations (4.16a) - (4.16d) are assembled in the global matrix equations to solve the nodal values of pressure, velocity components and temperature. The assembled matrix equations take the form,

$$A \lambda = F, \quad (4.17)$$

where, the chosen form for  $\lambda$  is,

$$\lambda_i = \begin{bmatrix} u_i \\ p_i \\ v_i \\ \theta_i \end{bmatrix}, \quad (4.18)$$

and  $A$  is generally denoted as the stiffness matrix in the FEM terminology. Due to the presence of the inertial terms in the momentum and energy equations,  $A$  is not symmetric. Because of the nonsymmetry of this matrix, the memory space and the inversion time are larger. Also the inertial terms in the governing equations make the matrix equation (4.17) nonlinear, hence an iterative solution procedure is required to be imposed. Using  $\bar{u}_k$  and  $\bar{v}_k$  values from the previous iteration, the stiffness matrix  $A$  is updated and the solution vector  $\lambda$  which contains all the nodal values of  $u$ ,  $p$ ,  $v$  and  $\theta$  is calculated. This is continued till the results do not change significantly from one iteration to the next.

The solution procedure used here for solving the assembled matrix equations is known as the FRONTAL METHOD. This method

leads to a significant reduction in the computer storage requirement and the execution time. In the present problem the assembled elemental coefficient matrix is itself large with a size of  $28 \times 28$ . Also there is a limitation on the minimum number of elements to be used to discretize the domain, in order to avoid the ill-conditioning of the global assembled matrix during inversion. A fairly large number of elements are used.

The frontal technique originally devised by Irons (1970), has proved to be very effective for solving positive definite matrices. This method has been modified by Taylor and Hughes(1981) for solving steady state Navier Stokes' equations. Originally this method was based on direct Gaussian elimination for solving symmetric matrices, where the leading diagonal is always used as pivot. For unsymmetric matrices encountered in wide range of problems in engineering fluid mechanics, the most suitable pivot is not always the leading diagonal, and frontal solutions exist for off-diagonal pivoting. These, however, tend to be more time consuming. The method used here uses only diagonal pivoting incorporating many features of the frontal method for solving symmetric matrices.

In Frontal method the reduction is carried out on an elemental basis, to avoid the difficulty of large storing space. The complete global matrix is never assembled fully. As soon as the contributions from all the elements to a particular nodal point have been completed, the corresponding variables associated with the node are eliminated. A preassigned global matrix core area is filled from contributing elements, the

largest diagonal entry in this is then found and used as a pivot in the direct Gaussian elimination process. The corresponding reduced equations written onto disk and more elements and corresponding equations are taken into the core. When all the elements have been included and the variables reduced, the back substitution process is initiated (Taylor and Hughes 1981).

The solution procedure involves the following steps:

- (i) Calculate the elemental coefficient matrix  $[A]_{28 \times 28}$  and  $[F]_{28 \times 1}$  for the element under consideration.
- (ii) Assemble the matrices into the global coefficient matrix and global right hand side vector.
- (iii) Introduce boundary conditions if any, for the particular element.
- (iv) Reduce the global matrix using the Gaussian elimination procedure.
- (v) Repeat the steps (i) to (iv) for the next element.

#### 4.5 RESULTS AND DISCUSSION

Numerical results using finite element method have been obtained for a wide range of dimensionless parameters. The solution domain has been discretized by using 100 rectangular elements, 10 in each direction. To test the applicability and accuracy of the present method, the results were obtained for the vertical cavity case and were compared with the solution obtained by finite difference method described in Chapter III. Both the methods yield comparable results confirming the validity of the present scheme.

The governing equations of the present problem are solved to first obtain the velocity and temperature fields. Subsequently the local Nusselt number and the average Nusselt number along the heated wall are evaluated using the expressions

$$Nu_y = \left. \frac{\partial \theta}{\partial r} \right|_{r=0}, \quad (4.19)$$

and

$$Nu = \int_0^A \left. \frac{\partial \theta}{\partial r} \right|_{r=0} dz, \quad (4.20)$$

respectively. These are evaluated by the method of numerical differentiation and integration.

The velocity and temperature fields for some typical values of  $Ra^*$ ,  $Da$ ,  $As$  and  $\alpha$  are presented in Figures 3 to 7. It is observed that the magnitude of  $u$  velocity (in the radial direction) first increases with distance away from the heated wall and then it decreases to zero. This feature can be explained in terms of the existence of a velocity boundary layer adjacent to the hot wall due to the buoyancy effects and the entrainment of the enclosure fluid into the boundary layer. The entrainment velocity will obviously have a maximum value at the edge of the boundary layer. The  $u$ -velocity is negative in the lower half of the enclosure and positive in the upper half. This indicates that the flow approaches towards the hot surface at the bottom of the enclosure and the hot fluid moves away from this surface at the top. This sense of flow circulation is also confirmed by velocity vector plots (Figures 10-12).



In Figure 4, it is seen that the magnitude of the velocity at the same location increases with radius ratio  $\alpha$ . The reason for this is that the ratio of area between the outer and inner cylinders increases with  $\alpha$ . Since at steady state same amount of heat flows from the hot wall to the cold, the heat flux on the hot wall is much larger (since its area is smaller) than that of the cold wall. The higher heat flux causes more buoyancy and it is therefore obvious that the velocity should increase with radius ratio. This fact is illustrated by the velocity vector plots (Figures 10-12).

The temperature distributions in Figures 5 to 7 clearly show the existence of a thermal boundary layer near the hot wall. Since the radius ratio is larger than one for all these plots, the heat flux near the hot wall is much larger than at the cold wall, thereby establishing a boundary layer type of temperature variation there.

It is seen in Figure 5, that the thermal boundary layer becomes steeper as  $Ra^*$  is increased. This confirms the known trend that as the effect of buoyancy increases (higher  $Ra$ ) the convective effects become stronger and the boundary layer becomes thinner. In the vertical direction, the boundary layer thickness increases with distance  $y$  as expected. The plots indicate that apart from steep gradients near the hot wall, moderately high gradients exist near the cold wall also. This is because the circulatory nature of the flow causes the hot fluid adjacent to the inner cylinder to come into contact with the cold wall at a subsequent time. It is also observed that

for radial positions which lie in the middle of the cavity the temperature variation in the radial direction is negligible.

As the radius ratio is increased (Figure 6), the boundary layer becomes steeper adjacent to the hot wall and simultaneously, the gradients at the cold wall decreases. Both the trends are the consequences of the higher area ratio between cylindrical surfaces at larger  $\kappa$ , with respect to the aspect ratio (Figure 7), however, it is observed that boundary layer becomes thicker, when  $As$  is increased. The temperature gradients on the cold wall also decrease with aspect ratio.

Local Nusselt number variation along the hot wall is plotted in Figures 8 and 9. The Nusselt number decreases with vertical distance since the thermal boundary layer thickness increases with distance.

For each radius ratio and Darcy number it is seen that Nusselt number increases with Rayleigh number. As explained earlier, this occurs due to the boundary layer thickness decreasing with Rayleigh number. It is interesting to note that the maximum Nusselt number does not occur at  $y = 0$  (bottom corner) but some distance above it. This is believed to be a consequence of the existence of the stagnation region in the corner zone with a decrease in the value of  $\kappa$ . The Nusselt number decreases obviously due to smaller ratio of the cold wall area and hot wall area. Finally, with increase in Darcy number, the Nusselt number decreases. This is because the viscous and thermal boundary layer thicknesses decrease when Darcy number is

decreased (higher resistance offered by the solid matrix). A thinner boundary layer, in turn, leads to larger Nusselt number.

The velocity vector plots for various parameters are shown in Figures 10 to 12. It is observed that the velocity values adjacent to the hot wall are always larger than those near the cold or adjacent to horizontal sides. This is the result of larger buoyancy force existing near the hot wall which has a smaller area near the cold wall. The magnitude of velocity decreases as one approaches the mid portion of the cavity. It is not surprising, since the natural convective flow is a phenomenon which is generated by buoyancy effects at the boundary walls and in the interior portion of the cavity the buoyancy effect is weak. The strength of the flow is observed to increase, as expected, with the radius ratio. Also, the magnitude of the velocity vector is larger, especially adjacent to the hot wall. Clearly this is the consequence of larger heat flux arising due to smaller heat transfer area, with the decrease in the value of  $\kappa$ . If the aspect ratio of the cavity is increased, then also the strength of the natural convective flow increases since the contact length with the non-adiabatic surfaces and the fluid increases.

Numerical results for Darcy law may be recovered by setting  $Da$  very small. The magnitude of the Darcy number in the present study is in the range  $10^{-5} \leq Da \leq 10^{-1}$ . Table 1 presents results of a parametric study of average Nusselt number along the heated wall as a function of  $Ra^*$ ,  $Da$ ,  $\kappa$  and  $As$ . Results are compared with those obtained for a Darcy flow regime by Prasad and

Kulacki (1984). An increase in the Rayleigh-Darcy number increases the average Nusselt number and an increase in the Darcy number produces a reverse trend. As the Darcy number increases, present results deviate from the results presented by Prasad and Kulacki (1984). The difference between the present results and the results corresponding to the Darcy flow is due to the inclusion of viscous and inertia terms in the momentum equation. Vafai and Tien (1981) have pointed out that the Nusselt number decreases when the inertia and boundary effects become significant. Results presented in Table 1 supplements this observation.

Table 1: Present Nusselt numbers compared with the results of Prasad and Kulacki

	$\alpha = 2.00$			$\alpha = 5.0$		
$Ra^*$	50	75	100	100	80	120
As	1	1	2	2	2.5	2.5
Prasad and Kulacki	2.77	3.59	4.05	5.72	4.83	5.79
Present results with $Da = 10^{-5}$	2.71	3.51	3.94	5.60	4.75	5.67
Present results with $Da = 10^{-4}$	2.65	3.39	3.83	5.49	4.68	5.56

## REFERENCES

- Bau, H. H., and Torrance, K. E., 1981. "Onset of convection in a permeable medium between vertical co-axial cylinders", *Phys. Fluids*, Vol. 24, pp.382-385.
- Havstad, M. A., and Burns, P. J., 1982, "Convective heat transfer in vertical cylindrical annuli filled with porous medium", *Int. J. Heat Mass Transfer*, Vol. 25, pp.1755-1766.
- Hickox, C.E., and Gartling, D. K., 1982, "A numerical study of natural convection in a vertical annular porous layer", ASME paper No. 82-HT-68.
- Philip, J. R., 1982, "Axysymmetric free convection at small Rayleigh number in porous cavities", *Int. J. Heat Mass Transfer*, Vol. 25, pp.1689-1699.
- Prasad, V., 1986, "Numerical study of natural convection in a vertical, porous annulus with constant heat flux on the inner wall", *Int. J. Heat Mass Transfer*, Vol. 29, pp.841-853.
- Prasad, V., and Kulacki, F. A., 1984, "Natural convection in a vertical porous annulus", *Int. J. Heat Mass Transfer*, Vol. 27, pp.207-219.
- Prasad, V., and Kulacki, F. A., 1985, "Natural convection in porous media bounded by short concentric vertical cylinders", *Trans. ASME J. Heat Transfer*, Vol.107, pp.147 - 154.
- Prasad, V., Kulacki, F. A., and Keyhani, M., 1985, "Natural convection in porous media", *J. Fluid Mech.*, Vol.150, pp.89 - 119.
- Prasad, V., Kulacki, F. A., and Kulkarni, A. V., 1986, "Free convection in a vertical porous annulus with constant heat flux on the inner wall - experimental results", *Int. J. Heat Mass Transfer*, Vol.29, pp.713 - 723.
- Reda, D. C., 1983, "Natural convection experiments in a liquid - saturated porous medium bounded by vertical co-axial cylinders", *Trans. ASME J. Heat Transfer*, Vol.105, pp.795 - 802.
- Taylor, C., and Hughes, T. G., 1981, *Finite Element Programming of the Navier - Stokes Equations*, Pineridge Press, Swansea, U.K.
- Vafai, K., and Tien, C.L., 1981, "Boundary and inertia effects on flow and heat transfer in porous media", *Int. J. Heat Mass Transfer*, Vol. 24, pp. 195-203.

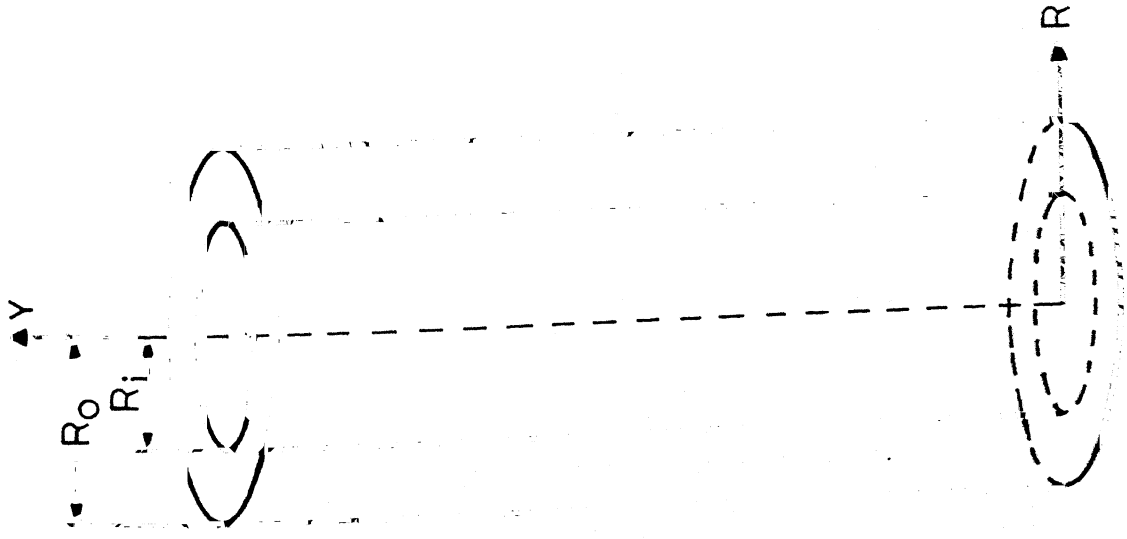


Figure 1 The Physical system

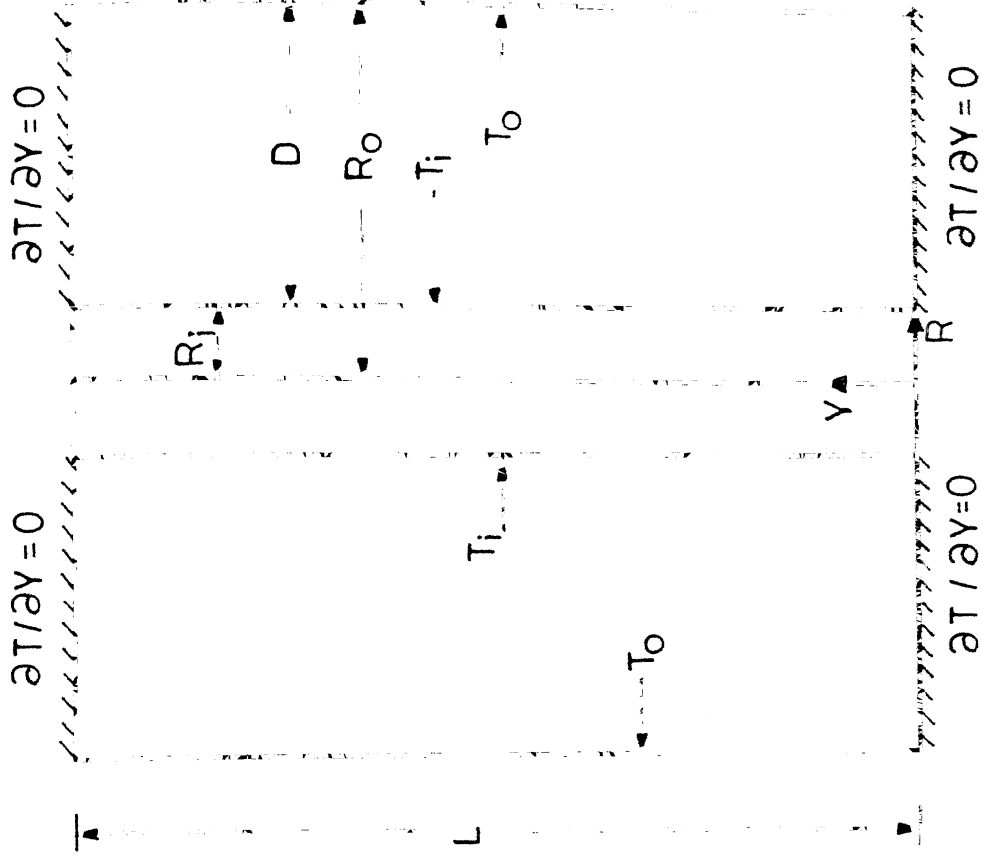


Figure 2 The two dimensional geometry and co-ordinate system

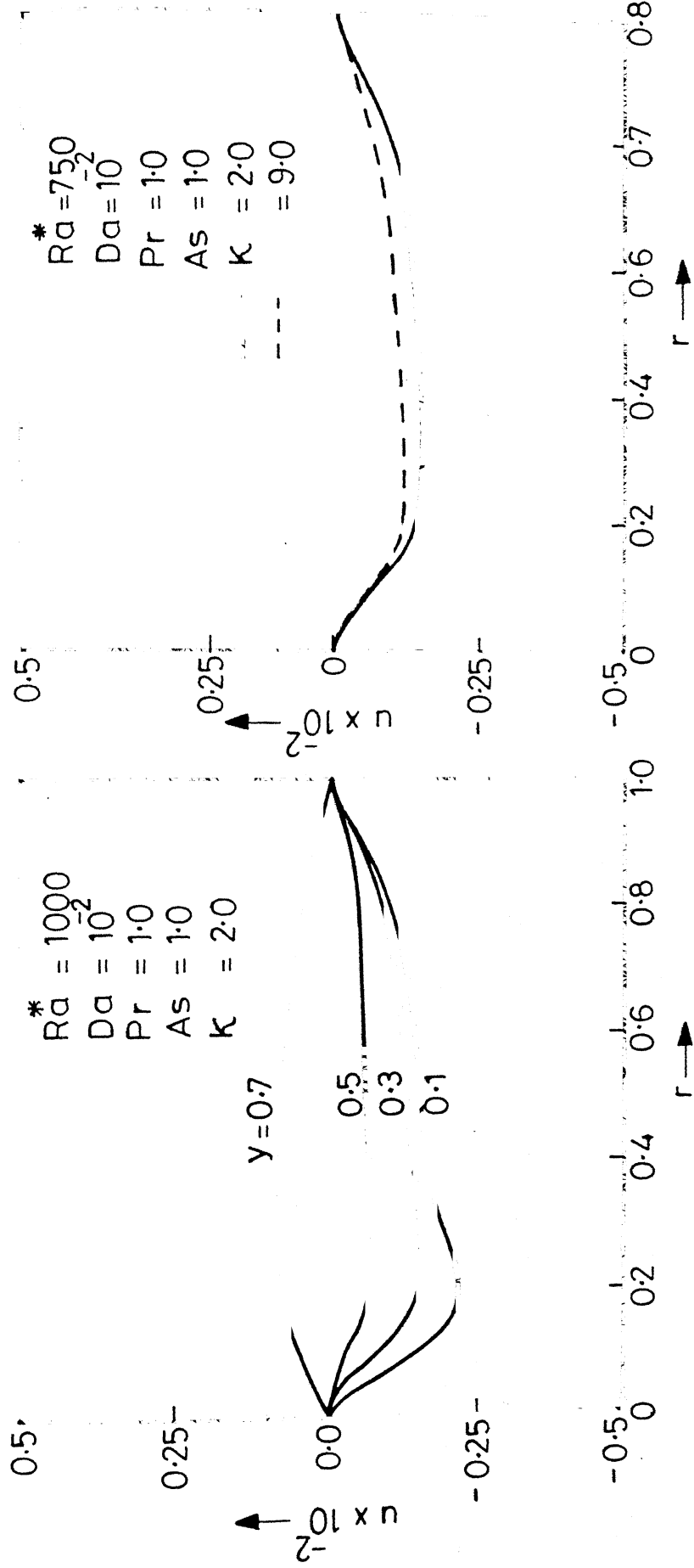


Figure 3 Velocity profile at different heights

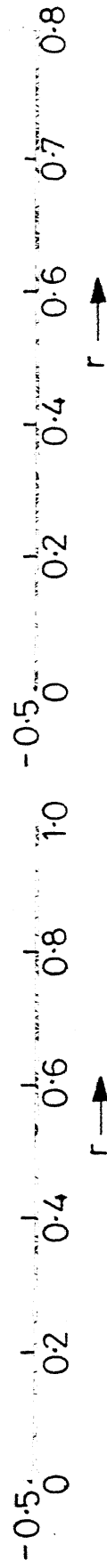


Figure 4 Effect of radius ratio on velocity at  $y=0.1$

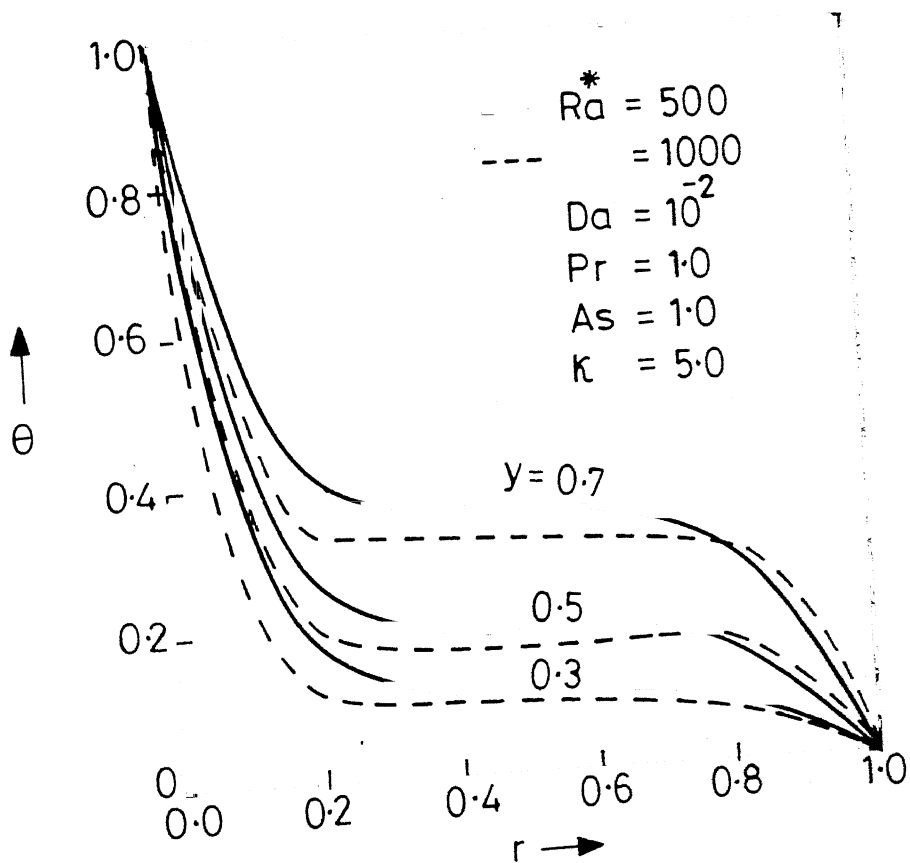


Figure 5 Temperature distribution at different heights



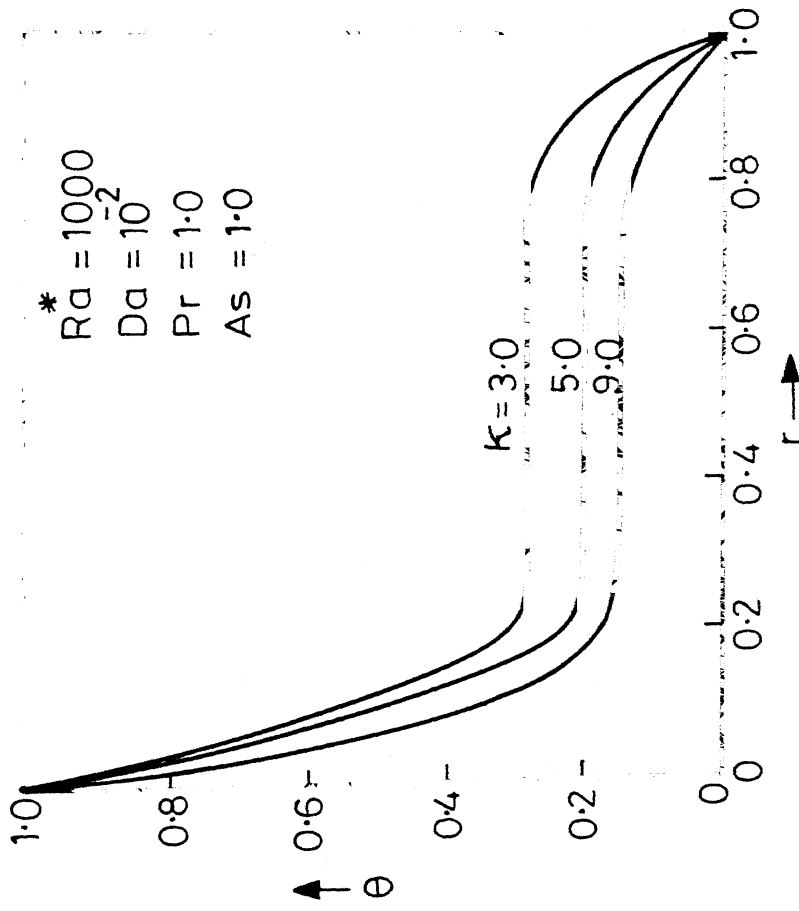


Figure 6 Temperature distribution at mid-height

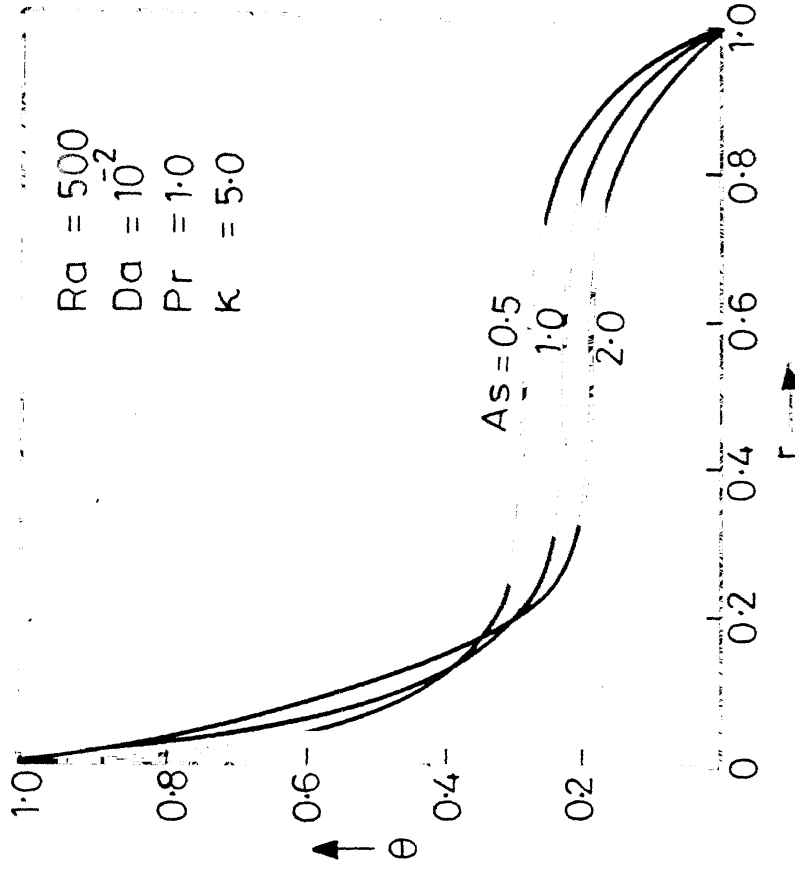


Figure 7 Temperature distribution at mid-height

15.0

10.0

$Ra^* = 1000$   
 $= 500$   
 $= 100$   
 $Da = 10^{-2}$   
 $Pr = 1.0$   
 $As = 1.0$

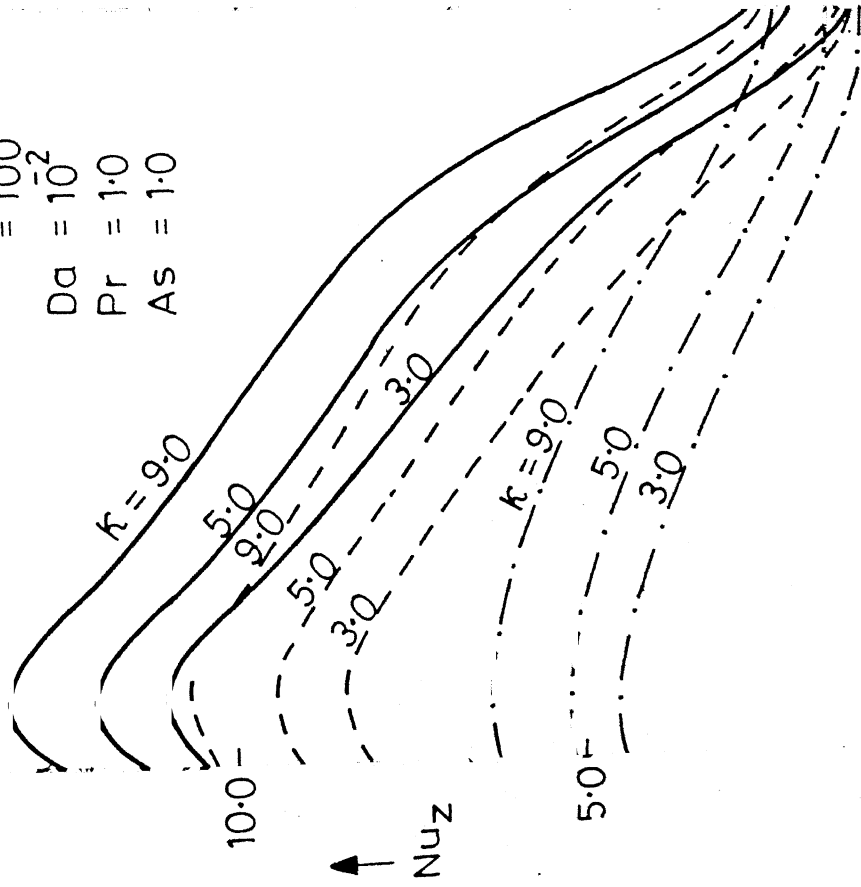


Figure 8 Local Nusselt number along the inner wall

$Ra^* = 100$   
 $Pr = 1.0$   
 $As = 1.0$   
 $\kappa = 2.0$

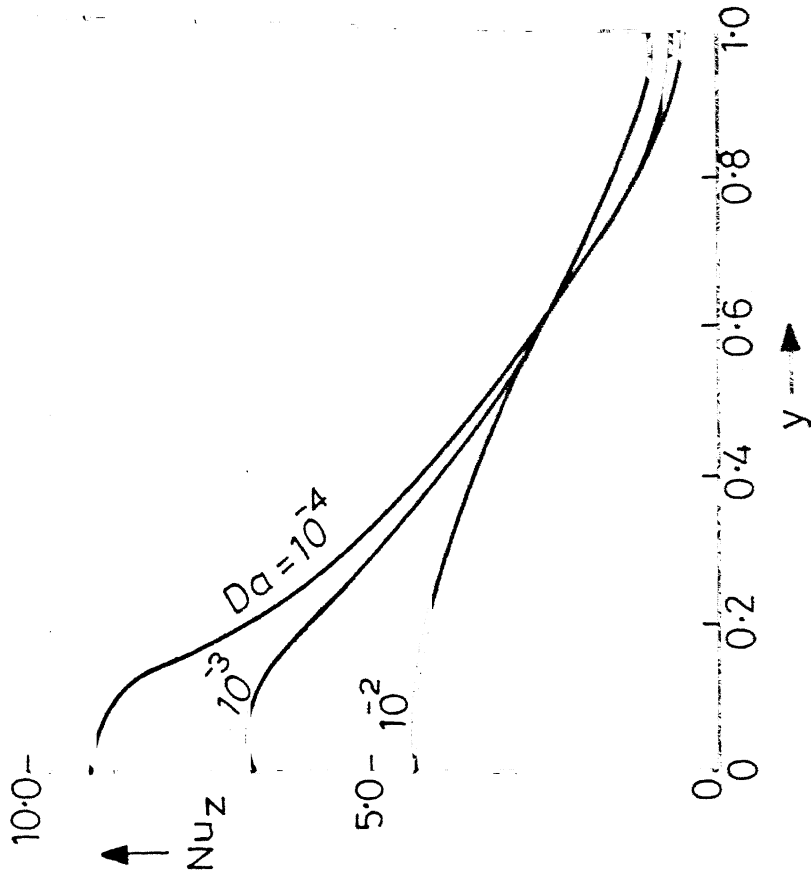


Figure 9 Local Nusselt number along the inner wall

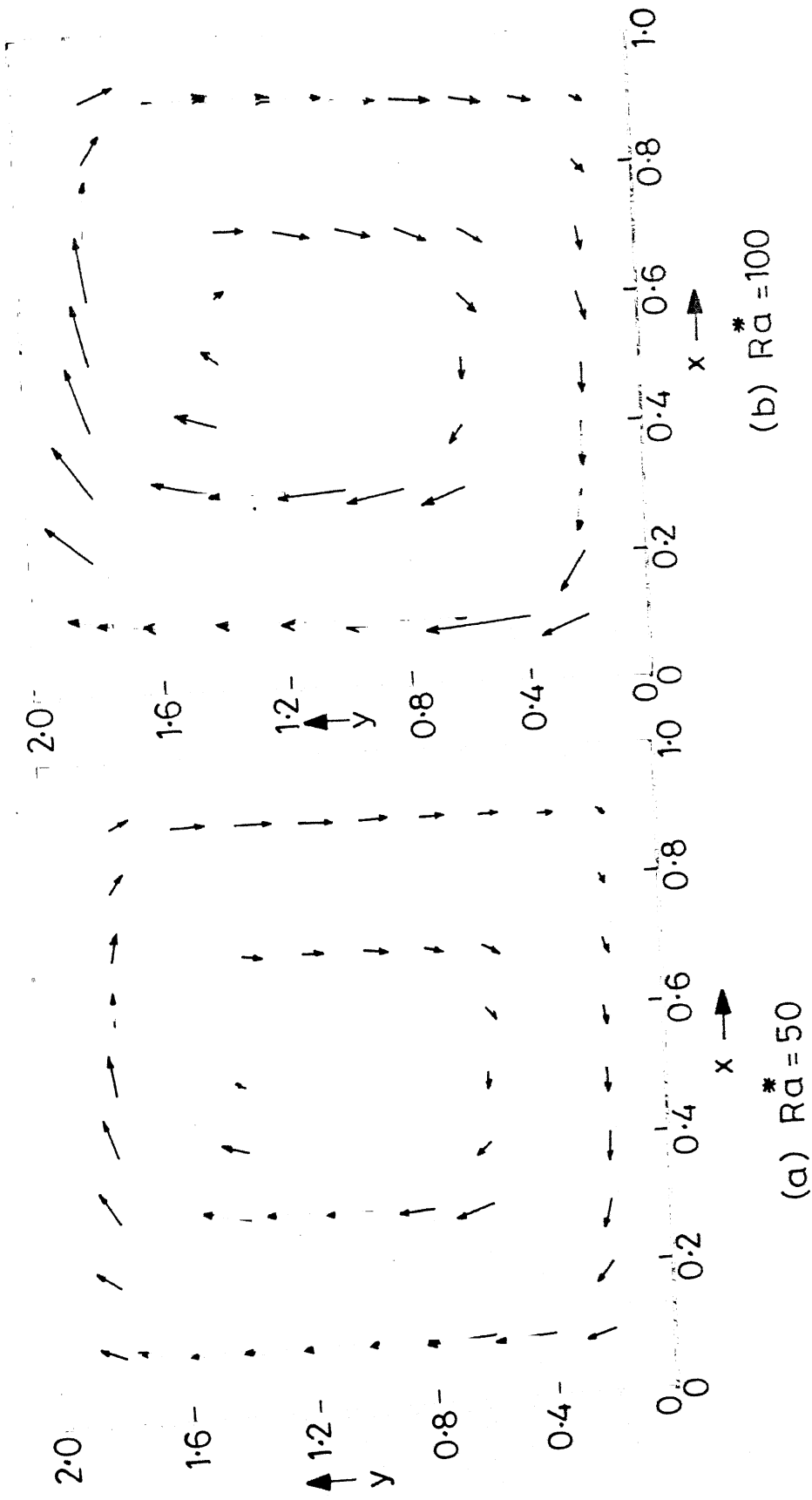


Figure 10 Velocity Vector for  $Pr = 1.0$ ,  $Da = 10^{-2}$ ,  $As = 2.0$ ,  $K = 4.0$   
 (1mm length of arrow = 1 unit of velocity)

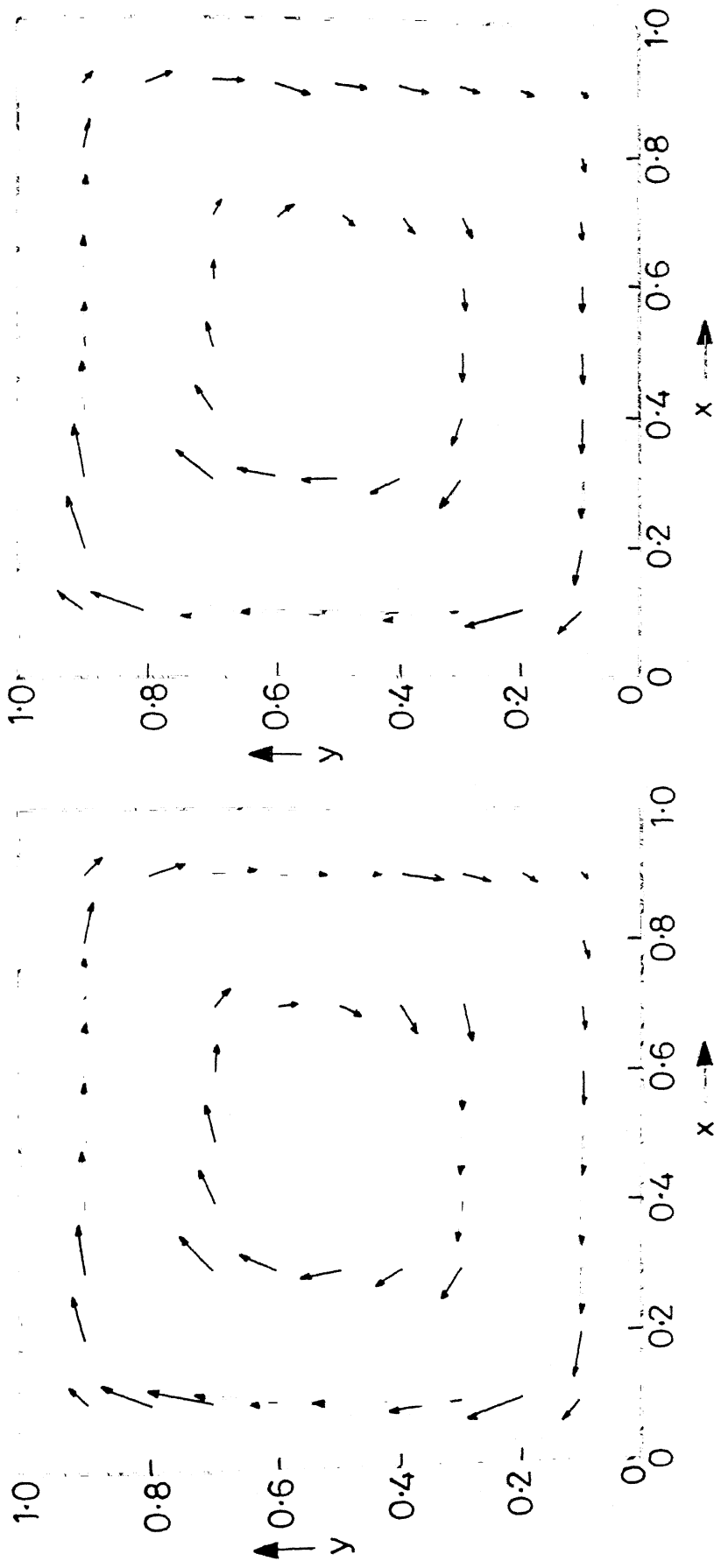
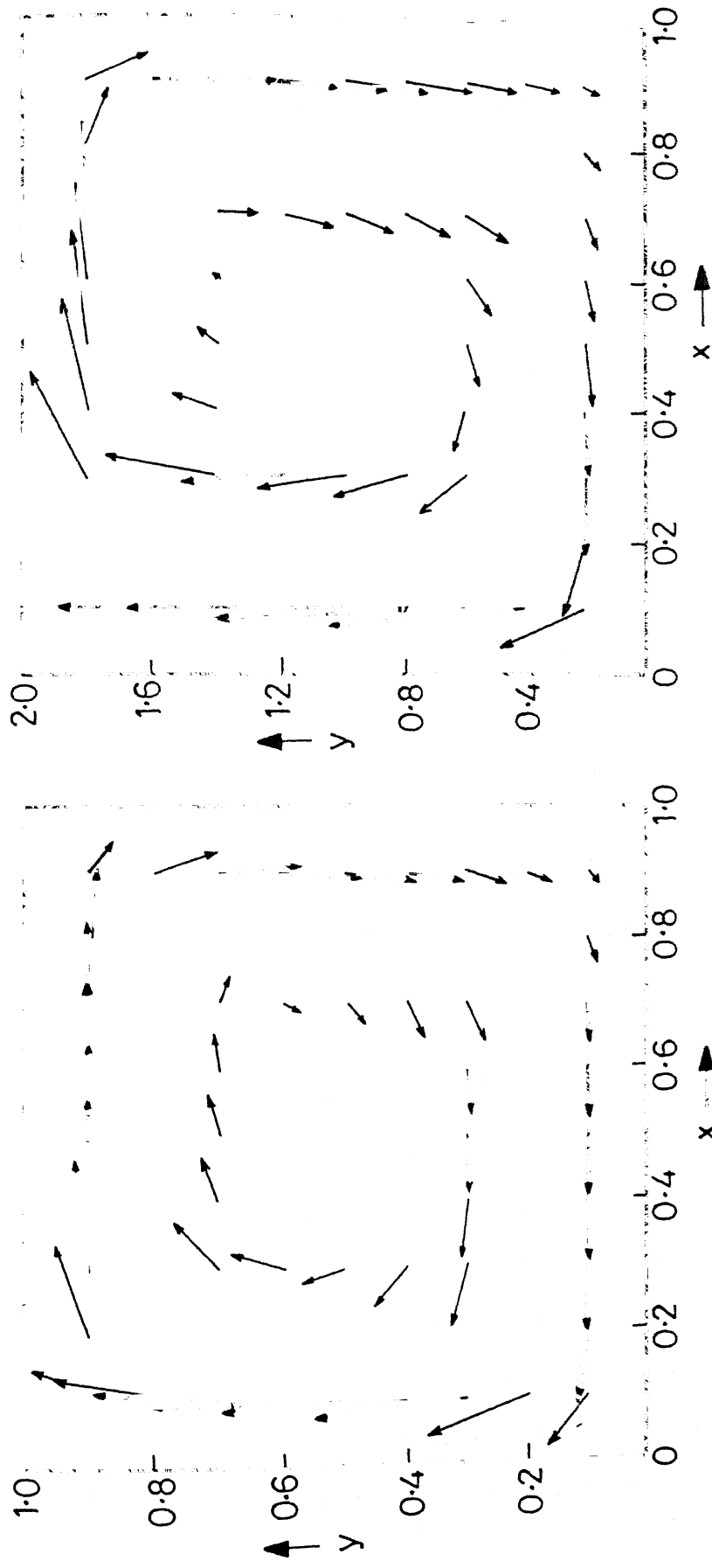


Figure 11 Velocity Vector for  $Pr=1.0$ ,  $Ra^*=100$ ,  $Da=10^{-2}$ ,  $As=1.0$   
(1mm length of arrow = 1 unit of velocity)



(a)  $As = 1.0$

(b)  $As = 2.0$

Figure 12 Velocity Vector for  $Pr=1.0$ ,  $Ra^*=250$ ,  $Da=10$ ,  $K=4.0$   
(1mm length of arrow = 1 unit of velocity)

## CHAPTER V

### A NUMERICAL STUDY OF OSCILLATORY CONVECTIVE FLOW THROUGH A POROUS MEDIUM

#### 5.1 INTRODUCTION

The problems of steady free or mixed convection adjacent to vertical flat plate embedded in a porous medium have been investigated extensively. Little attention, however, has been given to transient convection in a porous medium. The first paper on transient boundary layer flow in a porous medium is due to Johnson and Cheng (1978) who have obtained similarity solutions for specific variations of wall temperature in both time and position. Cheng and Pop (1984) presented approximate solutions for the transient free convection boundary layer in a porous medium adjacent to a vertical semi-infinite plate with a step increase in wall temperature or heat flux. Raptis (1983) considered two-dimensional unsteady free convective flow through a porous medium bounded by an infinite vertical plate, when the temperature of the plate is oscillating with time and obtained solutions with the restriction that the amplitude of oscillation is very small. Singh et al. (1986) studied the same problem without any restriction on amplitude by developing two asymptotic expansions in powers of the frequency parameter using a regular expansion technique for small frequency parameter and the method of matched asymptotic expansion for large frequency parameter.

Recently Raptis and Perdikis (1985) analyzed the effect of free convection on flow through a highly porous medium bounded by an infinite vertical wall of constant temperature absorbing the fluid with constant velocity when the free stream vibrates about a constant mean. The authors have shown their interest in the problem where the amplitude of free stream oscillations are very small. Nevertheless we may come across physical situations where the amplitude of oscillations will not be necessarily small.

With this motivation, the present work is devoted to the study of convective flow and heat transfer along an infinite vertical wall of constant temperature. The free stream temperature is also constant but differs from that of the wall. Due to differences of temperature, density gradients are setup giving rise to buoyancy forces. The fluid is being constantly absorbed by the vertical wall. The steady motion is disturbed due to oscillations in the free stream at  $t = 0$ . The velocity field subsequently differs from the steady state solution. The free stream velocity has been chosen of the form,

$$u = U_0 (1 + \epsilon \sin \omega t),$$

with no restriction on  $\epsilon$  except that it must be less than 1. The problem is solved by finite difference method using Crank Nicolson scheme. The flow behaviour has been computed for various values of  $\epsilon$ . Knowing the numerical values of the velocity field, the skin friction at the wall is computed using Newton's interpolation formula. The results obtained by this

method for small  $\epsilon$  agree satisfactorily with those given by Raptis and Perdikis (1985).

## 5.2 GOVERNING EQUATIONS

Consider an infinite vertical flat plate, with X-axis along the plate and Y-axis normal to it. The vertical plate is at constant temperature and absorbs the fluid at a constant velocity while the free stream velocity vibrates about a constant mean. We assume that all the fluid properties are constant except the density variation with temperature in the body force term. the governing equations for the problem are (Raptis and Perdikis 1985),

$$\frac{\partial V}{\partial Y} = 0, \quad (5.1)$$

$$\begin{aligned} \frac{\partial U}{\partial t'} + \nu \frac{\partial U}{\partial Y} = \frac{dU_{\infty}}{dt'} + g \beta (T - T_{\infty}) \\ + \nu \frac{\partial^2 U}{\partial Y^2} + \frac{\nu}{K'} (U_{\infty} - U), \end{aligned} \quad (5.2)$$

$$S \frac{\partial T}{\partial t'} + \nu \frac{\partial T}{\partial Y} = \alpha \frac{\partial^2 T}{\partial Y^2}. \quad (5.3)$$

The boundary conditions of the problem are,

$$Y = 0 : U = 0, V = -V_0 = \text{constant}, T = T_0.$$

$$Y \rightarrow \infty : U = U_{\infty} \rightarrow U_0 (1 + \epsilon \sin \omega' t'), T \rightarrow T_{\infty}. \quad (5.4)$$

Here,  $(U, V)$  are the velocity components along the axes,  $g$  is the acceleration due to gravity,  $\beta$  is the coefficient of thermal expansion,  $\nu$  the kinematic viscosity,  $K'$  the permeability of the porous medium,  $U_0$  a constant velocity,  $S$  is the heat capacity ratio of the fluid filled porous medium to that of fluid,  $\alpha$  the thermal diffusivity,  $T$  is the fluid temperature,  $T_0$  and  $T_{\infty}$  are



the surface temperature and temperature of the free stream and  $\epsilon$  and  $\omega'$  are amplitude and frequency of vibration of the free stream velocity respectively.

Introducing the dimensionless quantities,

$$u = \frac{U}{U_0}, \quad u^* = \frac{U_\infty}{U_0}, \quad \theta = \frac{T - T_\infty}{T_0 - T_\infty}, \quad t = \frac{t' V_0^2}{\nu}, \quad y = \frac{Y V_0}{\nu},$$

$$\omega = \frac{\nu \omega'}{V_0^2}, \quad Pr = \frac{\nu}{\alpha}, \quad Gr = \frac{\nu g \beta (T_0 - T_\infty)}{U_0 V_0^2}, \quad K = \frac{V_0^2}{\nu^2} K',$$

and substituting for the solution of the continuity equation,

$$V = -V_0 = \text{constant},$$

equations (5.2) and (5.3) become,

$$\frac{\partial u}{\partial t} - \frac{\partial u}{\partial y} = \frac{du^*}{dt} + \frac{\partial^2 u}{\partial y^2} + \frac{1}{K} (u^* - u) + Gr \theta, \quad (5.5)$$

$$S \frac{\partial \theta}{\partial t} - \frac{\partial \theta}{\partial y} = \frac{1}{Pr} \frac{\partial^2 \theta}{\partial y^2}. \quad (5.6)$$

The boundary conditions reduce to,

$$y = 0 : u = 0, \theta = 1,$$

$$y \rightarrow \infty : u \rightarrow 1 + \epsilon \sin \omega t, \theta \rightarrow 0. \quad (5.7)$$

### 5.3 SOLUTION OF THE TEMPERATURE FIELD

Since the suction velocity is constant, the temperature field remains unperturbed and hence the equation (5.6) takes the form,

$$Pr \frac{\partial \theta}{\partial y} + \frac{\partial^2 \theta}{\partial y^2} = 0. \quad (5.8)$$

The solution of (5.8) together with the boundary conditions (5.7) is given by,

$$\theta = e^{-Pr y}. \quad (5.9)$$

#### 5.4 NUMERICAL SOLUTION FOR THE VELOCITY FIELD

Substituting the expression for  $\theta$  from (5.9), the equation (5.5) is reduced to,

$$\frac{\partial u}{\partial t} - \frac{\partial u}{\partial y} = \frac{du^*}{dt} + \frac{\partial^2 u}{\partial y^2} + \frac{1}{K} (u^* - u) + Gr e^{-Pr y} \quad (5.10)$$

Equation (5.10) is to be solved numerically, together with the boundary conditions,

$$\begin{aligned} y = 0 : u &= 0, \\ y \rightarrow \infty : u &\rightarrow 1 + \epsilon \sin \omega t. \end{aligned} \quad (5.11)$$

The initial condition is obtained by solving the steady state equation corresponding to (5.10) which is given by,

$$t = 0 : u = 1 + \left\{ \frac{Gr}{(Pr + R_1)(Pr + R_2)} - 1 \right\} e^{R_1 y} - \frac{Gr e^{-Pr y}}{(Pr + R_1)(Pr + R_2)}, \quad (5.12)$$

$$\text{where, } R_1 = \frac{-1 - \sqrt{1 + 4/K}}{2} \text{ and } R_2 = \frac{-1 + \sqrt{1 + 4/K}}{2}.$$

The finite difference representation chosen for equation (5.10) is,

$$\begin{aligned} & \frac{u_{i,j+1} - u_{i,j}}{\Delta t} - \frac{1}{2} \left\{ \frac{u_{i+1,j+1} - u_{i,j+1}}{\Delta y} + \frac{u_{i+1,j} - u_{i,j}}{\Delta y} \right\} \\ &= \epsilon \omega \cos \omega j \Delta t + \frac{1}{2} \left\{ \frac{u_{i-1,j+1} - 2u_{i,j+1} + u_{i+1,j+1}}{(\Delta y)^2} \right. \\ & \quad \left. + \frac{u_{i-1,j} - 2u_{i,j} + u_{i+1,j}}{(\Delta y)^2} \right\} \\ & \quad + \frac{1}{K} \left\{ 1 + \epsilon \sin \omega j \Delta t - \frac{u_{i,j+1} + u_{i,j}}{2} \right\} + Gr e^{-Pr i \Delta y}. \end{aligned} \quad (5.13)$$

and the initial and boundary conditions take the form,

$$u_{i,0} = 1 + \left\{ \frac{Gr}{(Pr + R_1)(Pr + R_2)} - 1 \right\} e^{R_1 i \Delta y} - \frac{Gr e^{-Pr i \Delta y}}{(Pr + R_1)(Pr + R_2)},$$

$$u_{0,j} = 0. \quad (5.14)$$

$$u_{n+1,j} = 1 + \epsilon \sin \omega j \Delta t$$

The subscripts  $i$  and  $j$  appearing in (5.13) and (5.14) correspond to  $y$  and  $t$  respectively.

Equation (5.13) written for  $i = 1(1)n$  constitutes  $n$  linear equations in  $n$  unknowns,  $u_{i,j+1}$ , where  $n$  refers to the number of mesh points on  $y$ -axis. These equations may be written in the matrix form in which the coefficient matrix is tridiagonal and the method of Gaussian elimination is used to obtain a solution for  $u_{i,j+1}$ .

Knowing the numerical values of velocity field, the skin friction at the wall is calculated. In dimensionless form it is given by,

$$\tau = \left. \frac{\partial u}{\partial y} \right|_{y=0}.$$

This has been calculated by numerical differentiation using Newton's interpolation formula.

## 5.5 RESULTS AND DISCUSSION

The approximate analytical results obtained by Raptis and Perdakis (1985), for very small values of  $\epsilon$  show that  $u$  vary insignificantly after  $y \approx 7.5$ . Hence any value of  $y$  after 7.5 may be chosen to correspond to  $y \rightarrow \infty$ . To save computation time,

8.0 has been chosen to correspond to  $y \rightarrow \infty$ . In the entire computation,  $\Delta y$  and  $\Delta t$  are taken to be equal to 0.1 and 0.005 respectively. The solution procedure is repeated to get velocity field at different time step until  $t = 3.0$ . The computations are carried out for  $Pr = 0.71$ ;  $Gr = 1.0, 3.0$ ;  $K = 1.0, 4.0, 8.0$ ;  $\omega = 5.0$  and  $\epsilon = 0.1, 0.2, 0.5, 0.8$  on a DEC 1090 computer.

To see the correctness of taking  $y = 8.0$  corresponding to  $y \rightarrow \infty$ , we have also run the program for other values of  $y$  such as 8.5 and 9.0 corresponding to  $y \rightarrow \infty$  and we get the same numerical values for  $u$ . To judge the convergence of the numerical method used, different values of  $\Delta t$  such as  $\Delta t = 0.002, 0.003$  are chosen and no significant changes in the results are observed.

For the purpose of discussing the results, the velocity profiles are shown in Figures 1 and 2. The velocity field increases rapidly, attains its maximum and then decreases and at  $y \approx 8.0$  there is no significant variation.

In Figure 2, the velocity profiles are drawn for  $Pr = 0.71$ ,  $Gr = 1.0$ ,  $K = 4.0$ ,  $\omega = 5.0$ ,  $t = 1.5$  and for four different values of  $\epsilon = 0.1, 0.2, 0.5, 0.8$ . The velocity profiles have the same shape for all values of  $\epsilon$  but the maximum velocity which corresponds to  $y \approx 2.0$  increases significantly with the increase in  $\epsilon$ .

Figure 3, shows the variation in velocity with  $y$  for different values of  $Gr$  and  $K$ , when  $Pr = 0.71$ ,  $\epsilon = 0.8$ ,  $\omega = 5.0$  and  $t = 1.5$ . The velocity is shown to increase with  $Gr$  and  $K$  and the difference of the velocity are greater as  $Gr$  increases.

Figure 4 illustrates the variation in skin friction at the wall with time. Curves are drawn for  $Pr = 0.71$ ,  $Gr = 1.0$ ,  $K = 4.0$ ,  $\omega = 5.0$  and  $\epsilon = 0.2, 0.5$  and  $0.8$ . The skin friction at the wall is oscillatory in nature and the amplitude of oscillations increases with  $\epsilon$ .

The results obtained by the present numerical technique for small values of  $\epsilon$  are compared with the analytical approximate solutions of Raptis and Perdakis (1985) in Table 1. All the numerical results are calculated for the case in which the free stream velocity is of the form,

$$U_{\infty} = U_0 (1 + \epsilon \sin \omega t) .$$

The values of velocity distribution are found within 3 percent difference when  $\epsilon = 0.1$  but the difference increases slightly when  $\epsilon = 0.2$  as can be seen from Table 1. It is evident that as  $\epsilon$  increases the error involved in the analytical approximate method is more. Therefore, the present numerical method is preferable to the analytical method for solving this problem even for very small values of  $\epsilon$ . There is no solution available in the literature to compare present numerical results for larger values of  $\epsilon$ .

Table 1: Comparison of velocity distribution obtained by the approximate analytical method and the present numerical method for  $Pr = 0.71$ ,  $Gr = 1.0$ ,  $K = 1.0$ ,  $\omega = \frac{\pi}{2}$ ,  $t = \frac{1}{2}$ .

$\varepsilon$	$y$	$u$		% difference
		Analytical	Numerical	
0.1	0.2	0.4236	0.4111	2.95
	0.5	0.8187	0.8004	2.24
	1.0	1.1128	1.0982	1.31
	1.5	1.1960	1.1876	0.70
	2.0	1.2005	1.1965	0.33
	3.0	1.1554	1.1550	0.03
	4.0	1.1164	1.1167	0.03
	5.0	1.0940	1.0942	0.02
	6.0	1.0823	1.0823	0.00
0.2	0.2	0.4512	0.4371	3.13
	0.5	0.8705	0.8494	2.42
	1.0	1.1807	1.1631	1.49
	1.5	1.2677	1.2570	0.84
	2.0	1.2725	1.2670	0.43
	3.0	1.2266	1.2258	0.06
	4.0	1.1873	1.1874	0.01
	5.0	1.1647	1.1650	0.03
	6.0	1.1531	1.1531	0.00

## REFERENCES

- Cheng, P., and Pop, I., 1984, "Transient free convection about a vertical flat plate embedded in a porous medium", Int. J. Engng. Sci., Vol. 22, pp. 253-264.
- Johnson, C.H., and Cheng, P., 1978, "Possible similarity solutions for free convection boundary layers adjacent to flat plates in porous media", Int. J. Heat Mass Transfer, Vol. 21, pp. 709-718.
- Raptis, A., 1983, "Unsteady free convective flow through a porous medium", Int. J. Engng. Sci., Vol. 21, pp. 345-348.
- Raptis, A., and Perdikis, C.P., 1985, "Oscillatory flow through a porous medium by the presence of free-convective flow", Int. J. Engng. Sci., Vol. 23, pp. 51-55.
- Singh, P., Misra, J.K., and Narayan, K.A., 1986, "A mathematical analysis of unsteady flow and heat transfer in a porous medium", Int. J. Engng. Sci., Vol. 24, pp. 277-287.

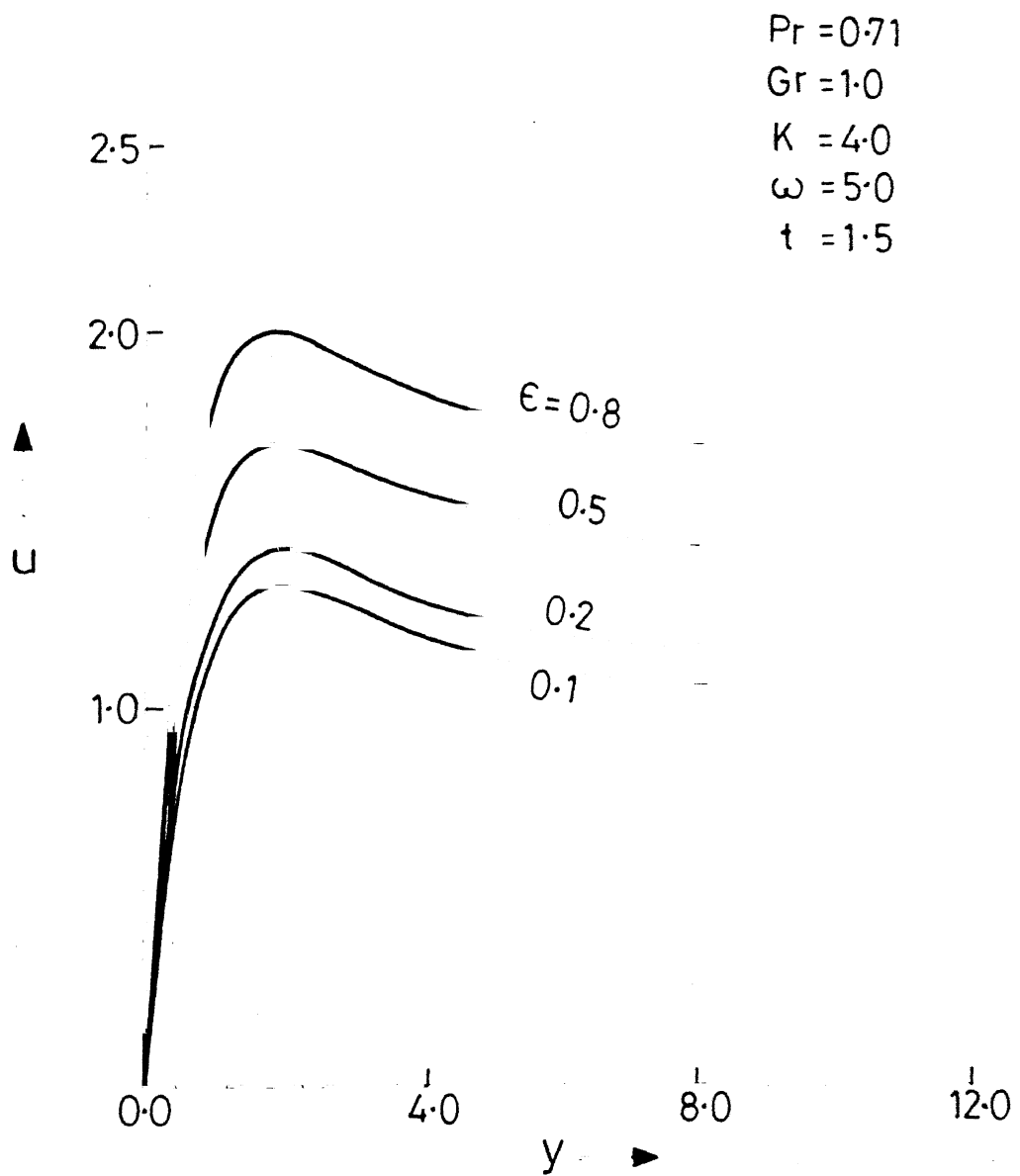


Figure 1 Variation in  $u$  velocity with  $y$



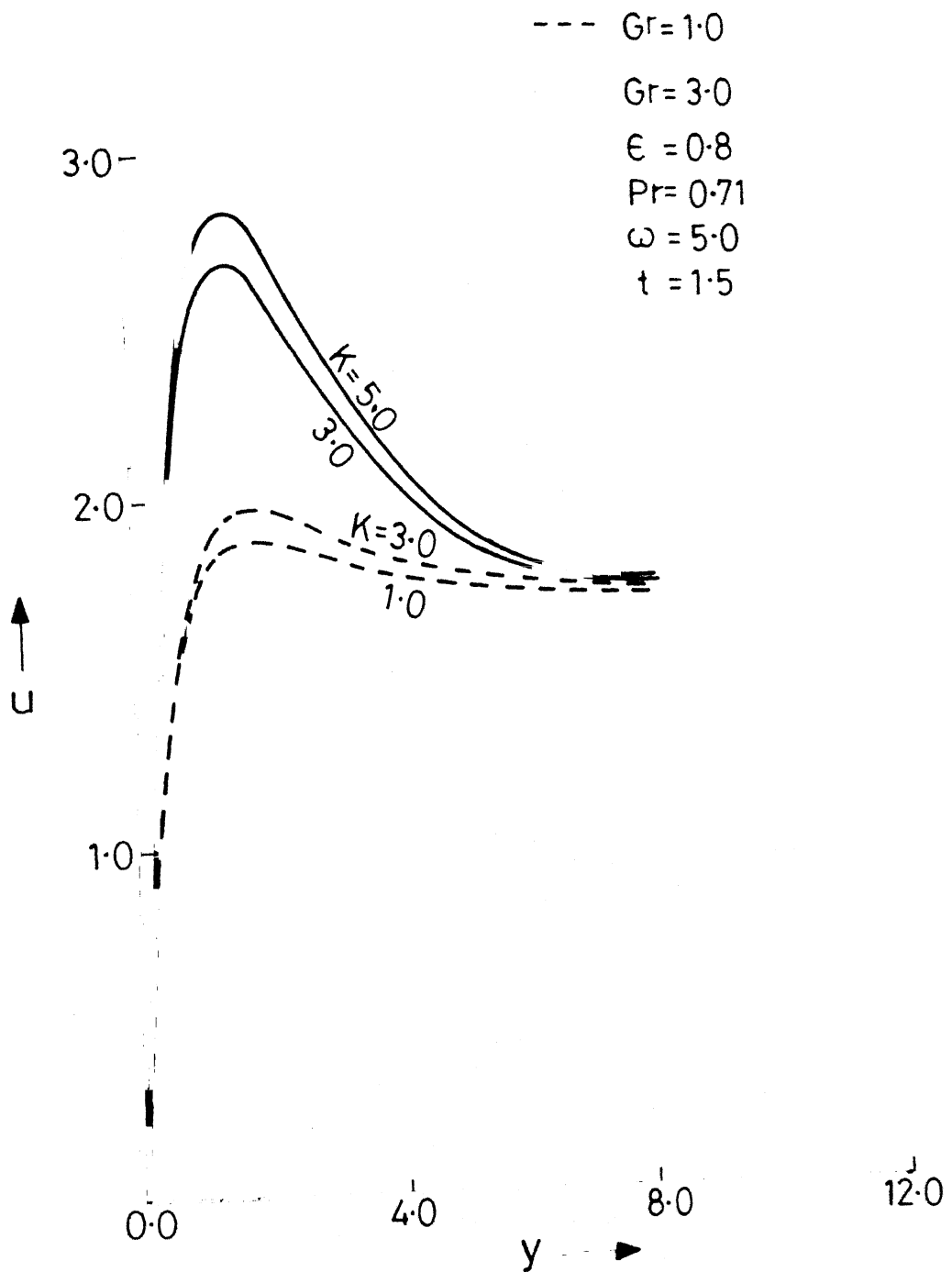


Figure 2 Variation in  $u$  velocity with  $y$

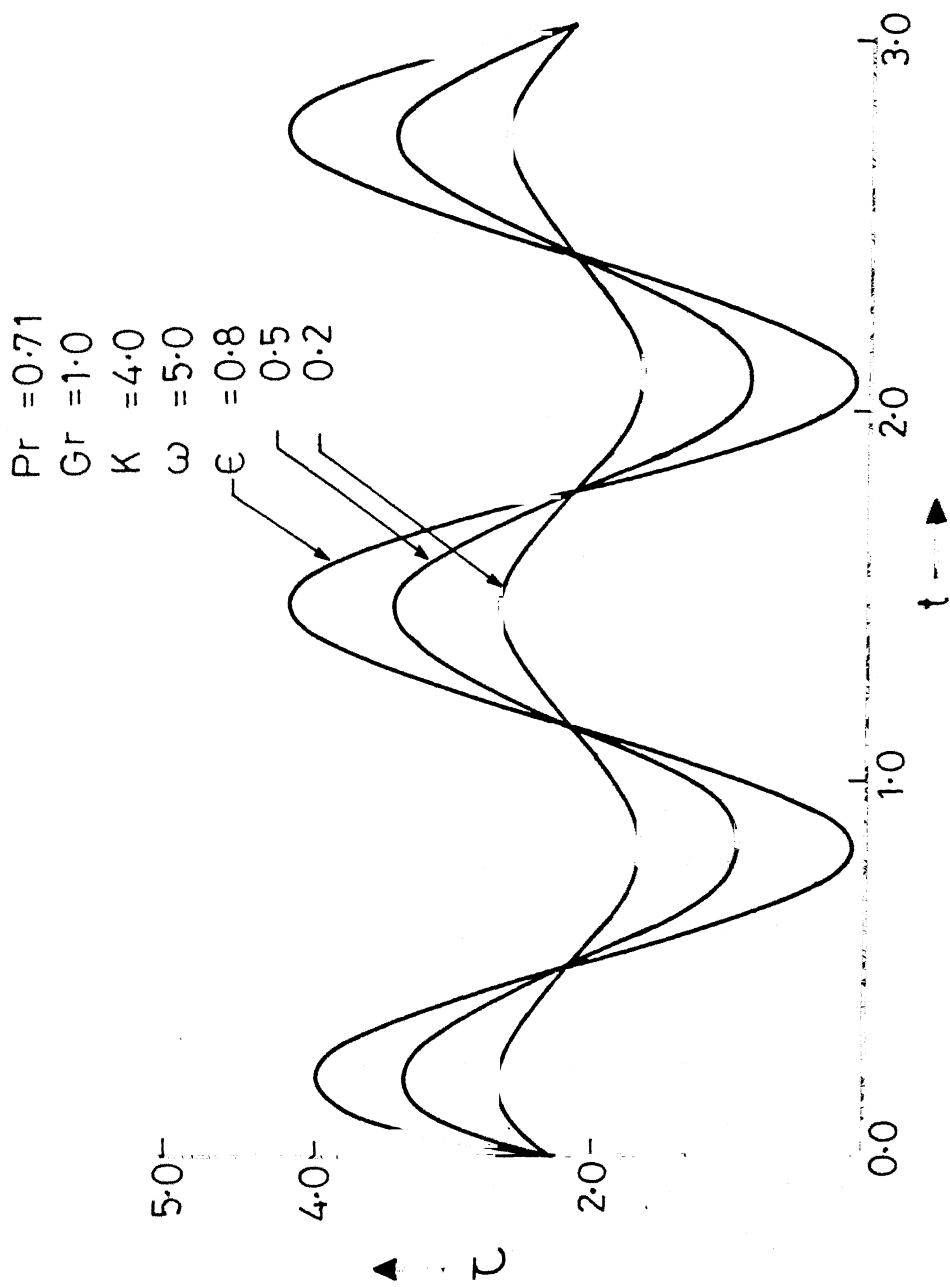


Figure 3 Variation of skin friction with time

## CHAPTER VI

### APPLICATION OF A THERMODYNAMIC METHOD TO BENARD CONVECTION IN HORIZONTAL POROUS LAYER

#### 6.1 INTRODUCTION

Present chapter deals with the breakdown of stability of a layer of fluid subject to a vertical temperature gradient in a porous medium bounded by two horizontal rigid walls. The Benard convection is the name used to describe the motions arising from the thermal instability of a thin horizontal layer of fluid when a steady temperature gradient is maintained across it. When a fluid filled porous layer is heated from below, a somewhat similar physical problem arises and was first studied theoretically by Lapwood (1948). Reviews of the contemporary investigations of the onset of convection in porous media have been presented by Cheng (1978), Nield (1985) and Bejan (1987). Recently, Lebon and Cloot (1986) employed extended irreversible thermodynamics to study natural convection in a thin porous layer heated from below. With few exceptions, most of the studies are based on either Darcy's law or Brinkman model.

The main aim of the present study is to apply a thermodynamic method to obtain neutral stability curve when a steady temperature contrast is maintained across a thin horizontal saturated porous medium bounded by two rigid walls. The generalized momentum equation is used to analyze the

problem, which has no exact solution and a variational technique based on the governing principle of dissipative processes (GPDP) proposed by Gyarmati (1969, 1970) is employed. The principle is quite applicable to various dissipative systems and is widely used to study the flow and heat transfer by Vincze (1973), Stark (1974), Singh (1976, 1980) and Singh and Raj (1985). The most general form of GPDP is represented by ,

$$\delta \int_V (\sigma - \psi - \phi) dV = 0 , \quad (6.1)$$

for any instant of time under the constraints that the balance equations ,

$$\dot{\rho}_i + \nabla \cdot J_i = \sigma_i, \quad (i = 1, 2, \dots, f) , \quad (6.2)$$

are satisfied. Here  $\sigma$  denotes the entropy production per unit volume and unit time.  $\psi$  and  $\phi$  are the local dissipation potentials and the integration is considered over the total volume  $V$  of the continuum.  $\dot{\rho}_i$  is the partial time derivative of the density  $\rho_i$ ,  $J_i$  is the corresponding current density and  $\sigma_i$  is the production per unit volume and unit time of the various attributes of the system. The entropy production,  $\sigma$ , in the case of irreversible processes taking place in continuum can always be written in the following bilinear form ,

$$\sigma = \sum_{i=1}^f J_i \cdot X_i \geq 0 , \quad (6.3)$$

where,  $J_i$  and  $X_i$  are the thermodynamic currents and forces respectively. Due to the second law of thermodynamics  $\sigma$  is a positive definite quantity. According to the Onsager's linear

theory of irreversible processes, the currents  $J_i$  and the dissipative forces  $X_i$  are given by the following constitutive laws,

$$J_i = \sum_{k=1}^f L_{ik} X_k, \quad X_i = \sum_{k=1}^f R_{ik} J_k, \quad (i, 1, 2, \dots, f), \quad (6.4)$$

where, the phenomenological coefficients  $L_{ik}$  and  $R_{ik}$  represent conductivities and resistances, respectively and are constants. They satisfy the famous Onsager's reciprocal relations ,

$$L_{ik} = L_{ki}, \quad R_{ik} = R_{ki}, \quad (i, k = 1, 2, \dots, f), \quad (6.5)$$

and their matrices are mutually reciprocal, i.e.,

$$\sum_{m=1}^f L_{im} R_{mk} = \sum_{m=1}^f R_{im} L_{mk} = \delta_{ik}, \quad (i, k = 1, 2, \dots, f). \quad (6.6)$$

Here,  $\delta_{ik}$  is the Kronecker symbol. The local dissipation potentials are the homogeneous quadratic functions of forces and currents respectively. These are defined as (Gyarmati 1970),

$$\psi = \frac{1}{2} \sum_{i,k=1}^f L_{ik} X_i \cdot X_k \geq 0, \quad (6.7)$$

$$\phi = \frac{1}{2} \sum_{i,k=1}^f R_{ik} J_i \cdot J_k \geq 0. \quad (6.8)$$

Since in the case of transport processes the forces can always be generated as the gradients of certain scalar parameters  $\Gamma_i$ , the thermodynamic forces,  $X_i$ , may be expressed as ,

$$X_i = \nabla \Gamma_i, \quad (6.9)$$

Using (6.3), (6.7), (6.8) and (6.9) the principle (6.1) takes the form ,

$$\delta \int_V \left[ \sum_{i=1}^f J_i \cdot \nabla \Gamma_i - \frac{1}{2} \sum_{i,k=1}^f L_{ik} \nabla \Gamma_i \cdot \nabla \Gamma_k - \frac{1}{2} \sum_{i,k=1}^f R_{ik} J_i \cdot J_k \right] dV = 0 . \quad (6.10)$$

## 6.2 THE DUAL FIELD METHOD

The two sets of independent variables  $[J_1, J_2, \dots, J_f]$  and  $[\nabla \Gamma_1, \nabla \Gamma_2, \dots, \nabla \Gamma_f]$  are connected with each other by the relations (6.4). In the dual field method we assume one set of these variables and obtain the other set with the help of the constitutive relations. In the irreversible transport phenomena, the variables  $\Gamma_i$  are fundamental ones, since their gradients,  $\nabla \Gamma_i$ , are the driving forces of dissipative transport processes. We, therefore, approximate the set  $[\nabla \Gamma_1, \nabla \Gamma_2, \dots, \nabla \Gamma_f]$  by another set  $[\nabla \Gamma_1^*, \nabla \Gamma_2^*, \dots, \nabla \Gamma_f^*]$ . Consequently the corresponding current densities are obtained by the following constitutive equations ,

$$J_i = \sum_{k=1}^f L_{ik} [\Gamma_1, \Gamma_2, \dots, \Gamma_f] \nabla \Gamma_k^* , \quad (i = 1, 2, \dots, f) . \quad (6.11)$$

It is remarkable that the duality property of the governing principle is preserved and the two sets of fundamental variables  $\Gamma_i$  and  $\Gamma_i^*$  coincide in the case of exact solution. The principle (6.10) with the help of (6.11) takes the form ,

$$\delta \int_V \left[ \sum_{i,k=1}^f \left( -\frac{1}{2} L_{ik} (\nabla \Gamma_i - \nabla \Gamma_i^*) \cdot (\nabla \Gamma_i - \nabla \Gamma_i^*) \right) \right] dV = 0, \quad (6.12)$$

which together with the balance equations ,

$$\dot{\rho}_i(\Gamma_i) + \sum_{k=1}^f \nabla \cdot (L_{ik} \nabla \Gamma_k^*) = \sigma(\Gamma_i), \quad (i = 1, 2, \dots, f), \quad (6.13)$$

serves the basis for the dual field method. We can, again, approximate the fundamental field  $\Gamma^{(n)}$  in the following form ,

$$\Gamma^{(n)} = \sum_{i=1}^n \alpha_i(t) g_i(\bar{x}), \quad (6.14)$$

where,  $[g_i(\bar{x})]_{i=1}^n$  are a set of linearly independent functions which satisfy the boundary conditions imposed on  $\Gamma$ . The coefficients,  $\alpha_i(t)$  are the variational parameters to be determined with the help of the principle. The balance equation takes the form ,

$$\frac{\partial \rho(\Gamma^{(n)})}{\partial t} + \nabla \cdot (L(\Gamma^{(n)}) \nabla \Gamma^{*(n)}) = \sigma(\Gamma^{(n)}), \quad (6.15)$$

where, the current density  $J$  is replaced by the constitutive law

$$J = L(\Gamma) \nabla \Gamma^*, \quad (6.16)$$

which, follows from the general constitutive laws (6.11). The balance equation (6.15) serves the purpose to determine the field  $\Gamma^*$  in the form  $\Gamma^{*(n)}$  and the solution of (6.15) with the appropriate boundary conditions may be written as ,

$$\Gamma^* \equiv \Gamma^{*(n)} = \Gamma^{*(n)}(\bar{x}, t, \alpha_1, \dots, \alpha_n, \dot{\alpha}_1, \dots, \dot{\alpha}_n). \quad (6.17)$$

The volume integral (6.12) is maximum at any instant of time for the real physical processes, that is; for the exact value of the

parameters  $\Gamma_i$  and the current densities  $J_i$ . It is fundamentally important that the maximum is zero for any time (Gyarmati 1969). In the application of approximate procedure, the volume integral generally becomes a function of time and therefore the volume integral may be integrated over the time interval  $0 < t < \infty$  during which the process is considered. Thus the principle (6.12) becomes ,

$$\delta \int_0^\infty \int_V \left[ -\frac{1}{2} L (\nabla \Gamma - \nabla \Gamma^*) \cdot (\nabla \Gamma - \nabla \Gamma^*) \right] dV dt = 0 . \quad (6.18)$$

In (6.18) we have confined our treatment for the case of one,  $\Gamma$ , parameter. The total variation of the principle (6.18) with the values of  $\Gamma$  and  $\Gamma^*$  from (6.14) and (6.17) becomes ,

$$\begin{aligned} & \int_V \left[ \left\{ \frac{\partial \rho^{(n)}}{\partial t} + \nabla \cdot (L^{(n)} \nabla \Gamma^{(n)}) - \sigma^{(n)} \right\} \frac{\partial \Gamma^{(n)}}{\partial \alpha_i} \right. \\ & + \frac{1}{2} \left[ \nabla \Gamma^{(n)} - \nabla \Gamma^{*(n)} \right] \frac{\partial L^{(n)}}{\partial \Gamma^{(n)}} \frac{\partial \Gamma^{(n)}}{\partial \alpha_i} \\ & + \left\{ \frac{\partial \rho^{(n)}}{\partial t} + \nabla \cdot (L^{(n)} \nabla \Gamma^{(n)}) - \sigma^{(n)} \right\} \frac{\partial \Gamma^{*(n)}}{\partial \alpha_i} \\ & - \frac{d}{dt} \left[ \left\{ \frac{\partial \rho^{(n)}}{\partial t} + \nabla \cdot (L^{(n)} \nabla \Gamma^{(n)}) - \sigma^{(n)} \right\} \frac{\partial \Gamma^{*(n)}}{\partial \alpha_i} \right] \Big] dV \\ & + \int_\Omega \left[ \left\{ L^{(n)} \nabla \Gamma^{(n)} - L^{(n)} \nabla \Gamma^{*(n)} \right\} \frac{\partial \Gamma^{(n)}}{\partial \alpha_i} \right. \\ & + \left\{ L^{(n)} \nabla \Gamma^{(n)} - L^{(n)} \nabla \Gamma^{*(n)} \right\} \frac{\partial \Gamma^{*(n)}}{\partial \alpha_i} \\ & - \frac{d}{dt} \left[ \left\{ L^{(n)} \nabla \Gamma^{(n)} - L^{(n)} \nabla \Gamma^{*(n)} \right\} \frac{\partial \Gamma^{*(n)}}{\partial \alpha_i} \right] \Big] \cdot d\Omega = 0 , \\ & (i = 1, 2, \dots, n) \quad (6.19) \end{aligned}$$



$$\begin{aligned}
& \text{and } \int_V \left[ \frac{\partial \rho^{(n)}}{\partial t} + \nabla \cdot (L^{(n)} \nabla \Gamma^{(n)}) - \sigma^{(n)} \right] \frac{\partial \Gamma^{*(n)}}{\partial \dot{\alpha}_i} \Big|_{t=\infty} dv \\
& + \int_{\Omega} \left[ L^{(n)} \nabla \Gamma^{(n)} - L^{(n)} \nabla \Gamma^{*(n)} \right] \frac{\partial \Gamma^{*(n)}}{\partial \dot{\alpha}_i} \Big|_{t=\infty} \cdot d\Omega = 0, \\
& (i = 1, 2, \dots, n). \quad (6.20)
\end{aligned}$$

In (6.20), the subscript denotes that the parameters,  $\alpha_i$ , are evaluated at the moment  $t = \infty$ . Taking into account the transversality conditions (6.20) and the given initial conditions, we can solve the second order ordinary differential equations (6.19) to get the parameters  $\alpha_i$  and thus the fields  $\Gamma^{(n)}$  and  $\Gamma^{*(n)}$  respectively.

### 6.3 FORMULATION OF GPDP FOR BENARD-DARCY PROBLEM

The balance equations of mass, momentum and energy for the linearized Benard convection in porous media are,

$$\nabla \cdot \mathbf{V} = 0, \quad (6.21)$$

$$\rho_0 \frac{\partial \mathbf{V}}{\partial t} + \nabla \cdot \overset{=}{\mathbf{P}} = \rho_0 g \alpha n T - \frac{\mu \mathbf{V}}{K}, \quad (6.22)$$

$$\rho_0 C_v \frac{\partial T}{\partial t} + \nabla \cdot \mathbf{J}_q = C_v \rho_0 \beta n \cdot \mathbf{V}, \quad (6.23)$$

where,  $\overset{=}{\mathbf{P}}$  is the pressure tensor and is given by ,

$$\overset{=}{\mathbf{P}} = p \delta + \overset{\circ}{\mathbf{P}}, \quad (6.24)$$

$p$  being the hydrostatic pressure and  $\overset{\circ}{\mathbf{P}}$  is the symmetrical part of the pressure tensor whose trace is zero.  $n = (0, 0, 1)$  is

the unit vector,  $\mathbf{V}$  and  $T$  are the perturbation velocity and temperature fields respectively.  $C_v$  denotes the specific heat at constant volume and  $\rho_0$  is the density at temperature  $T_0$ .  $\mathbf{J}_q$  denotes the heat current density,  $g$  is the acceleration due to gravity,  $\alpha$  the coefficient of volume expansion,  $\beta$  the temperature gradient,  $t$  the time and  $K$  represents the permeability of the porous medium.  $\delta$  is the unit tensor. In the formulation of Gyarmati's principle for thermohydrodynamical systems, it is preferable to use the energy picture of the principle. In the energy picture, the actual variable is  $\ln T$  instead of  $T$  and therefore, the balance equations (6.22) and (6.23) take the following form,

$$\rho_0 \frac{\partial \mathbf{V}}{\partial t} + \nabla \cdot \mathbf{P} = \rho_0 g \alpha \mathbf{n} \ln T - \frac{\mu \mathbf{V}}{K}, \quad (6.25)$$

$$\rho_0 C_v \frac{\partial \ln T}{\partial t} + \nabla \cdot \mathbf{J}_q = C_v \rho_0 \beta \mathbf{n} \cdot \mathbf{V}. \quad (6.26)$$

Since we use the energy picture of the principle instead of the entropy picture, we replace the entropy production,  $\sigma$ , by the energy dissipation,  $T\sigma$ . The energy dissipation for the problem is given by,

$$T\sigma = - \mathbf{J}_q \cdot \nabla \ln T - \mathbf{P} : \overset{\circ}{(\nabla \mathbf{V})}^s, \quad (6.27)$$

$$\text{where } \overset{\circ}{(\nabla \mathbf{V})}_{\alpha\beta}^s = \frac{1}{2} \left( \frac{\partial V_\alpha}{\partial x_\beta} + \frac{\partial V_\beta}{\partial x_\alpha} \right), \quad (\alpha, \beta = 1, 2, 3). \quad (6.28)$$

The linear laws in this case are ,

$$J_q = - L_\lambda \nabla \ln T, \quad (6.29a)$$

$$\begin{matrix} \circ \\ =VS \\ P \end{matrix} = - L_s \begin{matrix} \circ \\ (\nabla V)^s \end{matrix}, \quad (6.29b)$$

where,  $L_\lambda = \lambda$  is the coefficient of heat conduction and  $L_s = 2\mu$ ,  $\mu$  being the coefficient of viscosity. The dissipation potentials in the energy picture are ,

$$\psi^* = T\psi = \frac{1}{2} \left[ L_\lambda (\nabla \ln T)^2 + L_s \begin{matrix} \circ \\ (\nabla V)^s \end{matrix} : \begin{matrix} \circ \\ (\nabla V)^s \end{matrix} \right], \quad (6.30)$$

$$\phi^* = T\phi = \frac{1}{2} \left[ R_\lambda (J_q^2) + R_s \begin{matrix} \circ \\ =VS \\ P \end{matrix} : \begin{matrix} \circ \\ =VS \\ P \end{matrix} \right], \quad (6.31)$$

Here  $R_\lambda = \frac{1}{\lambda}$  and  $R_s = \frac{1}{2\mu}$ .

The energy picture of Gyarmati's principle is ,

$$\delta \int_V (T\sigma - \psi^* - \phi^*) dV = 0. \quad (6.32)$$

Principle (6.32), with the help of (6.27), (6.30) and (6.31) takes the form ,

$$\begin{aligned} \delta \int_V \left[ - J_q \cdot \nabla \ln T - \begin{matrix} \circ \\ =VS \\ P \end{matrix} : \begin{matrix} \circ \\ (\nabla V)^s \end{matrix} \right. \\ \left. - \frac{\lambda}{2} (\nabla \ln T)^2 - \mu \begin{matrix} \circ \\ (\nabla V)^s \end{matrix} : \begin{matrix} \circ \\ (\nabla V)^s \end{matrix} - \frac{1}{2\lambda} J_q^2 \right. \\ \left. - \frac{1}{4\mu} \begin{matrix} \circ \\ =VS \\ P \end{matrix} : \begin{matrix} \circ \\ =VS \\ P \end{matrix} \right] dV = 0. \quad (6.33) \end{aligned}$$

The use of the following vector identities ,

$$\nabla \cdot (J_q \ln T) = \ln T (\nabla \cdot J_q) + J_q \cdot \nabla \ln T , \quad (6.34)$$

$$\nabla \cdot (P^{VS} \cdot V) = V \cdot (\nabla \cdot P^{VS}) + P^{VS} : (\nabla V)^S , \quad (6.35)$$

reduces the principle (6.33) to the form ,

$$\delta \int_V \left[ \ln T \nabla \cdot J_q - \frac{\lambda}{2} (\nabla \ln T)^2 - \frac{1}{2\lambda} J_q^2 + V \cdot (\nabla \cdot P^{VS}) - \mu (\nabla V)^S : (\nabla V)^S - \frac{1}{4\mu} P^{VS} : P^{VS} \right] dV = 0 . \quad (6.36)$$

The surface integral vanishes due to the boundary conditions on the two surfaces. Substituting the values of  $\nabla \cdot J_q$  and  $\nabla \cdot P^{VS}$  from the balance equations (6.25) and (6.26) and using (6.24), we get the principle in the following form ,

$$\delta \int_V \left[ (\ln T) (\rho_0 C_v \beta n \cdot V - \rho_0 C_v \frac{\partial \ln T}{\partial t}) - \frac{\lambda}{2} (\nabla \ln T)^2 - \frac{1}{2\lambda} J_q^2 + V \cdot (\rho_0 g \alpha n \ln T - \rho_0 \frac{\partial V}{\partial t} - \frac{\mu V}{K}) - \mu (\nabla V)^S : (\nabla V)^S - \frac{1}{4\mu} P^{VS} : P^{VS} \right] dV = 0 . \quad (6.37)$$

The pressure term vanishes from the volume integral due to the boundary conditions,

$$\begin{aligned} x_3 = 0 : V_3 &= 0, \quad \ln T = 0, \\ x_3 = d : V_3 &= 0, \quad \ln T = 0. \end{aligned} \quad (6.38)$$

#### 6.4 APPLICATION OF DUAL FIELD METHOD

We introduce a second set of variables  $\ln T^*$  and  $V^*$  which are related with the thermodynamic currents through the following constitutive equations ,

$$J_q = - L_\lambda \nabla \ln T^* , \quad (6.39)$$

$$\begin{aligned} &^0 \\ &=VS \\ P &= - L_s (^0 \nabla V^*)^s . \end{aligned} \quad (6.40)$$

Here, the coefficients  $L_\lambda$  and  $L_s$  are unchanged. It may be assumed that  $\ln T^*$  and  $V^*$  satisfy the same boundary conditions as  $\ln T$  and  $V$ . These assumed temperature and velocity fields are to be determined with the help of balance equations (6.25) and (6.26) which become now ,

$$\rho_0 \frac{\partial V}{\partial t} - \nabla \cdot (2\mu (^0 \nabla V)^s) + \nabla p = \rho_0 g \alpha n \ln T - \frac{\mu V}{K} \quad (6.41)$$

$$\rho_0 C_v \frac{\partial \ln T}{\partial t} - \nabla \cdot (\lambda \nabla \ln T^*) = C_v \rho_0 \beta n \cdot V . \quad (6.42)$$

The principle (6.37) may now be written with the help of (6.39) and (6.40) as ,

$$\begin{aligned} \delta \int_V (\ln T) (\rho_0 C_v \beta n \cdot V - \rho_0 C_v \frac{\partial \ln T}{\partial t}) - \frac{\lambda}{2} (\nabla \ln T)^2 \\ - \frac{\lambda}{2} (\nabla \ln T^*)^2 + V \cdot (\rho_0 g \alpha n \ln T - \rho_0 \frac{\partial V}{\partial t} - \frac{\mu V}{K}) \\ - \mu (^0 \nabla V)^s : (^0 \nabla V)^s - \mu (^0 \nabla V^*)^s : (^0 \nabla V^*)^s \Big] dV = 0 , \end{aligned} \quad (6.43)$$

Integrating by parts the terms containing  $\ln T^*$  and  $V^*$  and then substituting the values of  $\nabla^2 \ln T^*$  and  $\nabla^2 V^*$  from (6.41) and (6.42), the principle (6.43) reduces to ,

$$\begin{aligned} \delta \int_V & \left[ (\ln T) \left( \rho_0 C_v \beta n \cdot V - \rho_0 C_v \frac{\partial \ln T}{\partial t} \right) - \frac{\lambda}{2} (\nabla \ln T)^2 \right. \\ & - \frac{1}{2} \ln T^* \left( \rho_0 C_v \beta n \cdot V - \rho_0 C_v \frac{\partial \ln T}{\partial t} \right) \\ & + V \cdot \left( \rho_0 g \alpha n \ln T - \rho_0 \frac{\partial V}{\partial t} - \frac{\mu V}{K} \right) - \mu (\nabla V)^s : (\nabla V)^s \\ & \left. - \frac{1}{2} V^* \cdot \left( \rho_0 g \alpha n \ln T - \rho_0 \frac{\partial V}{\partial t} - \frac{\mu V}{K} \right) \right] dV = 0 . \quad (6.44) \end{aligned}$$

Here, again the pressure term vanishes due to the boundary conditions.

To evaluate the principle, we expand each perturbation  $V$  and  $\ln T$  in complete two-dimensional series of normal modes over the plane  $x_1, x_2$ , perpendicular to the thermal gradient in the following way ,

$$\begin{aligned} \ln T &= \beta d \theta(x_3) \cos \frac{a_1 x_1}{d} \cos \frac{a_2 x_2}{d} e^{\omega t} , \\ V_3 &= \frac{\nu}{d} G(x_3) \cos \frac{a_1 x_1}{d} \cos \frac{a_2 x_2}{d} e^{\omega t} , \\ V_1 &= -\frac{a_1}{a^2} \nu \frac{dG}{dx_3} \sin \frac{a_1 x_1}{d} \cos \frac{a_2 x_2}{d} e^{\omega t} , \\ V_2 &= -\frac{a_2}{a^2} \nu \frac{dG}{dx_3} \cos \frac{a_1 x_1}{d} \sin \frac{a_2 x_2}{d} e^{\omega t} , \end{aligned} \quad (6.45)$$

where,  $a = (a_1^2 + a_2^2)^{1/2}$  is the wave number of the disturbance and  $\omega$  is the frequency which in principle, may be a complex number. The velocity components  $V_1, V_2$  and  $V_3$  satisfy the

$$\left( \frac{d^2}{dz^2} - a^2 \right) \theta^* = \rho_0 C_v \frac{d^4}{\lambda} \omega \theta - \rho_0 \frac{C_v}{\lambda} \nu G, \quad (6.48)$$

$$\begin{aligned} \left( \frac{d^4}{dz^4} - 2a^2 \frac{d^2}{dz^2} + a^4 \right) G^* &= g \alpha \beta \frac{d^4}{\nu^2} a^2 \theta \\ &+ \frac{1}{Da} \left( \frac{d^2}{dz^2} - a^2 \right) G + \frac{\omega d^2}{\nu} \left( \frac{d^2}{dz^2} - a^2 \right) G. \end{aligned} \quad (6.49)$$

For the linearized Benard convection, the principle of exchange of stability is valid, that is,  $\omega$  is real (Chandrasekhar 1961). The marginal stability curve can be obtained by setting Real  $\omega = 0$ . Since  $\omega$  is real in our case, we put  $\omega = 0$  in equations (6.47), (6.48) and (6.49). Thus the equations of motion and GPD reduce to

$$\left( \frac{d^2}{dz^2} - a^2 \right) \theta^* = - \rho_0 \frac{C_v}{\lambda} \nu G, \quad (6.50)$$

$$\begin{aligned} \left( \frac{d^4}{dz^4} - 2a^2 \frac{d^2}{dz^2} + a^4 \right) G^* &= g \alpha \beta \frac{d^4}{\nu^2} a^2 \theta \\ &+ \frac{1}{Da} \left( \frac{d^2}{dz^2} - a^2 \right) G. \end{aligned} \quad (6.51)$$

$$\begin{aligned} \delta \int_0^1 &\left[ \rho_0 C_v \nu \beta^2 G \theta - \frac{\lambda \beta^2}{2} \left\{ \left( \frac{d\theta}{dz} \right)^2 + a^2 \theta^2 \right\} - \frac{1}{2} C_v \rho_0 \nu \beta^2 G \theta^* \right. \\ &+ \left\{ \rho_0 g \alpha \beta \nu G \theta - \frac{\rho_0 \nu^3}{d^4 Da} \left\{ G^2 + \frac{1}{a^2} \left( \frac{dG}{dz} \right)^2 \right\} \right. \\ &\quad \left. \left. - \frac{\rho_0 \nu^3}{2d^4} \left\{ 2 \left( \frac{dG}{dz} \right)^2 + a^2 G^2 + \frac{1}{a^2} \left( \frac{d^2 G}{dz^2} \right)^2 \right\} \right\} \right. \\ &\left. - \frac{1}{2} \left\{ \rho_0 g \alpha \beta \nu G^* \theta - \frac{\rho_0 \nu^3}{d^4 Da} \left\{ GG^* + \frac{1}{a^2} \frac{dG}{dz} \frac{dG^*}{dz} \right\} \right\} \right] dz = 0. \end{aligned} \quad (6.52)$$

The equations of motion (6.50) and (6.51), the principle (6.52) and the boundary conditions (6.47) are quite general for the linearized Benard convection in porous media and they are applicable to any kind of bounding surfaces. We shall now consider the case of two rigid bounding surfaces.

## 6.5 SOLUTION FOR RIGID SURFACES

In the case of rigid surfaces, the boundary conditions are,

$$Z = 0 : G = 0, \frac{dG}{dz} = 0, \theta = 0,$$

$$Z = 1 : G = 0, \frac{dG}{dz} = 0, \theta = 0. \quad (6.53)$$

The similar conditions are to be satisfied by  $\theta^*$  and  $G^*$ . Consistent with the above boundary conditions, we choose very simple trial functions,

$$G = A (z^2 - 2z^3 + z^4), \quad (6.54)$$

$$\theta = B (z - z^2), \quad (6.55)$$

where, A and B are the two variational parameters and are to be determined from the variational formulation (6.52). Solving the equations (6.50) and (6.51) with the help of (6.54) and (6.55), we get  $\theta^*$  and  $G^*$  as,

$$\begin{aligned} \theta^* = A \frac{\rho_0 C_v \nu}{\lambda} & \left[ \frac{z^4}{2} - \frac{2z^3}{a^2} + \frac{(a^2+12)z^2}{a^4} - \frac{12z}{a^4} \right. \\ & \left. + \frac{(2a^2+24)z^2}{a^6} + \psi_1 e^{az} + \psi_2 e^{-az} \right], \end{aligned} \quad (6.56)$$



$$\begin{aligned}
 G^* = & \frac{B}{a^2} \frac{g\alpha\beta d^4}{\nu^2} \left[ -\frac{4}{a^2} + z - z^2 + (\psi_3 z + \psi_4) e^{az} \right. \\
 & \left. + (\psi_5 z + \psi_6) e^{-az} \right] \\
 & + \frac{2A}{a^4 Da} \left[ -1 - \frac{12}{a^2} + 6z - 6z^2 - \frac{a^2 z^2}{2} + a^2 z^3 - \frac{a^2 z^4}{2} + \right. \\
 & \left. (\phi_3 z + \phi_4) e^{az} + (\phi_5 z + \phi_6) e^{-az} \right], \quad (6.57)
 \end{aligned}$$

where,

$$\psi_1 = \frac{2(a^2+12)}{a^6} \frac{e^{-a}-1}{e^a-e^{-a}}, \quad \psi_2 = \frac{2(a^2+12)}{a^6} \frac{1-e^a}{e^a-e^{-a}},$$

$$\psi_3 = \frac{b_2 d_3 - b_3 d_2}{b_2 d_1 - b_1 d_2}, \quad \psi_4 = \frac{b_1 d_3 - b_3 d_1}{b_1 d_2 - b_2 d_1},$$

$$\psi_5 = \frac{4}{a} - 1 - 2a \psi_4 - \psi_3, \quad \psi_6 = \frac{4}{a^2} - \psi_4,$$

$$\phi_3 = \frac{b_2 d_4 - b_4 d_2}{b_2 d_1 - b_1 d_2}, \quad \phi_4 = \frac{b_1 d_4 - b_4 d_1}{b_1 d_2 - b_2 d_1},$$

$$\phi_5 = \frac{12}{a} - 6 + a - 2a \phi_4 - \phi_3, \quad \phi_6 = \frac{12}{a^2} + 1 - \phi_4,$$

$$b_1 = (1+a) e^{2a} + a - 1, \quad b_2 = a e^{2a} + 2a^2 - a,$$

$$b_3 = e^a - a + 5, \quad b_4 = 6e^a + a^2 - 6a + 18,$$

$$d_1 = e^{2a} - 1, \quad d_2 = e^{2a} - 2a - 1,$$

$$d_3 = \frac{4}{a^2} (e^a - 1) + 1 - \frac{4}{a},$$

$$d_4 = \frac{12}{a^2} (e^a - 1) + e^a - a - \frac{12}{a} + 5.$$

The expressions (6.56) and (6.57) satisfy the boundary conditions,

$$Z = 0: G^* = 0, \frac{dG^*}{dz} = 0, \theta^* = 0,$$

$$Z = 1: G^* = 0, \frac{dG^*}{dz} = 0, \theta^* = 0. \quad (6.58)$$

Finally the GDPD (6.52), with the substitution of the expressions for  $\theta$ ,  $G$ ,  $\theta^*$  and  $G^*$ , becomes,

$$\begin{aligned} & \delta \left[ \rho_0 C_v \nu \beta^2 \frac{AB}{140} - \frac{\lambda \beta^2}{2} \left( \frac{1}{3} + \frac{a^2}{30} \right) B^2 \right. \\ & \quad - \frac{1}{2\lambda} (\rho_0 C_v \nu \beta)^2 \beta_1 A^2 \\ & \quad + \left[ \rho_0 \frac{k\nu^2}{d^4} R \frac{AB}{140} - \frac{\rho_0 \nu^3 A^2}{d^4 Da} \left( \frac{1}{630} + \frac{2}{105} a^2 \right) \right] \\ & \quad - \frac{\rho_0 \nu^3}{2d^4} \left( \frac{4}{105} + \frac{a^2}{630} + \frac{4}{5a^2} \right) A^2 \\ & \quad - \frac{1}{2} \rho_0 \frac{k\nu^2}{d^4} R \left( \frac{Rk}{\nu} \frac{B^2}{a^2} \beta_2 + \frac{2}{a^4 Da} \frac{AB}{Da} \beta_3 \right) \\ & \quad + \frac{1}{2} \frac{\rho_0 \nu^3}{d^4 Da} \left( \frac{Rk}{\nu} \frac{AB}{a^2} \beta_4 + \frac{2A^2}{a^4 Da} \beta_5 \right) \\ & \quad \left. + \frac{1}{2} \frac{\rho_0 \nu^3}{d^4 Da a^2} \left( \frac{2Rk}{\nu} \frac{AB}{a^2} \beta_6 + \frac{4A^2}{a^4 Da} \beta_7 \right) \right] = 0, \quad (6.59) \end{aligned}$$

where,  $R = \frac{g\alpha\beta d^4}{k\nu}$  (Rayleigh number),  $k = \frac{\lambda}{\rho_0 C_v}$ .

$$\begin{aligned} \beta_1 = \frac{1}{a^4} \left[ \frac{4}{5a^2} - \frac{2}{105} + \frac{a^2}{630} \right] + \psi_1 (C_5 - 2C_7 + C_9) \\ + \psi_2 (C_6 - 2C_8 + C_{10}), \end{aligned}$$

$$\beta_2 = \frac{1}{30} - \frac{2}{3a^2} + \psi_3 (C_5 - C_7) + \psi_4 (C_3 - C_5) \\ + \psi_5 (C_6 - C_8) + \psi_6 (C_4 - C_6) ,$$

$$\beta_3 = \frac{1}{30} - \frac{2}{a^2} - \frac{a^2}{280} + \phi_3 (C_5 - C_7) + \phi_4 (C_3 - C_5) \\ + \phi_5 (C_6 - C_8) + \phi_6 (C_4 - C_6) ,$$

$$\beta_4 = \frac{1}{140} - \frac{2}{15a^2} + \psi_3 (C_7 - 2C_9 + C_{11}) + \psi_4 (C_5 - 2C_7 + C_9) \\ + \psi_5 (C_8 - 2C_{10} + C_{12}) + \psi_6 (C_6 - 2C_8 + C_{10}) ,$$

$$\beta_5 = \frac{1}{105} - \frac{2}{5a^2} - \frac{a^2}{1260} + \phi_3 (C_7 - 2C_9 + C_{11}) \\ + \phi_4 (C_5 - 2C_7 + C_9) + \phi_5 (C_8 - 2C_{10} + C_{12}) \\ + \phi_6 (C_6 - 2C_8 + C_{10}) ,$$

$$\beta_6 = \frac{1}{30} + \psi_3 \{ (C_3 - 3C_5 + 2C_7) + a (C_5 - 3C_7 + 2C_9) \} \\ + a \psi_4 (C_3 - 3C_5 + 2C_7) \\ + \psi_5 \{ (C_4 - 3C_6 + 2C_8) - a (C_6 - 3C_8 + 2C_{10}) \} \\ - a \psi_6 (C_4 - 3C_6 + 2C_8) ,$$

$$\beta_7 = \frac{1}{5} - \frac{a^2}{210} + \phi_3 \{ (C_3 - 3C_5 + 2C_7) + a (C_5 - 3C_7 + 2C_9) \} \\ + a \psi_4 (C_3 - 3C_5 + 2C_7) \\ + \phi_5 \{ (C_4 - 3C_6 + 2C_8) - a (C_6 - 3C_8 + 2C_{10}) \} \\ - a \psi_6 (C_4 - 3C_6 + 2C_8) ,$$

$$C_1 = \int_0^1 e^{az} dz = \frac{e^a - 1}{a},$$

$$C_2 = \int_0^1 e^{-az} dz = \frac{1 - e^{-a}}{a},$$

$$C_3 = \int_0^1 ze^{az} dz = \frac{e^a}{a} - \frac{C_1}{a},$$

$$C_4 = \int_0^1 ze^{-az} dz = -\frac{e^{-a}}{a} + \frac{C_2}{a},$$

$$C_5 = \int_0^1 z^2 e^{az} dz = \frac{e^a}{a} - \frac{2C_3}{a},$$

$$C_6 = \int_0^1 z^2 e^{-az} dz = -\frac{e^{-a}}{a} + \frac{2C_4}{a},$$

$$C_7 = \int_0^1 z^3 e^{az} dz = \frac{e^a}{a} - \frac{3C_5}{a},$$

$$C_8 = \int_0^1 z^3 e^{-az} dz = -\frac{e^{-a}}{a} + \frac{3C_6}{a},$$

$$C_9 = \int_0^1 z^4 e^{az} dz = \frac{e^a}{a} - \frac{4C_7}{a},$$

$$C_{10} = \int_0^1 z^4 e^{-az} dz = -\frac{e^{-a}}{a} + \frac{4C_8}{a},$$

$$C_{11} = \int_0^1 z^5 e^{az} dz = \frac{e^a}{a} - \frac{5C_9}{a},$$

$$C_{12} = \int_0^1 z^5 e^{-az} dz = -\frac{e^{-a}}{a} + \frac{5C_{10}}{a}.$$

Taking variation of (6.59), the marginal stability curve is obtained as ,

$$R = \frac{a^2(a^2+10) \left(1 + \frac{E}{Da}\right)}{30\beta_2} ,$$

$$\text{where, } E = \frac{140}{a^4} (-\beta_3 + \frac{\beta_4 a^2}{2} + \beta_6) .$$

## 6.6 RESULTS AND DISCUSSION

The critical wave numbers and the corresponding Rayleigh-Darcy numbers (DaR) are obtained for various values of Da. These results are shown in Table 1.

Table 1 Critical values of  $a$  and DaR

Da	$a$	DaR
$\infty$ (Navier-Stokes)	3.12	1748.697 ( $= R_c$ )
$10^{-3}$	3.30	44.794
$10^{-6}$	3.31	42.537
$10^{-9}$	3.31	42.535

The results given in Table 1 show that when the permeability of the medium tends to infinity, the system behaves like an ordinary fluid, with critical wave and Rayleigh-Darcy number equal to 3.12 and 1748.697 respectively. These two values are remarkably close to the exact values of 3.117 and 1707.762 given by Chandrasekhar (1961). Results obtained for different values

of Rayleigh-Darcy number are also comparable with the critical wave number and corresponding Rayleigh-Darcy number determined by Lebon and Cloot (1986) which differ by less than 3% . This shows that the governing principle of dissipative processes proposed by Gyarmati is well suited for analyzing the Benard convection in porous media.

## REFERENCES

- Bejan, A., 1987, "Convective heat transfer in porous media", In Handbook of Single-phase convective heat transfer (Edited by Kakac, S., Shah, R.K., and Aung, W.), Chapter 16, Wiley, New York.
- Chandrasekhar, S., 1961, Hydrodynamic and Hydromagnetic Stability, Clarendon Press, Oxford.
- Cheng, P., 1978, "Heat transfer in geothermal systems", Advances in Heat Transfer, vol. 14, pp. 1-105.
- Gyarmati, I., 1969, "On the governing principle of dissipative processes and its extension to non-linear problems", Ann. Phys., Vol. 23, pp. 353-378.
- Gyarmati, I., 1970, Non-Equilibrium Thermodynamics Field Theory and variational Principles, Springer-Verlag, Berlin.
- Lapwood, E.R., 1948, "Convection in a porous medium", Camb. Phil. Soc., Vol. 44, pp. 508-521.
- Lebon, G., and Cloot, A., 1986, "A thermodynamical modelling of fluid flows through porous media : application to natural convection", Int. J. Heat Mass Transfer, Vol. 29, pp. 381-390.
- Nield, D.A., 1985, "Recent research on convection in a saturated porous medium", Convective flows in Porous Media, Proceedings of a seminar organized by DSIR and CSIRO, Institute of Physical Sciences, Wairakei, New Zealand (1984), DSIR Science Information Publishing Centre, Wellington.
- Singh, P., 1976, "The application of the Governing Principle of Dissipative Processes to Bénard convection", Int. J. Heat Mass Transfer, Vol. 19, pp. 581-588.
- Singh, P., 1980, "Formulation of Gyarmati Principle for Heat conduction equation", Wärme-und Stoffübertragung, Vol. 13, pp. 39-45.
- Singh, P., and Raj, S.A., 1987, "Analytical study of laminar boundary layers with non-uniform main stream velocity and wall temperature", J. Non-Equilib. Thermodyn., Vol. 10, pp. 287-304.
- Stark, A., 1974, "Approximation methods for the solution of heat conduction problems using Gyarmatis Principle", Ann. Phys., vol. 31, pp. 53-75.
- Vincze, Gy., 1973, "On the treatment of Thermo-Electrodynamical Processes by Gyarmati's Principle", Ann. Phys., vol. 30, pp. 55-61.